The Effects of Endocannabinoid Modulation and Neurogenic Inflammation in Experimental Knee Joint Arthritis

by

Eugene Krustev

Submitted in partial fulfillment of the requirements for
the degree of Master of Science

at

Dalhousie University
Halifax, Nova Scotia
July 2015

For my mother, Mia

Table of Contents

List of Tables

List of Figures

Abstract

Arthritis is a debilitating condition, and a leading cause of disability worldwide. Despite the prevalence of arthritis, few therapies are satisfactorily efficacious, and many are limited by serious adverse effects. It is for these reasons that the development of newer, safer and more efficacious arthritis therapies is essential.

The knee is the second largest joint in the human body, and is one of the most affected joints in osteoarthritis. Furthermore, the knee is easily accessible in mice, making it an ideal joint for inducing experimental arthritis in rodents.

Local neurogenic inflammation is mediated by the release of neuropeptides from the peripheral terminals of nociceptive fibres. Neurogenic inflammation has been implicated in a number of inflammatory conditions, including arthritis; therefore, understanding how neurogenic inflammation contributes to joint inflammation may help in the development of novel arthritis therapeutics.

One family of molecules that shows tremendous promise for the management of arthritic inflammation and pain are the cannabinoids. These compounds were first identified in the *Cannabis* plant, but subsequent research has identified an endogenous cannabinoid system, that plays a role in both health and disease. One method that is used to increase endocannabinoid activity is inhibiting the enzymes responsible for their degradation. Using a drug called URB597, we can block fatty acid amide hydrolase, increasing articular endocannabinoids.

The aim of this thesis was to investigate the contribution of neurogenic inflammation in experimental knee joint disease, as well as the therapeutic potential of the endocannabinoid system in joint inflammation and the development of arthritic pain.

List of Abbreviations and Symbols Used

2-AG	2-Arachidonoyl glycerol
ACEA	Arachidonyl-2-chloroethylamide
ACL	Anterior cruciate ligament
ACR	American College of Rheumatology
AS	Amidase signature
ATP	Adenosine triphosphate
CAM	Cell adhesion molecule
cAMP	cyclic adenosine monophosphate
CB1R	Cannabinoid receptor type 1
CB2R	Cannabinoid receptor type 2
CGRP	Calcitonin gene related peptide
CNS	Central nervous system
COX	Cyclooxygenase
DAGL	Diacylglycerol-lipase
DAMP	Damage associated molecular pattern
DMARD	Disease modifying anti-rheumatic drug
DMSO	Dimethyl sulfoxide
DRG	Dorsal root ganglion
DWB	Dynamic weight bearing
EC50	Half Maximal Effective Concentration
eNOS	Endothelial nitric oxide synthase
ERRα	estrogen-related receptor α

EULAR	European League Against Rheumatism
FAAH	Fatty acid amide hydrolase
GAPDH	Glyceraldehyde-3-phosphate dehydrogenase
G_i	Inhibitory heterotrimeric G-protein
GM-CSF	Granulocyte-macrophage colony stimulating factor
GPCR	G protein coupled receptor
hr	Hour
Hz	Hertz
i.p.	Intra-peritoneal
i.v.	Intravenous
ICAM-1	Intercellular adhesion molecule-1
IL	Interleukin
IVM	Intravital microscopy
KC	Kaolin-carrageenan
LCL	Lateral collateral ligament
LFA-1	Lymphocyte function associated antigen-1
MAGL	Monoacylglycerol lipase
MAP	Mean arterial pressure
MCL	Medial collateral ligament
MIA	Sodium monoiodoacetate
MMP	Matrix metalloproteinases
mRNA	Messenger ribonucleic acid
MSU	Monosodium urate

NAPE-PLD	N-acyl phosphatidylethanolamine phospholipase-D
NF-κB	nuclear factor kappa-light-chain-enhancer of activated B cells
NK	neurokinin
NLP3	NOD-like receptor family, pyrin domain containing 3
NO	Nitric oxide
NSAID	Non-steroidal anti-inflammatory drug
OA	Osteoarthritis
OEA	Oleoylethanolamide; oleamide
PACAP-38	Pituitary adenylate cyclase-activating polypeptide-38
PAMP	Pathogen associated molecular pattern
PAR	Proteinase activate receptor
PCL	Posterior cruciate ligament
PEA	Palmitoylethanolamide
PG	Prostaglandin
PRR	Pattern recognition receptor
PSGL-1	P-selectin glycoprotein ligand-1
R6G	Rhodamine 6G
RA	Rheumatoid arthritis
RAGE	Receptor for advanced glycation endproducts
s	Second(s)
s.c.	Subcutaneous
SDF1-α	Stromal cell-derived factor 1-α
SEM	Standard error of the mean

SP	Substance P
SWB	Static weight bearing
TLR	Toll like receptor
TNF-α	Tumor necrosis factor-α
TRPV1	Transient receptor potential cation channel subfamily V member 1
TRPV4	Transient receptor potential cation channel subfamily V member 4
VCAM-1	Vascular cell adhesion molecule 1
VIP	Vasoactive intestinal peptide
wk	Week
Δ9-THC	Tetrahydrocannabinol

Acknowledgements

First and foremost I would like to thank my supervisor Dr. Jason J McDougall. Your mentorship over the past few years has been indispensable, and you have been fundamental in sparking my ever-growing interest in science.

I would also like to acknowledge the past and present members of the McDougall Lab with whom I have the chance to work. Most importantly, I would like to thank Allison Reid, to whom I am forever grateful for her help throughout all aspects of this project. Also, Milind Muley, your help over the past few months has been tremendously appreciated, and your passion for science is contagious.

I am also grateful to the members of my advisory and defense committees, Dr. Jana Sawynok, Dr. Melanie Kelly, and Dr. Christian Lehmann, all of whom have helped tremendously in shaping this thesis.

Furthermore, I would like to thank our current graduate student coordinator, Dr. Kishore Pasumarthi, for all of his help in finalizing my thesis.

I cannot thank Luisa Vaughan, Sandi Leaf, and Cheryl Bailey enough for all they do as the administrative staff in the office.

A special thank you goes to Bridget Higgins for lending me her artistic talent and contributing the anatomical figures presented here.

To my friends and family, thank you for all of your support over the course of my studies.

Lastly, I would like to thank everyone in the Department of Pharmacology for a great past few years!

Chapter 1: Introduction

1.1 Anatomy of the knee

The knee is a synovial joint and the second largest joint in the body. The knee joint functions primarily as a hinge, allowing leg flexion and extension, but is also capable of moderate rotation, which grants us the ability to perform complex manoeuvres while walking and running. Furthermore, during movement and standing, both knees share 100% of total body weight, subjecting them to numerous forces. Given the important role that each knee plays in stance and locomotion, it is no wonder that proper joint function requires intricate interactions between musculoskeletal, neuronal and vascular components.

The knee joint consists of three bones, the femur, patella and tibia; and five ligaments, the lateral collateral ligament (LCL), the medial collateral ligament (MCL), the anterior cruciate ligament (ACL), the posterior cruciate ligament (PCL) and the patellar ligament (Figure 1.1). One more bone, the fibula, provides an attachment point for the LCL, but does not contact the synovial space of the knee. The knee joint is encased in an articular capsule that is composed of an outer avascular fibrous layer and an inner membranous layer, also known as the synovial membrane. The synovial membrane is highly vascularized and supplies the joint with sustenance, as well as secretes the synovial fluid that fills the joint space. Each human knee contains approximately 1ml of synovial fluid (Ropes et al., 1940), which is composed of filtered plasma, hyaluronic acid and lubricin, the latter two components being secreted from synovial cells (Hui et al., 2012). The molecular content of synovial fluid increases its viscosity, allowing almost frictionless contact and movement between the two articulating bones. The two adjacent

surfaces of the femur and tibia are also coated with cartilage, which provides an additional protective layer. Furthermore, each knee contains two crescent-shaped menisci, one lateral and one medial, which provide increased cushioning, and aid in stabilizing the knee during joint loading.

1.1.1 Neuroanatomy of the knee

The knee joint communicates regularly with the central nervous system (CNS), a process facilitated by both efferent and afferent neurons, which carry nerve impulses to and from the knee, respectively. Efferent neurons transmit sympathetic signals to the knee, which control articular vasomotor tone. These sympathetic nerve fibres primarily originate from the paravertebral ganglia at L3-L6 in cats (Heppelmann & Schaible, 1990), rodents (Catre & Salo, 1999), and humans, with slight differences between species. By terminating near joint blood vessels, these sympathetic efferents control vasoconstriction by releasing noradrenaline. Articular sympathetic tone controls normal vasomotor responses in healthy joints; however, changes to the articular adrenergic system may contribute to pathology in diseased knees (McDougall et al., 1995; McDougall, 2001).

The afferent signals that originate from the joint convey somatosensory information with respect to joint movement, proprioception and pain. The afferent neurons that carry these signals are divided into four groups (Table 1.1). Class I (Aα) primary afferents are the largest diameter and fastest conducting neurons that innervate the joint. Aα neurons are myelinated, innervate the surrounding ligaments, and conduct proprioceptive information from the joint to the CNS. Class II (Aβ) primary afferents also conduct proprioceptive information to the spinal cord, but more commonly innervate the joint capsule. Class III (Aδ) primary afferents are thinly myelinated, and are responsible for

conveying nociceptive signals from the joint to the CNS. Lastly, Class IV (C) primary afferents are unmyelinated fibres that conduct nociceptive information from the joint to the CNS. These are the smallest diameter fibres that innervate the joint, and also the slowest conducting (Freeman & Wyke, 1967).

Table 1.1 Innervation of the joint

Signal Direction	Fibre Subtype	Myelination	Diameter	Conduction Velocity	Function
Efferent	Sympathetic	No	0.4 - 2.4 μm	1m/s	Sympathetic tone
Afferent	Class I (Aα)	Yes	10 - 18μm	60 - 100m/s	Proprioception
Afferent	Class II (Aβ)	Yes	5 - 13μm	20 - 70m/s	Proprioception
Afferent	Class III (Aδ)	Thinly	1 - 5μm	2.5 - 20m/s	Nociception
Afferent	Class IV (C)	No	<1μm	<1m/s	Nociception

(Adapted from Krustev et al., 2015).

1.1.2 Knee joint vasculature

In humans, the vascular supply of the knee is comprised of various branches of the femoral artery and vein (Figure 1.2). On the medial side of the femur, just before reaching the knee, the articular genicular artery branches from the femoral artery, begins to loop around the anterior of the femur, and travels down the anterior portion of the knee. A saphenous branch also forms from the genicular artery, which travels the anteromedial portion of knee. At the point where the genicular artery branches, the femoral artery becomes the popliteal artery, and travels along the posterior side of knee, producing several branches that vascularize this area. The anterolateral portion of the knee is vascularized by the descending branch of the lateral circumflex femoral artery (Gray,

1989). Similar to humans, rodent knee joint vascularization is also derived from articular branches of the genicular and saphenous branches of the femoral artery and vein.

Similar to their differences in cell type, the different components of the knee receive different degrees of vascularization. The outer third of the meniscus, which is closest to the synovium, is vascularized, while the inner two thirds are avascular (Petersen & Tillmann, 1999). As for the knee joint ligaments, only their outer most layers contain blood vessels. The cartilage is normally avascular, and is sustained primarily by the diffusion of nutrients and oxygen from synovial capillaries into the synovial fluid. The synovium is highly vascularized, affording it the responsibility of supplying the knee with plasma, nutrients and oxygen (Smith, 2011), as well as being the primary site of normal and pathological articular inflammation.

1.2 Inflammation

Inflammation is characterized by five cardinal signs, *rubor* (redness), *calor* (heat), *tumor* (swelling), *dolor* (pain), and *functio laesa* (loss of function) (Celsus and Galen, as cited in Lawrence et al., 2002). Under normal conditions, acute inflammation is beneficial, protecting us from invading pathogens, and promoting tissue remodelling and repair. Conversely, chronic inflammation (≥6wk) serves no beneficial purpose and can result in chronic pain and tissue damage. There are a number of different mechanisms and mediators that drive joint inflammation, which involve numerous cell types and molecules. In autoimmune arthropathies, like rheumatoid arthritis (RA), inflammation is primarily the result of T and B cell driven immunity, in which the body's own defense systems mount an immune response targeted at self-antigens (Van Boxel & Paget, 1975). On the other hand, in osteoarthritis (OA), the breakdown of joint constituents activates

innate immune responses, which are beneficial for clearing damaged cells, but, when chronic, can lead to further joint damage (Sokolove & Lepus, 2013).

Vertebrates have developed two distinct immune systems, which are responsible for protecting us against microorganisms, as well as promoting tissue repair following injury. The innate immune system provides us with an acute non-specific initial response to invading pathogens, facilitates the clearance of dead cells, and repairs damaged tissues. Meanwhile, the adaptive immune system is slower but adaptable, insofar as it "remembers" invading pathogens, thus optimizing responsiveness to these organisms in the future.

1.2.1 The innate immune system

The innate immune system is considered the more simple of the two; however, its role in host survival is equally, if not more important. On their surface, pathogenic organisms express distinct molecular patterns (pathogen-associated molecular patterns; PAMPs), to which, through evolution, we have developed specific pattern recognition receptors (PRRs). PRRs also recognize molecular patterns that are released during tissue damage (damage associated molecular patterns; DAMPs), thus enabling tissue damage-induced immune responses. This sterile form of inflammation is driven by tissue damage without pathogen infiltration, and is especially important in understanding inflammation in degenerative joint disease.

1.2.1.1 Damage associated molecular patterns

There are a number of different DAMPs, which are released following cell injury or death. The release of DAMPs during the initial stages of OA is thought to be a key

initiator in driving joint inflammation. Several DAMPs have been identified in the synovial fluids of OA patients, and their corresponding PRRs have also been elucidated (Table 1.2). These OA DAMPs can be fragments of degraded cartilage, plasma proteins or intracellular components that are released following cell damage (alarmins) (Sokolove & Lepus, 2013).

PRRs can be divided into two categories, circulating PRRs, which are released from remote organs and travel in the blood (Litvack & Palaniyar, 2010), and cell expressed PRRs, which are either surface expressed, endosomal or cytosolic (Kawai & Akira, 2010). Both circulating and cellular PRRs play different, but important roles in identifying and eliminating invading organisms. Cellular PRRs include the toll like receptors (TLR1 - TLR4), NOD-like receptor family, pyrin domain containing 3 (NLP3), and receptor for advanced glycation endproducts (RAGE). These PRRs are expressed in a number of different immune and non-immune cell types, including, but not limited to, circulating and resident leukocytes (Nalubamba et al., 2007), endothelial cells (Fitzner et al., 2008), and the peripheral terminals of nociceptive free nerve endings (Diogenes et al., 2011; Qi et al., 2011). When activated by a molecular pattern, PRRs initiate intracellular signalling cascades that differ depending on the effector cell type. One example is MyD88, the adapter molecule for the TLRs (except TLR3), which then activates other intracellular adapter molecules and subsequent gene expression (Rhee & Hwang, 2000). Although the intracellular pathways and cellular responses may differ between cell types, the general outcome of PRR activation is increased local inflammation. PRR activation increases the expression of pro-inflammatory molecules like cytokines and prostaglandins. Furthermore, PRR activation promotes the recruitment of white blood

cells to the site of injury, which facilitates the uptake and clearance of damaged cells; however, chronic activation of the innate immune system, as a result of repeated trauma or impaired resolution mechanisms, may result is dysregulated tissue remodelling, which can exacerbate joint damage (see Section 1.2.3).

Table 1.2 Osteoarthritis associated DAMPs and PRRs

DAMP	PRR
Fragmented extracellular matrix components	
Biglycan [1]	TLR2, TLR4, NLRP3
Decorin [1]	TLR2, TLR4
Fibronectin	TLR2, TLR4
Low molecular weight hyaluronic acid	TLR2, TLR4
Tenascin C	TLR4
Lumican [1]	Unknown; enhances TLR4 activation
Keratocan [1]	Unknown; neutrophil infiltration
Extravasated plasma proteins	
α1 microglobulin	TLR4
α2 microglobulin	TLR4
Fibrinogen	TLR4
Gc-globulin	TLR4
Alarmins	
High mobility group box 1	TLR2, TLR4, RAGE
S100 proteins	TLR4

Adapted and expanded from (Sokolove & Lepus, 2013)
[1](Melrose et al., 2008)

1.2.1.2 Cellular effectors of the innate immune system

Almost any articular cell can contribute to joint inflammation in one way or another; however, the most important cells involved in the development of joint inflammation are resident and infiltrating immune cells, vascular endothelial cells, and innervating neurons.

1.2.1.2.1 Resident immune cells

Resident mast cells, macrophages and dendritic cells all contribute to local immune responses; however, mast cells and macrophages are more involved in innate immune responses, while dendritic cells are essential components of the adaptive immune system.

The following section on resident innate immune cells will, therefore, only focus on mast cells and resident macrophages.

1.2.1.2.1.1 Mast cells

In the joint, connective tissue mast cells reside in the synovium, and express numerous immune receptors on their outer membranes, including PRRs (Applequist et al., 2002). When activated, mast cells work rapidly and release pre-stored granules of histamine, in a process called degranulation (Masini et al., 1987). Mast cells are also capable of synthesizing and releasing other pro-inflammatory molecules, like prostaglandins (Tolone et al., 1978), leukotrienes (Malaviya & Abraham, 2000), cytokines (Galli et al., 1991), proteinases (Wenzel et al., 1988), and granulocyte-macrophage colony stimulating factor (GM-CSF) (Wodnar-Filipowicz et al., 1989); however, the release of these pro-inflammatory molecules, which must be synthesized on demand, is much slower than histamine release. Histamine and synthesized immunomodulators act on endothelial cells, producing vasodilation and widening fenestrations, and this increases vascular perfusion and permeability, respectively (Flynn & Owen, 1979). Increased blood flow is responsible for the characteristic redness of inflamed tissues, and promotes the transport of plasma proteins and leukocytes to the site of inflammation. Furthermore, increased vascular permeability promotes plasma and protein extravasation, resulting in oedema and swelling. In addition to facilitating these non-specific hemoresponses, mast cell-released pro-inflammatory molecules can specifically promote leukocyte transmigration by inducing cell adhesion molecule (CAM) expression on vascular endothelial cells (Yamaki et al., 1998).

1.2.1.2.1.2 Resident macrophages

Macrophages are phagocytic cells that engulf and neutralize invading pathogens, as well as dead or damaged cells. In the knee joint, where infections are quite rare, the duties of macrophages are primarily to mediate tissue repair following injury. During joint trauma, DAMPs activate TLRs on resident macrophages, initiating phagocytic mechanisms that promote the removal of damaged cell constituents, which undergo enzymatic digestion once inside the phagosome (Savill & Fadok, 2000). Macrophages are also capable of releasing matrix metalloproteinases (MMPs), a family of enzymes responsible for extra-cellular matrix remodelling. Macrophages can also stimulate MMP expression by chondrocytes, thus enabling these cartilaginous cells to mediate their own cartilage remodelling (Dreier et al., 2001). Under normal conditions, these events are beneficial and are an essential part of cartilage turnover; however, when dysregulated, these finely tuned processes can result in aberrant remodelling mechanisms that may contribute to joint degeneration.

1.2.1.2.2 Small diameter nociceptors and neurogenic inflammation

'*On the origin from the spinal cord of the vaso-dilator fibres of the hind-limb, and on the nature of these fibres'*, by William Bayliss (1901) is the seminal paper on neurogenic inflammation. In this paper, Bayliss described how he observed increased blood flow in canine hindlimbs following electrostimulation of the ipsilateral sciatic nerve. He further concluded that this effect was mediated by small diameter nociceptive afferents. Given that these neurons were believed to only transmit signals towards the CNS, Bayliss coined the term 'antidromic signalling' to describe the propagation of signals in the opposite direction, towards the periphery. It was later noted that

electrostimulation and chemostimulation of these nociceptors, using the transient receptor potential cation channel subfamily V member (TRPV) 1 (TRPV1) agonist capsaicin, also induces plasma extravasation and subsequent oedema (Jancsó et al., 1967). Janscó and colleagues (1967) showed that denervating local nociceptors, using neurotoxic doses of capsaicin, abolished experimentally-induced neurogenic inflammation. The work of Bayliss, Jancsó, and others, showed that electrical impulses could travel down nociceptive fibres, towards the periphery, where they then elicited local inflammatory responses. As for how these impulses develop naturally, two theories dominate the field, both holding their own merits and limitations.

1.2.1.2.2.1 Generating antidromic action potentials

The axon reflex is the more Occamian of the two theories, and suggests that the neuroanatomical machinery required for generating antidromic signals is entirely peripherally located. The first step of the axon reflex is the activation of free nerve ending nociceptors by a nociceptive stimulus, which in turn produces an action potential. Once elicited, the action potential then propagates along the neuron, in the orthodromic direction, towards the spinal cord; however, once reaching a dendritic branch, the action potential can bifurcate, with one stimulus continuing towards the CNS and the other commencing its antidromic route down the intersecting branch (Bruce, 1913). One fallacy of this theory is that severing the nerve proximal to the dorsal root ganglion (DRG) almost completely abolishes capsaicin-induced skin neurogenic inflammation, suggesting that central mechanisms are involved (Lin et al., 1999)

The dorsal root reflex theory suggests that antidromic impulse generation requires spinal mechanisms (Sluka et al., 1995). Similar to the axon reflex, the first step in this

process is the generation of an action potential by a nociceptive stimulus. This signal then travels towards the spinal cord, eventually reaching a network of interneurons. Spinal interneurons are important for processing nociceptive information en route to the brain; however, according to the dorsal root reflex theory, these neurons are also involved in generating antidromic signals, which then leave the spinal cord via an afferent nociceptive neuron (Eccles et al., 1963; Evans & Long, 1989). This theory is also subject to debate, as some neurogenic responses are maintained even when a local anaesthetic is applied to the DRG, suggesting that peripheral mechanisms are also at play (Groetzner & Weidner, 2010).

1.2.1.2.2.2 Inflammatory neuropeptides

Regardless of how they are generated, sufficient antidromic signalling at the peripheral terminals of nociceptive afferents results in the release of pro-inflammatory neuropeptides. These neuropeptides include substance P (SP), calcitonin gene related peptide (CGRP), vasoactive intestinal peptide (VIP), somatostatin, and endomorphin-1 (Figure 1.3).

Von Euler and Gaddum first discovered SP in 1931, while studying intestinal contractions *in vitro*. Nearly a half a century later, SP expression in both the somas (Hökfelt et al., 1975) and peripheral terminals (Cuello et al., 1978) of DRG neurons provided the first clues that SP was involved in neurogenic inflammation. When stimulated with capsaicin, DRG neurons were capable of releasing SP from their peripheral and central terminals (Gamse et al., 1980). Peripherally acting SP induces both vasodilation and plasma extravasation in rats, and these effects are partially mediated by histamine release from mast cells (Lembeck & Holzer, 1979). SP also increases the

expression of lymphocyte function associated antigen-1 (LFA-1) and intercellular adhesion molecule-1 (ICAM-1) on leukocytes and endothelial cells, respectively. By inducing the expression of these CAMs, SP promotes leukocyte recruitment to areas of inflammation (Vishwanath & Mukherjee, 1996). In addition to stimulating CAM expression on leukocytes, SP can also induce cytokine production and release from immune cells (Azzolina et al., 2003).

There are two isoforms of CGRP, α-CGRP and β-CGRP, which are both composed of thirty-seven amino acids, sharing thirty-four and differing by three (Morris et al., 1984). In the periphery, CGRP is expressed in DRG neurons (Noguchi et al., 1990), and acts as a potent vasodilator following release (Brain et al., 1985). CGRP can also stimulate plasma extravasation when administered alone (Karimian & Ferrell, 1994), as well as promote plasma and leukocyte extravasation in IL-1 treated tissues (Buckley et al., 1991). CGRP is also chemotactic, and can attract passing leukocytes (Foster et al., 1992), and stimulate their adherence to the local vasculature (Zimmerman et al., 1992). Paradoxically, CGRP can also have anti-inflammatory effects, and has been shown to attenuate cytokine-induced oedema (Raud et al., 1991), and decrease macrophage activity *in vitro* (Nong et al., 1989).

As its name suggests, VIP was first discovered in the intestine, where it plays an important role in regulating gastric secretions (Barbezat & Grossman, 1971). VIP is also released from DRG neurons, and modulates local immune responses by recruiting human T cells and stimulating their adhesion to the local vasculature, in areas of inflammation (Johnston et al., 1994). VIP also increases articular blood flow in normal and chronically inflamed rat knee joints, but this hyperaemic effect is abolished in acutely inflamed joints

(McDougall & Barin, 2005). Conversely, like CGRP, VIP can also have anti-inflammatory effects, and when human monocytes were treated with VIP, their ability to produce IL-8 was hindered (Delgado & Ganea, 2003).

Originally, somatostatin was discovered in the hypothalamus, where it has numerous signalling functions (Ling et al., 1973). In the periphery, somatostatin is expressed in DRG neurons (Hökfelt et al., 1976), and transported down the axon towards the peripheral nerve endings (Rasool et al., 1981). Interestingly, somatostatin appears to be purely anti-inflammatory and counteracts some of the effects of co-released neuropeptides. Stromal cell-derived factor 1-α (SDF1-α) is a potent chemokine, capable of inducing T cell infiltration *in vitro*. When leukocytes were treated with somatostatin, their chemokinesis towards SDF1-α was significantly reduced (Talme et al., 2004). Furthermore, somatostatin reduces histamine release from human basophils *in vitro* (Goetzl & Payan, 1984), and is capable of inhibiting the chemotactic effects of SP (Kolasinski et al., 1992).

1.2.1.2.3 Endothelial cells

Infiltrating leukocytes and plasma proteins reach the joint via the circulatory system, and enter through fenestrations between activated endothelial cells. During inflammation, changes to the endothelial cells and the proteins they express promote the infiltration of circulating inflammatory mediators. When activated by histamine, endothelial nitric oxide synthase (eNOS) begins synthesizing nitric oxide (NO), which in turn has activity on the vascular smooth muscle causing relaxation and subsequent vasodilation (Fiscus, 1988). Furthermore, pro-inflammatory molecules like histamine promote the phosphorylation of endothelial tight junction proteins, thus widening the

fenestrations between endothelial cells and permeabilizing the endothelium (Boucher et al., 1978). These two effects promote blood flow and vascular leakage, both non specific events; however, local inflammation can also specifically activate leukocyte recruitment by increasing CAM expression on endothelial cells, which will be discussed in detail below.

1.2.1.2.4 Infiltrating immune cells

In normal joints, most leukocytes will pass through the area at the same speed as the surrounding flow of blood; however, during articular inflammation a number of vascular changes occur that promote the transmigration of white blood cells into the inflamed joint (Figure 1.4) (reviewed Ley, 1996). These infiltrating leukocytes promote local inflammation by releasing cytokines. As for how these cells get into the joint, the recruitment of leukocytes involves a well-defined cascade of events.

1.2.1.2.4.1 Leukocyte recruitment cascade

The first step in this cascade is leukocyte capture, which involves interactions between CAMs, specifically, P-selectin on endothelial cells, and P-selectin glycoprotein ligand-1 (PSGL-1) on leukocytes (Mayadas et al., 1993). PSGL-1 is constitutively expressed on the surface of circulating neutrophils, monocytes and granulocytes (Laszik et al., 1996), but P-selectin expression on the luminal endothelial surface only occurs following activation of the endothelium. In the absence of inflammation, P-selectin is stored inside the endothelial cells, within storage granules called Weibel-Palade bodies. Upon activation by pro-inflammatory molecules, endothelial cells rapidly mobilize P-

selectin to their membranes (Dole et al., 2005), where it can interact with PSGL-1, and this interaction decreases the kinetic energy of passing leukocytes.

Leukocytes that are moving slower than the surrounding flow of blood are called rolling leukocytes, and, like capture, leukocyte rolling also involves P-selectin-mediated leukocyte-endothelial interactions. Interestingly, L-selectin can also facilitate leukocyte rolling when P-selectin ligand expression is experimentally decreased, suggesting a role for other selectins in this process (von Andrian et al., 1993). As CAM interactions between endothelial cells and leukocytes increase or become stronger, leukocytes will continue to lose kinetic energy, and, once completely stopped, are defined as firmly adherent leukocytes.

Leukocyte adherence involves another family of CAMs, the integrins. Blocking CD18, which is the β subunit of several integrin complexes, has profound negative effects on leukocyte adherence (Vedder et al., 1990). Of the CD18 containing integrins, LFA-1 appears to play the most significant role in leukocyte adherence, as it is expressed on leukocyte membranes and interacts with endothelial ICAM-1 (Dustin, 1988). In addition to ICAM-1, vascular cell adhesion molecule 1 (VCAM-1) is also involved in leukocyte adherence in the peripheral (Sans et al., 1999), and cerebral microcirculation (Norman et al., 2008).

Adherent leukocytes transmigrate though endothelial fenestrations in response to chemoattractants, which are secreted by both the endothelium and local immune cells. Once a leukocyte exits the blood vessel, it will continue to follow the chemoattractant gradient, navigating through the extra-cellular matrix until it reaches the site of inflammation (Ebnet & Vestweber, 1999). Here, it can promote or attenuate the

inflammatory response by releasing cytokines, as well as phagocytose unwanted pathogens or damaged cellular constituents.

1.2.2 Adaptive immunity

The adaptive immune system is beyond the scope of this thesis, as all of the models used here are driven by innate immune mechanisms; however, given its importance in autoimmune arthropathies, like RA, a brief discussion has been included. The adaptive immune system is unique to mammals, and affords our immune system the ability to "remember" invading pathogens and mount more efficient immune responses in the future. T cells, which mature in the thymus, and B cells, which mature in the bone, are the two most important cells involved in adaptive immunity. These cells possess specialized surface receptors that allow them to recognize foreign antigens and become activated. Following activation, both T cells and B cells produce different clones, some to fight off the current infection, and others that act as memory cells. Memory T and B cells express receptors to the invading pathogen, and, in the future, if the pathogen invades again, then a more efficient immune response can occur (Ward & Rosenthal, 2014).

1.2.3 Pathological outcomes of chronic joint inflammation

Acute joint inflammation is beneficial, as it warns us of injury, deters us from using an injured joint, and contributes to the repair process. On the other hand, chronic inflammation, which persists more than 6 weeks, is detrimental because of the discomfort it causes and the negative effects it can have on joint morphology.

1.2.3.1 Inflammatory joint pain

Non-steroidal anti-inflammatory drugs (NSAIDs) are frequently prescribed for the treatment of mild to moderate OA pain; therefore, implicating inflammation as a source of pain in OA (Felson, 2000). Furthermore, the inflammatory flares that afflict RA sufferers are characterized by periods of moderate to severe pain. The pro-nociceptive effects of inflammation are a consequence of inflammatory molecules acting directly on the free nerve endings of small diameter afferents. Prostaglandins, cytokines, proteinases and neuropeptides are all capable of sensitizing these nociceptors, increasing their propensity to fire in response to painful stimuli (hyperalgesia), as well as previously non-painful stimuli (allodynia).

1.2.3.1.1 Prostaglandins

NSAIDs inhibit either one or both cyclooxygenase enzymes (COX; COX1 and COX2), which catalyse the conversion of arachidonic acid into prostaglandin (PG)H2. Subsequently, PGH2 is hydrolysed into PGD2, PGE2, PGF2α, PGI2, or thromboxane, a family of pro-inflammatory molecules that drive local inflammatory responses and sensitize nociceptors (reviewed Camu et al., 2003).

PGE2 seems to have the greatest effect on joint pain, and activation of PGE2 receptors, which are localized on joint nociceptors, produces peripheral sensitization and enhanced neuronal sodium currents (Gold et al., 1998). Prostacyclin (PGI2) is also involved in the development of joint pain, albeit less so than PGE2. Prostacyclin receptor antagonism attenuates pain behaviours in the sodium monoiodoacetate (MIA) model of

OA in rats, and this effect is comparable to that of the classic NSAID diclofenac (Pulichino et al., 2006).

1.2.3.1.2 Cytokines

Cytokines are involved in both adaptive and innate immune responses, and contribute to the development of pain during inflammation. Cytokines can be released from both resident and infiltrating leukocytes, as well as endothelial cells and fibroblasts. During joint inflammation, articular cytokine concentrations are increased drastically (McInnes & Schett, 2007). Tumor necrosis factor-α (TNF-α), IL-6 and IL-1β, are all capable of activating receptors on joint nociceptors, and sensitizing these neurons (Kidd & Urban, 2001). The synovial samples from both OA and RA patients are positive for cytokines, with higher concentrations in RA samples (Farahat et al., 1993). Levels of IL-1α, IL-1β, and TNF- α are positively correlated with disease progression in OA patients (Smith et al., 1997), and these results are in accordance with pre-clinical studies where cytokine levels were elevated in both the MIA model of OA (Orita et al., 2011), and an antigen-induced rat RA model (Lewthwaite et al., 1995; Szekanecz et al., 2000).

When injected into an inflamed joint, TNF-α decreases ipsilateral hindlimb weight bearing, which is indicative of pain (Tonussi & Ferreira, 1999). Two TNF- α receptors, TNFR1 and TNFR2, are expressed on nociceptive afferents, and TNF- α-induced pain is a product of their activation (Schaible et al., 2010). TNFR activation increases neuronal TRPV1 expression, an ion channel that is primarily responsible for recognizing nociceptive heat stimuli (Hensellek et al., 2007). IL-1β can also increase TRPV1 expression on DRG neurons, as well as sensitize articular C-fibres, but not Aδ fibres (Ebbinghaus et al., 2012). Lastly, IL-17 also appears to play a role in nociceptor

sensitization, as it increases expression of TRPV4, an ion channel involved in mechanosensation. Furthermore, IL-17 deficient mice show decreased mechanosensitization following induction of experimental RA (von Banchet et al., 2013).

1.2.3.1.3 Neuropeptides

As mentioned above, neurogenic inflammation involves the release of inflammatory neuropeptides from Aδ and C fibre peripheral terminals following antidromic signalling. In addition to its immunomodulatory effects, SP is capable of sensitizing joint nociceptors; therefore, increasing their propensity to fire and contributing to inflammatory joint pain (McDougall & Schuelert, 2007). Furthermore, when treated with VIP, nociceptors become hyper-responsive to mechanical stimulation (Schuelert & McDougall, 2006), while VIP antagonism is analgesic in experimental OA joints (McDougall et al., 2006).

Interestingly, joint nociceptors are also capable of releasing analgesic molecules. Endomorphin-1 is an endogenous opioid that is released from articular nociceptors, and is capable of reducing nociceptor activation in normal joints; however, the analgesic effect of endomorphin-1 was lost in chronically inflamed joints, as peripheral opioid receptor expression was down-regulated by chronic inflammation (Li et al., 2005). Somatostatin is another nociceptor derived signalling molecule that is released during neurogenic inflammation and decreases inflammatory pain. Both normal and arthritic rat DRG neurons express somatostatin receptors, but acute and chronic inflammation decreases their expression (Bär et al., 2004). Furthermore, somatostatin receptor agonists decrease nociceptor firing and painful behaviours in rodents (Carlton et al., 2001). Pituitary adenylate cyclase-activating polypeptide-38 (PACAP-38) is a nociceptor-released

neuropeptide that is capable of decreasing carrageenan-, burn- and formalin-induced nocifensive behaviours, but increases rotation-induced primary afferent firing; therefore, showing opposite effects depending on the model tested (Sándor et al., 2009).

1.2.3.1.4 Proteinases

Proteinases are hydrolytic enzymes essential for tissue repair and remodelling; however, unchecked proteinase activity can result in joint damage and pain. Proteinases can also act as signalling molecules by activating a particular group of G protein-coupled receptors (GPCRs) called proteinase-activated receptors (PARs). The receptors in this family are unique, as activation requires the enzymatic cleavage of the N-terminus, which exposes a moiety that then binds and activates the same receptor. Currently, there are four known PARs, and PARs 1, 2 and 4 are involved in inflammatory pain. In the mouse hindpaw, PAR1 activation is analgesic and decreases carrageenan-induced pain (Kawabata et al., 2002). Conversely, PAR2 activation sensitizes articular nociceptors and is pro-nociceptive in joints (Russell et al., 2012). Neuronal PAR2 activation also promotes the release of SP and CGRP, which results in local neurogenic inflammation (Steinhoff et al., 2000), and subsequent leukocyte rolling and adherence within the synovial microcirculation (Russell et al., 2012). At low doses, PAR2 agonists sensitize nociceptors without producing inflammation, and this effect is mediated by SP release at the spinal terminals of these nociceptors (Vergnolle et al., 2001). In rodent joints, PAR4 activation promotes inflammation and pain, via mast cell- and bradykinin-dependent mechanisms (McDougall et al., 2009).

1.2.3.2 Inflammation-induced joint damage

For many years, inflammation was simply thought of as a symptom of OA, with little to no role in disease progression; however, in recent years, a body of literature has begun to accrue suggesting that inflammation does play a role in joint degeneration (reviewed Scanzello & Goldring, 2012). Inflammatory cytokines and complement factors are capable of inducing the expression of matrix degrading enzymes, which promote cartilage degradation and pathological bone remodelling. Interestingly, pharmacological and genetic inhibition of complement activation significantly reduced joint damage in three different OA models (Wang et al., 2011). Chronic inflammation also causes synovial hyperplasia and fibrosis, resulting in a dysfunctional synovium. These actions contribute to disease progression and joint damage in multiple different arthritic conditions.

1.3 Arthritis

Arthritis is a broad term, and can be any one of over 100 disorders that affect the joint. The word arthritis, when dissected into its Greek roots, literally means joint (*arth-* as from *arthron*) inflammation (*-itis*). Two of the most common forms of arthritis are OA, a degenerative joint disease, and RA, an autoimmune disorder that primarily affects the joints (March et al., 2014). In addition to OA and RA, there are numerous other arthritic disorders, whose causes range from crystal deposits in joints (e.g. gout and pseudogout), to articular bacterial infections (e.g. septic arthritis). Due to their differing aetiologies, the definitions and techniques used for diagnosing these conditions can differ greatly. Furthermore, arthritic conditions can differ in which and how many joints they affect, thereby adding another layer of complexity to the diagnosis and treatment of these diseases.

1.3.1 Osteoarthritis

OA is the most prevalent form of arthritis and normally affects large weight bearing joints, like the hip and knee, as well as the small joints of the hand. Based on the results of the 2010 Global Burden of Disease study, knee OA affects close to 4% of people worldwide, while hip OA has a prevalence of 1% (Cross et al., 2014). When combined, 1 in 4 persons over the age of 45 are afflicted by OA in one of more of their joints, and, given our aging global population, this number is expected to rise in the near future (Turkiewicz et al., 2014).

The primary symptom that OA patients find burdensome is joint pain, which can result from structural changes, inflammation and joint neuropathy. In OA, joint structures can be compromised due to cartilage degradation and aberrant bone remodelling, as a result of excessive or abnormal joint usage. Furthermore, obesity and acute injuries can add additional strain to the joints, resulting in an exacerbation of the damage. There is evidence to suggest that genetic factors also play a role in the development of OA, and the disease is more likely to develop in persons with a family history of OA; however, the precise genes that increase susceptibility are difficult to elucidate, because they are numerous. Genes that code for collagen (COL2A1), interleukins (IL-1A, IL-1B, IL1RN, IL4R, IL-17F, IL-6) and bone metabolism mediators (vitamin D receptor, Frizzled Related Protein Gene) have all been implicated as potential candidates in the development OA (Fernández-Moreno et al., 2008). Pathological changes in joint morphology lead to chronic low-grade inflammation, which eventually results in inflammatory joint pain. The contribution of joint inflammation in OA pain has long been recognized, as anti-inflammatory drugs are efficacious for treating OA pain; however, in recent years,

researchers have started placing greater emphasis on the role that inflammation plays in joint destruction (Sokolove & Lepus, 2013). The inflammatory mediators that are found in the synovial fluid of OA patients can activate MMPs, leading to cartilage degeneration and pathological joint remodelling. The literature concerning the role of inflammation in joint destruction is still lacking; therefore, a better understanding of how inflammation contributes to OA pathogenesis is necessary in order to understand how this debilitating disease progresses.

1.3.2 Rheumatoid arthritis

RA is a systemic autoimmune disorder that normally affects multiple joints, as well as extra-articular organs like the eyes and heart. The precise aetiology of RA is unknown, and undoubtedly differs between patients. Several candidate triggers have been linked to the development of pathological RA immunity, and these include genetic susceptibility (Hunt & Emery, 2014), Epstein Barr viral infections (Costenbader & Karlson, 2006), and smoking (Lahiri et al., 2012). As for how the disease manifests, RA is characterized by inflammatory flares that are separated by periods of little to no disease activity. These flares can last anywhere from a single day to over two weeks, and are characterized by joint swelling, redness, and pain.

Several different organizations have released criteria outlining how RA should be diagnosed. Of these, a joint effort by the American College of Rheumatology (ACR) and the European League Against Rheumatism (EULAR) in 2010 produced the most widely accepted and used set of criteria. According to the ACR, potential RA patients must first be identified by the presence of one or more swollen joints that cannot be explained by another cause or disease (i.e. OA, gout, infection, injury). Next, the patient is assessed for

several different criteria (Table 1.3), which take into account number and type of joints involved, circulating antibodies, acute phase reactants, and disease history. A score of 6 or higher is satisfactory for diagnosing a patient with RA (Aletaha et al., 2010).

Table 1.3 American College of Rheumatology/European League Against Rheumatology - Classification Criteria for the Diagnosis of Rheumatoid Arthritis

Criterion	Score
Joints Involved	
• 1 large joint	0
• 2-10 large joints	1
• 1-3 small joints (with or without large joint involvement)	2
• 4-10 small joints (with or without large joint involvement)	3
• >10 joints (including at least 1 small joint)	5
Serology	
• Negative for RF and ACPA	0
• Low-positive RF *or* ACPA	2
• High-positive RF *or* ACPA	3
Acute-phase reactants (at least 1 test result is needed for classification)	
• Normal CRP *and* normal ESR	0
• Abnormal CRP *or* ESR	1
Duration of symptoms	
• <6 weeks	0
• ≥6 weeks	1

Large joints: shoulders, elbows, hips, knees and ankles. Small joints: metacarpophalangeal joints, proximal interphalangeal joints, second through fifth metatarsophalangeal joints, thumb interphalangeal joint, and wrists. Excluded joints: distal interphalangeal joints, first carpometacarpal joints, and first metatarsophalangeal joints. ACPA, anti-citrullinated protein antibody; CRP, C-reactive protein; ESR, erythrocyte sedimentation rate; RF, rheumatoid factor. (Adapted from Aletaha et al., 2010).

Disease-modifying anti-rheumatic drugs (DMARDs) and biologic therapies have revolutionized outcomes for RA patients. Methotrexate has been used to decrease immune activation since the 1950's, and is still widely used in the clinic today (Favalli et al., 2014). The role of cytokines in RA has been known since the early 1970's, and it has been almost 20 years since Drs. Ravinder Maini and Mark Feldmann began targeting cytokines, specifically TNF-α, with biologics to treat inflammation in RA (Codreanu & Damjanov, 2015). DMARDs have helped millions of patients manage their symptoms; however, unfortunately, these drugs are not effective in all patients, and only maintain satisfactory clinical efficacy in 30% of patients after 2yrs of use (van der Kooij et al., 2007). Furthermore, because of their immunosuppressive effects, DMARDs are associated with adverse events like serious infections, tuberculosis reactivation, and increased rates of skin cancer (Codreanu & Damjanov, 2015). Lastly, DMARDs are outrageously expensive, with the most expensive biologic treatment, infliximab, averaging as much as $20,000 per year (Curtis et al., 2015); therefore, the development of more efficacious, safer, and cost effective drugs for the management of RA is paramount.

1.4 Cannabinoids

One system that has been implicated as a potential target for new arthritis therapies is the endocannabinoid system. The earliest mention of the medicinal use of *Cannabis* can be dated back to the 28th century B.C., where it was reportedly used by the emperor and healer Shen Nung for the treatment of multiple conditions, including rheumatism (Mack, 2001). Medicinal cannabis is again mentioned in the 16th century

B.C., in the Ebers Papyrus, an Egyptian text of herbal medical knowledge. In the Papyrus, *cannabis* is mentioned as a useful remedy for treating the effects of gonorrhoea, as well as pain and inflammation (Dawson, 1934; Zias et al., 1993). Since then, the use of medicinal *cannabis* has fluctuated, being plagued by both legal issues, and public opinion. Currently, research surrounding the medicinal properties of *cannabis,* as well as its active compounds, seems to be at an all time high. In 1964, Mechoulam and Gaoni published a seminal paper, where they isolated and synthesized delta-9 tetrahydrocannabinol (Δ9-THC), a bioactive *cannabis* constituent that is responsible for the majority of the plant's psychotropic effects. Soon after the discovery of Δ9-THC, other *cannabis* compounds were synthesized, some of the most notable being cannabidiol, cannabinol, and cannabigerol. As a family, these *cannabis*-derived molecules were collectively named the cannabinoids. Following their discovery, many scientists began to hypothesize how cannabinoids might exert their biological effects. Given their high lipophilicity, many cannabinoid researchers postulated that these compounds were working by disrupting the cell membrane. It was not until the early 1990's that actual Δ9-THC responsive membrane receptors were discovered, and aptly named cannabinoid receptor type 1 (CB1R) and 2 (CB2R) (Matsuda et al., 1990; Munro et al., 1993). This was followed by the discovery of N-arachidonoylethanolamine (anandamide) (Devane et al., 1992), and 2-arachidonoyl glycerol (2-AG) (Mechoulam et al., 1995), the endogenous cannabinoid (endocannabinoid) ligands of CB1R and CB2R.

1.4.1 The endocannabinoid system

Endocannabinoids, their receptors, and the enzymes responsible for their breakdown, form the endocannabinoid system, which is involved in a plethora of biological functions throughout the mammalian body (Figure 1.5 and 1.6).

1.4.1.1 Endocannabinoid receptors

The cannabinoid receptors are seven-transmembrane domain GPCRs, that are normally paired with an inhibitory G-protein (G_i); therefore, primarily function by decreasing cellular activity. CB1R and CB2R activation decreases adenylate cyclase activity and cyclic adenosine monophosphate (cAMP) production, decreases cation influx, and promotes rectifying K^+ efflux (reviewed Demuth & Molleman, 2006). The main difference between CB1R and CB2R is their localization. CB1R was first identified in the rat brain (Matsuda et al., 1990), and is primarily expressed in neuronal tissues. Conversely, CB2R was first identified on peripheral immune cells, and is primarily localized to the periphery (Munro et al., 1993); however, recent evidence suggests that CB2R is also expressed in the CNS (Onaivi et al., 2006).

The cannabinoid receptors are so named because their first known ligands were plant-derived cannabinoids; however, it is evident that endocannabinoids can also activate several other receptors. TRPV1, the capsaicin and heat sensitive ion channel, is responsive to anandamide (Zygmunt et al., 1999; Smart et al., 2000). One previously orphaned receptor, GPR18, is now known to be activated by anandamide and Δ9-THC (reviewed Alexander, 2012). Another recently deorphanized GPCR is GPR55, which is activated by 2-AG, anandamide, and Δ9-THC (Reviewed Shore & Reggio, 2015). The discovery of non-CB1R/CB2R receptors that are sensitive to

endocannabinoids may help explain some endocannabinoid related effects that previously appeared to be non-receptor mediated.

1.4.1.2 Endocannabinoids

Endocannabinoids are highly lipophilic arachidonic acid derivatives, that are unlike most signalling molecules insofar as anandamide and 2-AG are not stored in vesicles, but rather are synthesized on demand in response to increased intracellular calcium. N-acyl phosphatidylethanolamine phospholipase-D (NAPE-PLD) and diacylglycerol-lipase (DAGL), are the two enzymes responsible for the synthesis of anandamide and 2-AG, respectively (Figure 1.5). Following synthesis, anandamide and 2-AG are secreted by the cell; however, the exact mechanism by which they are released has yet to be characterized.

Once outside the cell anandamide and 2-AG are both capable of activating CB1R and CB2R, with Ki's in the nM range. Depending on the assay used, the pharmacological constants of anandamide and 2-AG have been quite variable, preventing comparisons between studies. As a rule of thumb, anandamide appears to have slightly greater affinity for rodent CB1R (Ki=89+/-10 nM), when compared to CB2R (Ki=371+/-102 nM) (Showalter et al., 1996), as does 2-AG (CB1R Ki=472+/-55 nM; CB2R Ki =1400+/-172 nM) (Mechoulam et al., 1995). Additionally, anandamide is a partial agonist at CB1R and CB2R, while 2-AG is a full agonist at both receptors.

As mentioned in the previous section, in addition to its actions on canonical cannabinoid receptors, anandamide also activates TRPV1 and GPR55. The affinity of anandamide for TRPV1 is quite low, with a Ki of ~2μM (De Petrocellis et al., 2001),

and this is comparable to capsaicin's affinity for the receptor (Ross et al., 2001). The potency of anandamide differs between recombinant and native TRPV1 expressing cells. Anandamide's EC50 can range between 0.7-5.0μM in recombinant cell lines, 0.3-0.8μM in blood vessels, and 6-10μM in sensory neurons and bronchi smooth muscle cells (Ross, 2003). Similarly, the efficacy of anandamide on TRPV1 activation differs tremendously between systems, ranging from 22-100% of capsaicin depending on the cell type (Ross, 2003). Anandamide is capable of stimulating GPR55-meditated increases in intracellular calcium at concentrations in the micromolar range (Lauckner et al., 2008).

1.4.1.3 Endocannabinoid degradation

Following release, the window of opportunity for endocannabinoid activity is limited, as they are taken up quickly by the cell and degraded within minutes in peripheral tissues such as the adrenal gland. The mechanism by which endocannabinoid uptake occurs, resembles facilitated diffusion; however, the transporter(s) involved in this process have yet to be identified. For the time being, the putative transporter has been named the endocannabinoid membrane transporter (EMT). Once inside the cell, anandamide and 2-AG are primarily neutralized by two different hydrolyzing enzymes, but can also be broken down via alternative pathways (Figures 1.6).

1.4.1.3.1 Fatty acid amide hydrolase

Fatty acid amide hydrolase (FAAH) was originally identified as a hydrolytic enzyme, capable of metabolizing the fatty acid amide, oleamide (OEA) (Cravatt et

al., 1996). Soon after, it was discovered that FAAH was responsible for the breakdown of all fatty acid amides, including palmitoylethanolamide (PEA) and anandamide (Thomas et al., 1997). In humans, there are two FAAH enzymes, FAAH-1 and FAAH-2. FAAH-1 is a 65-kDa membrane associated serine hydrolase, encoded by a gene located on chromosome 1 in humans, and chromosome 4 in mice. The FAAH-2 gene is located on the X chromosome in humans; however, neither mice nor rats have a FAAH-2 gene (Wei et al., 2006).

FAAH is the only mammalian expressed member of the larger amidase signature (AS) family, which, given their serine nucleophiles, are part of the larger serine protease family. When hydrolyzed, fatty acid amides produce a free fatty acid and ethanolamine. More specifically, the products of anandamide hydrolysis are arachidonic acid and ethanolamine (McKinney & Cravatt, 2005).

1.4.1.3.1.1 URB597

Probably the most popular FAAH inhibitor used for research purposes is URB597, which has an IC50 of 5nM in rat cortical membranes, and 3nM in human liver microsomes. *In vivo*, rat FAAH is 50% inhibited following systemic administration of 0.15mg/kg (i.p.). Furthermore, URB597 does not appear to have off-target effects on other enzymes or receptors within the endocannabinoid system, nor any cytochrome P450 enzymes. Following oral administration, the half-life of URB597 is approximately 2h; however, because it binds FAAH irreversibly, a 90% reduction in enzyme activity was maintained after 12h, and 60% FAAH inhibition was maintained after 24h (Piomelli et al., 2006). In addition to systemic

administration, URB597 is also capable of modulating articular neuron activity when administered locally to the joint (Schuelert et al., 2011).

1.4.1.3.2 Monoacylglycerol lipase (MAGL)

Monoacylglycerol lipase (MAGL), another serine protease, is responsible for the breakdown of 2-AG. In humans, the gene for this 33kDa membrane bound protein is located on chromosome 3, while the mouse ortholog is located on chromosome 6. MAGL catalyzes the degradation of 2-AG into arachidonic acid and glycerol (Dinh et al., 2002).

1.4.1.3.3 Cyclooxygenase 2 (COX2)

Given the structural similarity of anandamide and 2-AG to arachidonic acid, the endocannabinoids also act as substrates for COX2, which is more commonly known for converting arachidonic acid into PGH2. Endocannabinoid-derived COX2 products are PG derivatives, with anandamide producing PG-ethanolamides (prostamides) and 2-AG producing PG-glycerol esters. Interestingly, although COX1 and COX2 are 77% similar at the amino acid level, with the catalytic regions being even more conserved, there are small, but important, differences between the two enzymes. These differences allow COX2 specificity by certain NSAIDs (Gierse et al., 1996), in addition to making anandamide and 2-AG poor substrates for COX1 (Kozak et al., 2002).

1.4.2 Cannabinoids and disease

Given the widespread expression of the endocannabinoid system, it is no wonder that it has been implicated in a number of different diseases. Changes in cannabinoid receptor expression have been observed in CNS disorders like multiple sclerosis, and Parkinson's, Alzheimer's and Huntington's diseases (reviewed Fagan & Campbell, 2014). Endocannabinoid levels are also altered in a number of peripheral diseases, including myocardial trauma, inflammatory bowel disease, and diabetes (reviewed Maccarrone et al., 2015). Furthermore, in arthritis patients, major changes are observed in the expression of joint endocannabinoid levels, as a result of joint disease (Richardson et al., 2008).

1.4.2.1 Endocannabinoids and arthritis

In the UK, the largest group of medicinal *cannabis* users are those suffering from arthritis and chronic pain, representing 46% of those prescribed (Ware et al., 2005). One common misconception is that the CNS effects of medicinal cannabis are responsible for all of its beneficial effects in treating arthritis pain. Although the 'high' produced by cannabis is the most renowned effect of the drug, the endocannabinoid system is also expressed in arthritic joints, suggesting a possible local mechanism of action. When synovial fluid samples were compared between arthritis patients and healthy controls, it was discovered that anandamide and 2-AG expression was turned on during arthritic conditions. Furthermore, both CB1R and CB2R, as well as FAAH were also expressed in these samples (Richardson et al., 2008).

Although upregulated during arthritis, it would appear that endocannabinoids play a role in decreasing arthritic symptoms. Blocking endocannabinoid breakdown, with the potent and selective FAAH inhibitor URB597, decreased pain behaviours in the kaolin-carrageenan (KC) inflammatory arthritis model (Krustev et al., 2014), and nociceptor firing in both the MIA rat model and a spontaneous guinea pig model of OA (Schuelert et al., 2011). In both studies, these anti-nociceptive effects were mediated through CB1R dependant mechanisms. Furthermore, the synthetic CB1R agonist, arachidonyl-2-chloroethylamide (ACEA), decreased nociceptor firing in experimental OA, while CB1R antagonism exacerbated neuronal nociceptor responses (Schuelert & McDougall, 2008). Although these effects suggest that endocannabinoid signalling is analgesic, anandamide is also capable of increasing nociceptor firing through a TRPV1 dependent mechanism (Gauldie et al., 2001).

Given the expression of CB2R on circulating and resident immune cells, as well as CB1R expression on neuropeptide-containing free nerve endings, the cannabinoid system is also an attractive target for decreasing joint inflammation (Munro et al., 1993; McDougall, 2009). In DRGs, CB1R messenger ribonucleic acid (mRNA) expression is co-localized with CGRP and SP (Hohmann & Herkenham, 1999). Furthermore, anandamide decreases capsaicin-induced CGRP release from free nerve endings (Richardson et al., 1998). Anandamide also decreased plasma extravasation and subsequent oedema in a model of acute inflammatory arthritis (Richardson et al., 1998). The anti-inflammatory effects of CB2R activation are numerous. When leukocytes are treated with the CB2R agonist JWH-015, surface CAM expression is decreased, and leukocyte transmigration is attenuated (Montecucco et al., 2008).

Furthermore, CB2R agonism is also capable of decreasing plasma extravasation *in vivo* (Fukuda et al., 2010).

1.5 Arthritis models

1.5.1 Kaolin-carrageenan inflammatory arthritis

The KC arthritis model is a widely used unilateral model of joint pathology. This model produces a well-defined pattern of inflammation and pain and has been established in primates, cats, and rodents. Kaolin, also known as China clay, is an inorganic substance that is composed of hydrate aluminum silicate ($H_2Al_2Si_2O_8.H_2O$). When injected into the joint as an aqueous suspension, kaolin produces robust mechanical damage to the articular cartilage, resembling that observed in OA. Additionally, kaolin increases carrageenan-induced synovitis by irritating joint tissues. λ-Carrageenan Type IV (carrageenan) is a sulfated polysaccharide derived from Irish moss, and so named after the Irish town Carragheen. Carrageenan produces a robust inflammatory response via TLR4 activation, which leads to the phosphorylation of BCL10, and subsequent nuclear factor kappa-light-chain-enhancer of activated B cells (NF-κB) activation. This chain of events results in increased IL-8 production, which, promotes local inflammation (Bhattacharyya et al., 2008).

KC-induced joint inflammation has a well-defined time course, where signs of inflammation are apparent 1-3h following injection, peak and plateau around 5-6h, and are maintained for several days (Neugebauer et al., 2007). This inflammatory phase is characterized by hyperaemia, oedema and immune cell infiltration (Muirden & Peace, 1969). In addition to inflammation, this model also produces a number of behavioural and neuronal responses that are characteristic of joint pain. Animals show

decreased weight bearing on the inflamed limb, decreased withdrawal thresholds to von Frey hairs (Andruski et al., 2008), increased guarding (Sluka & Westlund, 1993), and pain-induced vocalizations (Han & Neugebauer, 2005). Furthermore, articular afferents and dorsal horn neurons show increased electrical activity following intra-articular injection of KC (Neugebauer & Schaible, 1988). Because of the well-defined and consistent pain and inflammation that this model produces, it is frequently used to test new anti-inflammatory and analgesic compounds.

1.5.2 Saphenous nerve stimulation-induced neurogenic inflammation

In mice, the saphenous nerve innervates the anteromedial portion of the knee, providing the free nerve endings responsible for obtaining nociceptive information, as well as immunomodulatory neuropeptides during neurogenic inflammation (Greene, 1968). By electrostimulating the saphenous nerve at specific parameters, it is possible to induce the release of immunomodulatory neuropeptides from the nerve terminals and promote neurogenic hyperaemia (McDougall et al., 1999), and extravasation (Lembeck et al., 1982).

1.5.3 Sodium monoiodoacetate (MIA) osteoarthritis model

When injected into the joint, MIA causes cartilage damage resembling that observed in OA, as well as nociceptive behaviours. This model is widely used because of the quick and consistent symptoms that arise ~14d after injection (Kobayashi et al., 2003). MIA inhibits glyceraldehyde-3-phosphate dehydrogenase (GAPDH), which is the enzyme responsible for the conversion of glyceraldehyde-3-phosphate to D-glycerate 1,3,-biphosphate (Foxall et al., 1984). This process is the

sixth step in the glycolysis chain, and, therefore, GAPDH inhibition attenuates the production of adenosine triphosphate (ATP). When injected into the knee, MIA is taken up articular chondrocytes, preventing their ability to produce energy and effectively killing these cells. Chondrocyte death results in thinning of the cartilage, joint space narrowing, and eventual bone fracturing and spurring (Kobayashi et al., 2003). These structural changes produce joint pain, which has nociceptive, inflammatory and neuropathic components (reviewed Zhang et al., 2013).

1.6 Measuring joint inflammation and pain

1.6.1 Inflammation

1.6.1.1 Knee joint diameter

Oedema is a characteristic sign of inflammation, and is especially evident in experimental models of knee joint inflammation. One method that is used to assess knee joint swelling is measuring the distance between the medial and lateral femoral condyles. This method is primarily used to assess proper induction of joint inflammation in models of arthritis. One limitation of this technique is that knee diameter is affected by local drug administrations, as local treatments are usually injected as a bolus, either subcutaneous (s.c.) atop the knee, or into the joint space. The volume of the bolus increases joint diameter, making this a poor method for assessing the anti-inflammatory effects of localized treatments shortly after administration. Furthermore, this technique has poor inter-experimenter reproducibility and is fairly subjective, especially when assessing the small knee joints of mice.

1.6.1.2 Leukocyte-endothelial interactions

The leukocyte recruitment cascade is activated by inflammation; therefore, increased leukocyte rolling and adherence within the synovial microcirculation is indicative of articular inflammation. Using intravital microscopy (IVM), we can visualize the microcirculation of the joint, and assess the number of rolling and adherent leukocytes. Circulating leukocytes are fluorescently labelled with rhodamine 6G (R6G), which accumulates within the mitochondria of these white blood cells (Gear, 1974; Baatz et al., 1995;). The spectral absorption of R6G ranges between 440 and 570nm, and peaks at 530nm (Brackmann, 1986). Furthermore, when excited, R6G emits light between 550 and 620nm, depending on the solvent used and the concentration of the solution (Zehentbauer et al., 2014).

When passing through areas of inflammation, leukocytes will interact with the vascular endothelium of post-capillary venules. These interactions promote leukocyte rolling, which is when leukocytes begin moving slower than the normal flow of blood, and adherence, which is when leukocytes firmly adhere to the venule wall and stop moving. Both of these steps are important, as they precede leukocyte extravasation. Using IVM, we are able to visualize leukocyte-endothelial interactions within the microcirculation of the knee joint *in vivo*. By quantifying the number of R6G-stained leukocytes that are rolling and adherent, we can assess the degree of joint inflammation. Furthermore, by measuring leukocyte rolling and adherence, before and after drug treatment, we can quantify the effects of our compounds on leukocyte-recruitment and joint inflammation. In terms of inflammation, leukocyte

adherence is considered a more robust measure of inflammation when compared to rolling, as it is the step that directly precedes extravasation.

1.6.1.3 Articular blood flow

Hyperaemia is another characteristic sign of joint inflammation, and measuring changes in blood flow between naïve and arthritic knee joints, as well as between drug treatments, provides another measure of the degree of inflammation. Laser speckle contrast analysis (LASCA) is a useful technique that allows the assessment of local fluid dynamics, which, in tissues, is primarily local blood flow.

When a beam of monochromatic light (laser) hits tissue, some of the light is absorbed, some is transmitted to deeper tissues, and some is reflected back, as scattered light, towards the source. As a result of scattering, the reflected light produces a speckle pattern, with alternating points of low and high light intensity. Stationary surfaces produce maximal scattering, which results in maximal speckle contrast (i.e. large intensity differences between light and dark points). Conversely, when the surface is moving, the scattering of reflected light is blurred, which results in a reduction in speckle contrast (i.e. little to no difference between light and dark points). The LASCA apparatus has a sensor that recognizes differences in speckle contrast, and calculates an arbitrary measure of surface movement that is inversely proportional to speckle contrast. When visualizing tissues *in vivo*, the moving surface is flowing blood, and therefore the units have been termed Perfusion Units (Boas & Dunn, 2010).

1.6.2 Pain

1.6.2.1 Hindlimb weight bearing

Spontaneous pain is characteristic of many inflammatory diseases (Griffioen et al., 2015); therefore, measuring non-evoked painful behaviours in animal models is essential in understanding this clinically relevant phenomenon. One technique used to measure spontaneous arthritis pain is hindlimb incapacitance, in which the difference in weight bearing between both hindlimbs is assessed (Griffioen et al., 2015). Normally, rodents distribute their weight equally between both hindlimbs; however, following induction of unilateral knee joint inflammation, rodents tend to favour the non-inflamed hindlimb. This shift in weight bearing can be measured in stationary animals (static weight bearing; SWB), as well as free moving animals (dynamic weight bearing; DWB). SWB requires that the animal rear on both hindlimbs while standing on two force plates, one under each hindpaw. On the other hand, when measuring DWB, the animal is placed in a chamber with pressure sensitive flooring, which allows weight bearing to be assessed at any point on the sensor, both when the animal is stationary and during movement. In both techniques, the weight borne by each hindlimb is measured, and the difference between the two is calculated. Hindlimb incapacitance measurements are useful in testing weight bearing changes in models of inflammatory arthritis, osteoarthritis, neuropathic pain, and bone cancer, as reductions in hindlimb weight bearing have been observed in all of these models (Tétreault et al., 2011).

1.6.2.2 Von Frey hair tactile sensitivity

Joint inflammation and neuropathy can alter the neuronal architecture of a joint's nociceptive pathway. These changes can occur along the peripheral nerves, spinal cord, or even within the brain, and result in neuropathic pain. In the periphery, inflammation and neuronal damage can result in changes to voltage-gated cation channels (Luo et al., 2001), and adrenergic receptor expression (Birder & Perl, 1999), increasing their propensity to fire and responsiveness to sympathetic tone, respectively. Furthermore, changes within the CNS have also been attributed to heightened von Frey hair sensitivity following induction of arthritis. Central sensitization can result from altered pain processing in the spinal cord (Menétrey & Besson, 1982) and brain (Staud et al., 2007), insufficient descending inhibitory signals (Vaccarino & Chorney, 1994), excessive descending facilitatory signals (Urban et al., 1996), or changes in synaptic plasticity in the anterior cingulate cortex (Zhuo, 2007), and all can contribute to pro-nociceptive neuronal activity. One method that is used to test peripheral and central sensitization is von Frey hair algesiometry. Von Frey hairs are thin filaments that were developed by Maximilian von Frey for testing algesia. Von Frey hairs come as a set, and increase in thickness as well as bending force. Normally, mice show little to no response when stimulated with a range of von Frey hairs applied to the planter surface of the hindpaw; however, following arthritic induction, mice become hypersensitive to von Frey stimuli. This is the result of changes along the shared pain pathway of the knee and hindpaw, and provides a measure of allodynia and referred pain.

1.7 Objectives and hypotheses

This project had two main objectives: 1) to explore the effects of endocannabinoid modulation on experimental knee joint arthritis, and 2) to identify the contribution of neurogenic mechanisms to joint inflammation. Within each of these main objectives there were several sub-objectives, which will be described in greater detail within the corresponding chapters.

We hypothesized that decreasing endocannabinoid breakdown, using the potent and selective FAAH inhibitor URB597, would decrease joint inflammation, as well as attenuate the development of joint pain. Furthermore, we hypothesized that neurogenic mechanisms would play a pro-inflammatory role in joint inflammation.

1.8 Figures

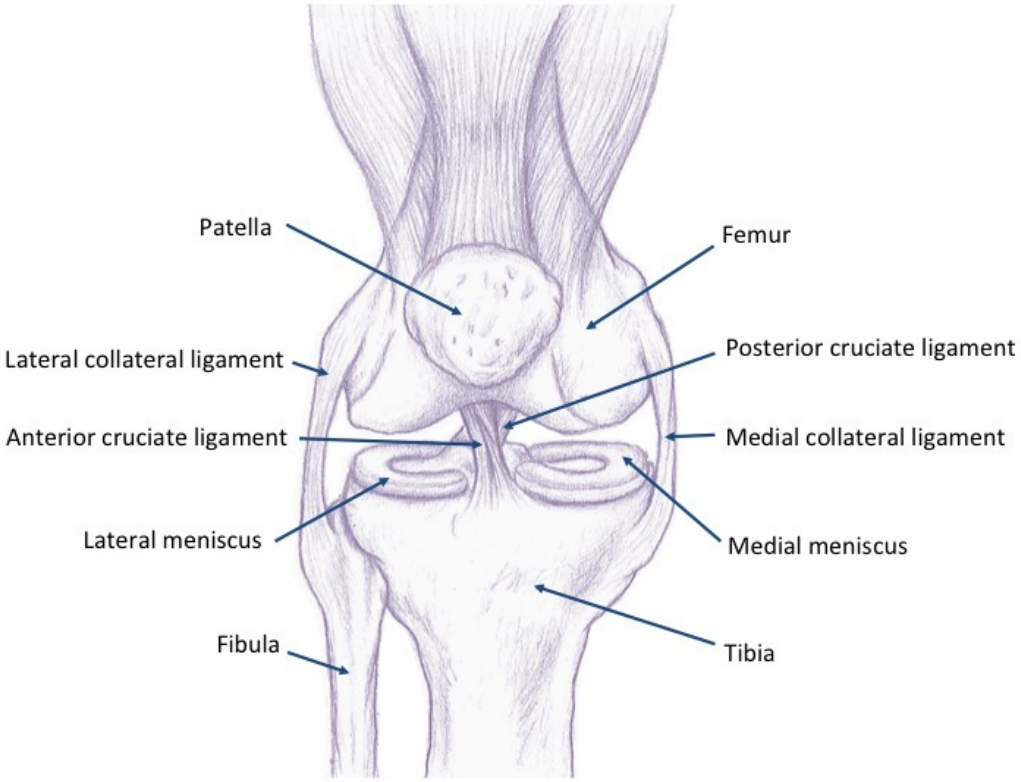

Figure 1.1 Anatomy of the human knee joint. (Artwork by Bridget Higgins).

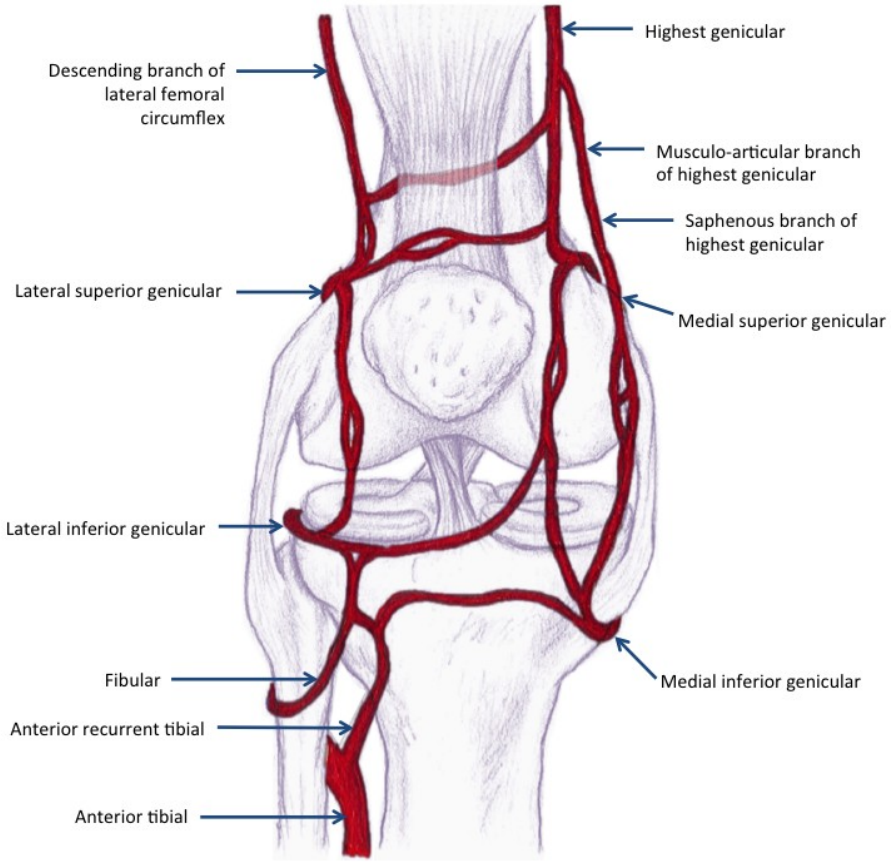

Figure 1.2 Vasculature of the human knee joint. (Artwork by Bridget Higgins).

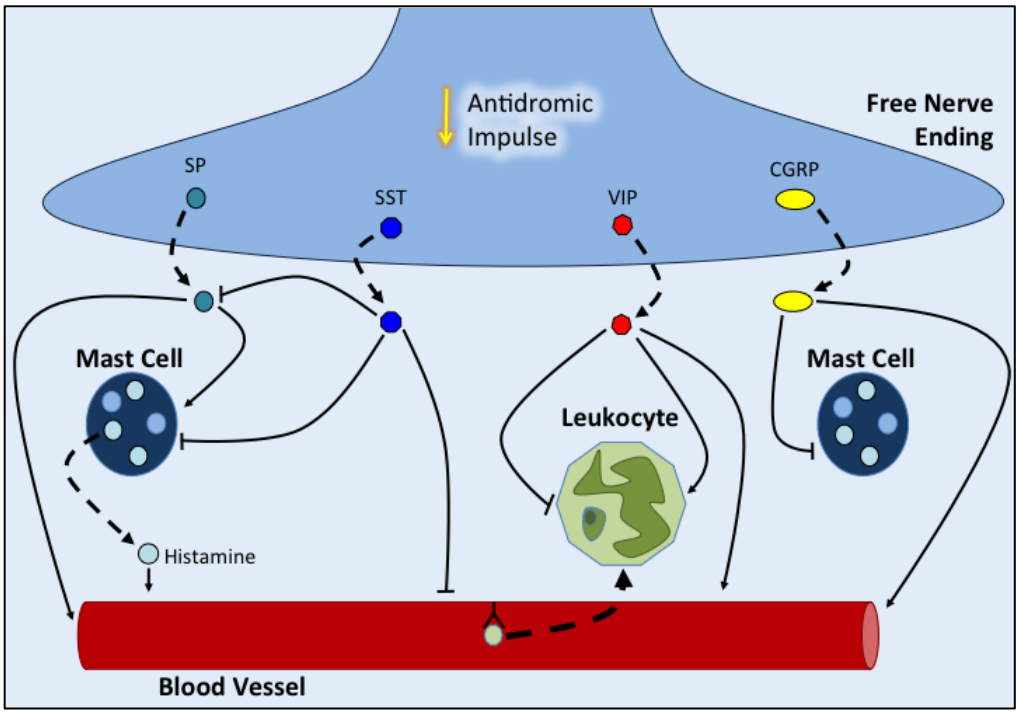

Figure 1.3 Mediators of neurogenic inflammation. SP is capable of acting directly on the vasculature, as well as resident mast cells. When acting on the vasculature, SP induces vasodilation, as well as increases the expression of endothelial CAMs, which promote leukocyte recruitment. Furthermore, SP activity on mast cells induces the release of histamine, as well as other pro-inflammatory molecules. SST acts primarily as an anti-inflammatory mediator, and inhibits many of the actions of SP, as well as decreases activation of vascular endothelial cells. VIP has been shown to have both pro-inflammatory and anti-inflammatory activity. VIP activates and inhibits leukocytes, depending on the context. Furthermore, VIP is also capable of causing vasodilation *in vivo*. CGRP can inhibit the release of pro-inflammatory molecules from mast cells, as well as increase inflammatory vascular responses, promoting leukocyte recruitment and vasodilation. (See Section 1.2.1.2.2.2). CGRP, calcitonin gene related peptide; SST, somatostatin; SP, substance P; VIP, vasoactive intestinal peptide.

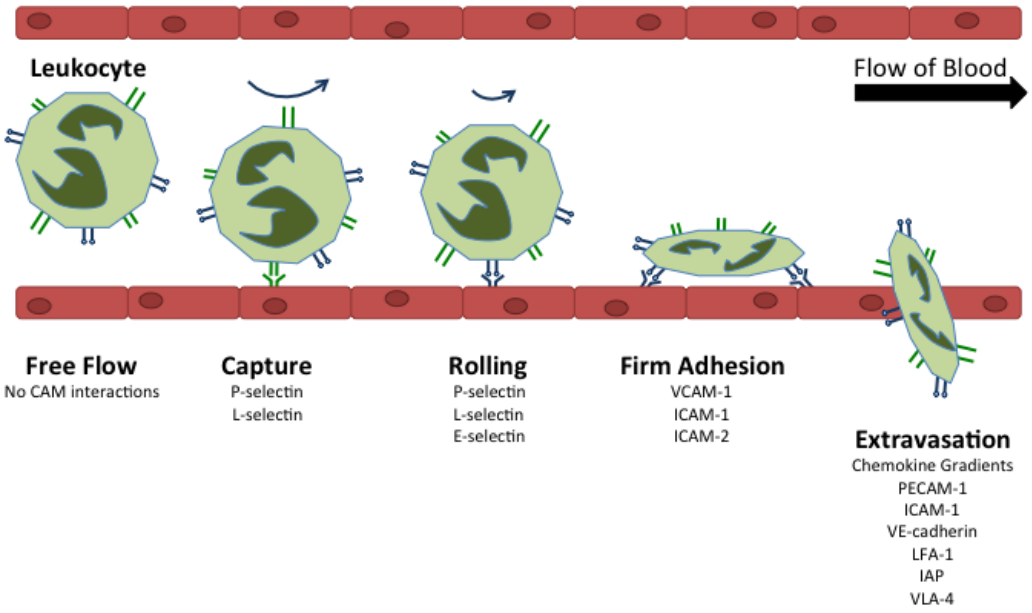

Figure 1.4 Leukocyte extravasation cascade and the CAMs involved in each step.

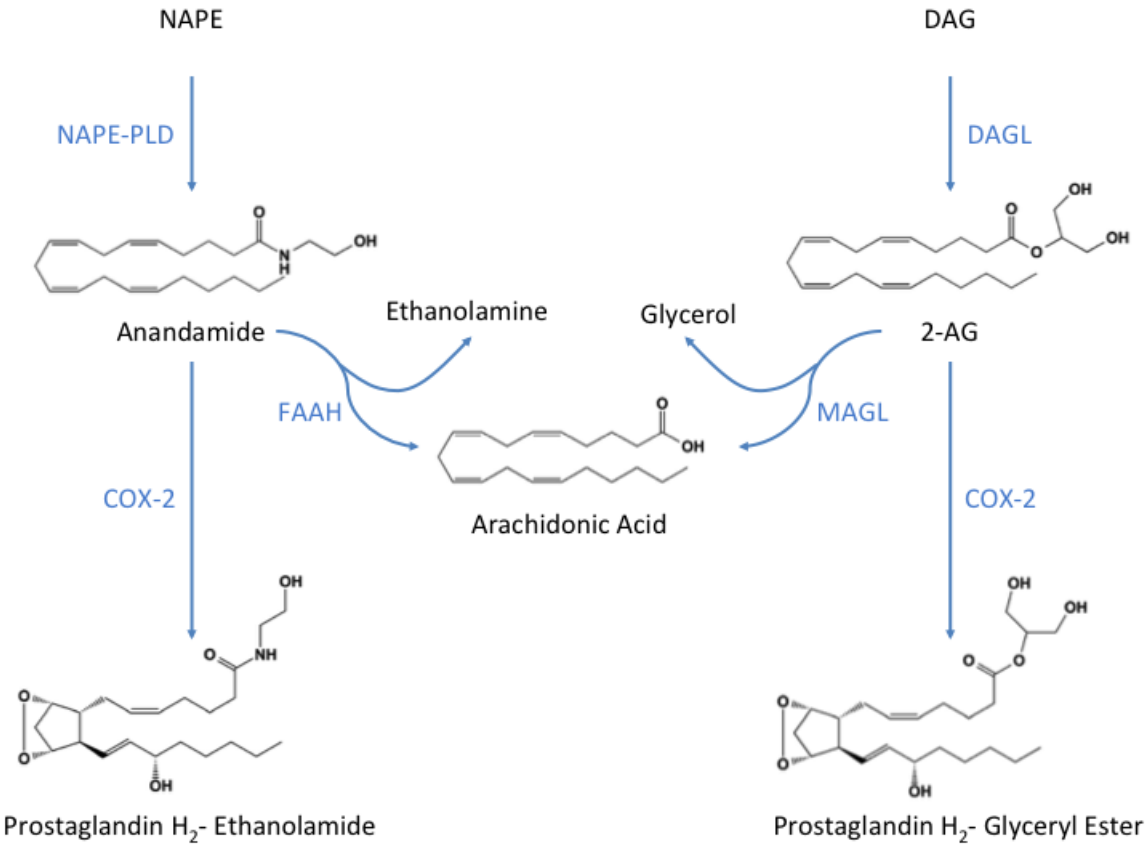

Figure 1.5 Endocannabinoid synthesis and degradation. 2-AG, 2-arachidonoylglycerol; COX-2, cyclooxygenase 2; DAGL, diacylglycerol lipase; FAAH, fatty acid amide hydrolase; MAGL, monoacylglycerol lipase; NAPE, N-acyl-phosphatidylethanolamine; NAPE-PLD, NAPE phospholipase D.

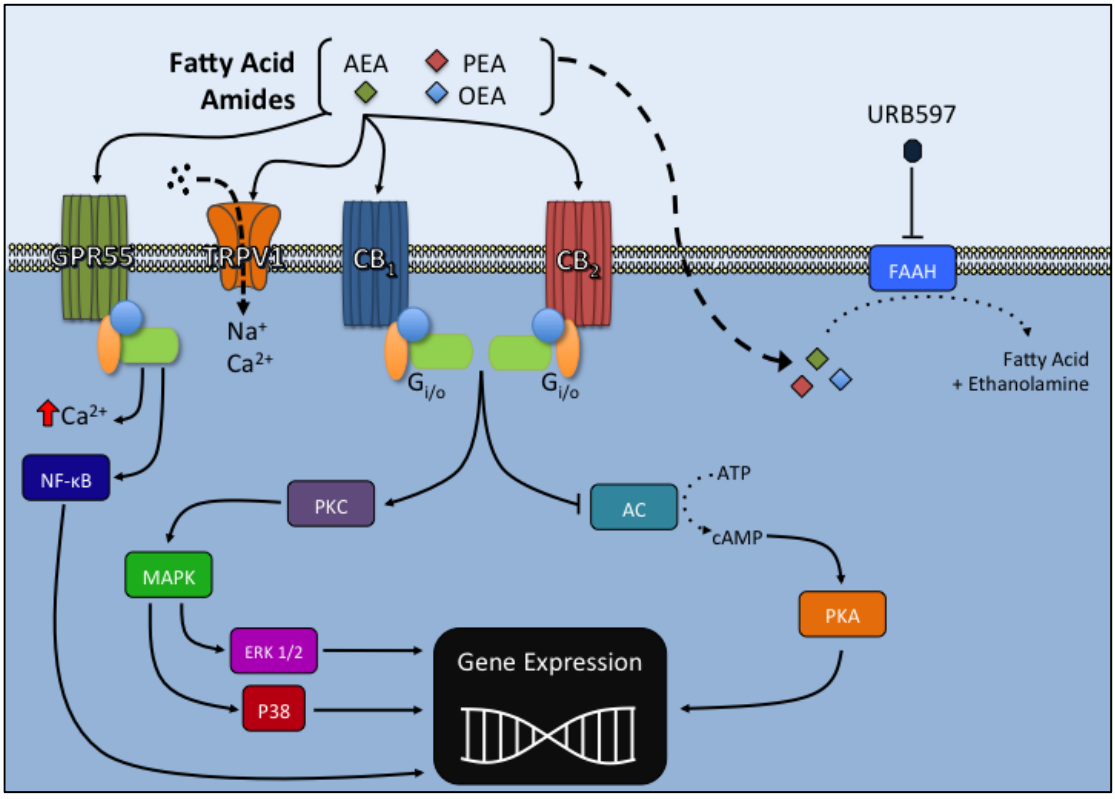

Figure 1.6 Fatty acid amide pharmacology, showing the main receptors activated and intracellular signalling cascades. AC, adenylate cyclase; AEA, anandamide; ATP, adenosine triphosphate; CB1, cannabinoid receptor type 1; CB2, cannabinoid receptor type 2; ERK 1/2, extracellular signal-regulated kinases 1/2; FAAH, fatty acid amide hydrolase; MAPK, mitogen activate protein kinase; NF-kB, nuclear factor kappa-light-chain-enhancer of activate B cells; OEA, oleoylethanolamide; PEA, palmitoylethanolamide; PKA, protein kinase A; PKC, protein kinase C.

Chapter 2: Methods and Materials

2.1 Animals

All experimental protocols were approved by the Dalhousie University Committee on Laboratory Animals, which acts in accordance with the standards put forth by the Canadian Council for Animal Care. Protocols Numbers: 12-041 and 14-056.

C57BL/6 mice (6-12 weeks; 20-42g; Charles River, Quebec, Canada) were housed in ventilated racks at 22 ± 2°C on a 12:12hr light:dark cycle (light-on from 7:00-19:00) in the Carleton Animal Care Facility, Faculty of Medicine, Dalhousie University, Halifax, Nova Scotia, Canada. Following arrival at the facility, all animals were allowed at least 1wk to acclimatise to their new environment. Cages were lined with woodchip bedding and animals were provided with environmental enrichment. Standard lab chow and water were provided *ad libitum*.

2.2 Arthritis models

2.2.1 Kaolin-carrageenan monoarthritis

For experiments involving KC-induced joint inflammation, animals were deeply anaesthetized (2-4% isoflurane; 100% oxygen at 1L/min) and an acceptable plane of anaesthesia was confirmed by failure to produce a hindpaw withdrawal reflex. The right knee was shaved and knee joint diameter was assed by measuring the distance between both femoral condyles using a digital micrometer (VWR, Friendswood, Texas, USA). The knee area was then swabbed with 100% ethanol, allowed to dry, and 10µl of kaolin (2% in saline) was injected into the intra-articular space. The knee

was then manually extended and flexed for 10min to disperse the kaolin throughout the joint and irritate the synovium. Next, 10μl of carrageenan (2% in saline) was injected in the same manner, and followed by 30s of hindlimb flexion and extension. Animals were returned to their cages for 24hr, after which inflammation was assessed.

2.2.2 Saphenous nerve stimulation

Animals were deeply anesthetised with urethane (25%; 0.25 - 0.40ml), and a surgical plane of anaesthesia was confirmed by failure to elicit a hindpaw withdrawal reflex. The animals were then prepped for vascular assessment (described in detail below), after which a longitudinal incision (1cm) was made perpendicular to the inguinal-femoral border using surgical scissors, and both flaps of skin were separated with forceps. The underlying muscle was blunt dissected to expose the saphenous nerve, which was isolated using watchmaker forceps. A small piece (<3cm) of moistened (saline, 0.9%) thread was placed under the nerve, and any remaining connective tissue was dissected away using watchmaker forceps. The thread was then tied into a knot near the most proximal end of the exposed portion of the nerve. The nerve was then cut proximal to the knot, and the distal section of the nerve was placed over a pair of silver wire electrodes (Figure 2.1), then covered with mineral oil to prevent nerve desiccation.

An electric pulse generator (CD9 Stimulator, Grass Technologies, Warwick, Rhode Island, USA) was used to electrostimulate the saphenous nerve. Voltage (10V) and pulse width (1ms) were fixed, as these parameters were shown to be effective in previous studies (Escott & Brain, 1993; Zeller et al., 2008). A range of frequencies

(0.5, 1.0, 2.0, and 5.0Hz) were tested, with 2 and 5min stimulation periods, in order to identify the ideal parameters for inducing synovial leukocyte-endothelial interactions. Based on our frequency response profile, 2Hz stimulation for 5min was chosen as the optimal protocol for eliciting neurogenic leukocyte-rolling; therefore, all following experiments used the parameters:

Voltage	Pulse Frequency	Pulse Width	Duration
10V	2Hz	1ms	5min

2.2.3 Sodium monoiodoacetate osteoarthritis

Animals were deeply anaesthetized (2-4% isoflurane; 100% oxygen at 1L/min) and an acceptable plane of anaesthesia was confirmed by failure to produce a hindpaw withdrawal reflex. The right knee was shaved and the distance between both femoral condyles was measured using a digital micrometer (VWR, Friendswood, Texas, USA). The knee area was then swabbed with 100% ethanol, allowed to dry, and 10µl of MIA (0.3mg in saline) was injected into the synovial space of the right knee joint. The knee was then manually extended and flexed for 30s to disperse the solution throughout the joint. Animals were returned to their cages and allowed at least 24hr to recover. In separate groups of animals, inflammation was assessed on day 1, and pain was assessed on day 14.

2.3 Measuring inflammation and pain

2.3.1 Knee joint diameter

Joint swelling was assessed by measuring the change in joint diameter, along the transverse plane of the knee, between both femoral condyles using a digital

micrometer (VWR, Friendswood, Texas, USA). These measures were used to confirm positive induction of inflammation, but not to test the effects of drugs on inflammation. Measures were taken before and 24hrs after injection of either KC or MIA.

2.3.2 Synovial vascular assessment

2.3.2.1 Surgical preparation

The following preparation was conducted before IVM and LASCA of the inflamed knee vasculature. Animals were anaesthetised with urethane (25% in saline; 0.25 - 0.4ml i.p.) and a surgical plane of anaesthesia was confirmed by failure to elicit a hindpaw withdrawal reflex. A longitudinal incision was made in the skin of the neck to expose the trachea, left carotid artery and left jugular vein, which were individually cannulated to provide a clear airway, mean arterial pressure (MAP) monitoring, and intravenous (i.v.) access, respectively (the jugular vein was not cannulated if the animal was not undergoing IVM). PE-60 tubing was used for the tracheal cannulation, while PE-10 tubing, filled with heparinized saline (1U/ml), was used for the blood vessel cannulations. The capsular microcirculation of the right knee was exposed by surgically removing a small ellipse of overlying skin (<1cm long; <0.5cm wide), and the knee was immobilized. Physiological buffer (37^{o}C) was immediately and continuously perfused over the exposed joint.

2.3.2.2 Intravital microscopy

IVM was used to assess leukocyte trafficking within the microcirculation of the knee joint, as previously described (Andruski et al., 2008). After surgical preparation,

the synovial microcirculation was visualized under incident fluorescent light using one of three intravital microscopes:

I. Leica DM2500 microscope with a HCX APO L 20X objective and an HC Plan 10X eyepiece (Leica Microsystems Inc., Ontario, Canada; final magnification 200X), with a BC-71 AVT camera (Horn Imaging, Aalen, Germany).

II. Leica DM5000B with an N-Plan 20x objective and an HC Plan 10x eyepiece (Leica Microsystems Inc., Ontario, Canada; final magnification 200X), and a Hamamatsu EM-CCD camera (Hamamatsu Phototonics, Hamamatsu City, Japan).

III. Leica DM2500 microscope with a HCX APO L 20X objective and an HC Plan 10X eyepiece, and a Leica DFC 3000 camera (Leica Microsystems Inc., Ontario, Canada; final magnification 200X).

Three different microscopes were used because experiments were begun using the microscope in the neighbouring lab of Dr. Christian Lehmann, continued on one borrowed from Dr. Brent Johnson, and finished on a newly-purchased one of our own. *In vivo* leukocyte staining was achieved by i.v. administration of R6G (0.05%; 0.05ml; saline). Straight, unbranched, postcapillary venules (15-50μm in diameter) overlying the knee capsule were selected for visualization. Videos (1min duration) of leukocyte kinetics were captured using the attached camera.

Two measures of leukocyte-endothelial interactions were used to assess inflammation: [i] number of rolling leukocytes and [ii] number of adherent leukocytes per 50 or 100μm of vessel length. Two different lengths of vessel were used because, after switching microscopes, the field of view was larger, allowing visualization of a larger portion of vessel; therefore, for increased precision, we began analyzing a

larger section of vessel in our latter studies. Rolling leukocytes are defined here as R6G-stained cells travelling slower than the surrounding flow of blood in the vessel of interest. The rolling leukocyte measure was obtained by counting the number of rolling leukocytes per minute to pass an arbitrary line perpendicular to the vessel of interest. Adherent leukocytes were defined as R6G-stained cells that remained stationary for a minimum of 30s. Total leukocyte adhesion was quantified by counting the number of adherent cells within a defined portion of the vessel (50 or 100μm).

2.3.2.3 Laser speckle contrast analysis

After surgical preparation, synovial vascular perfusion was assessed using a PeriCam PSI System (Perimed Inc., Ardmore, PA). Recordings of the exposed knee joint were taken at a working distance of 10cm with a frame rate of 25 images per second, which were then averaged to create 1 perfusion image per second using the provided software (PIMSoft, Version 1.5.4.8078). A 1min LASCA recording was taken of the entire hindlimb at each time point of interest; however, during data analysis only vascular perfusion within the knee joint area was analyzed. Furthermore, after euthanizing the animal a dead scan of the knee was taken *post-mortem* and this value was subtracted from all measurements to account for any optical noise in the tissue.

2.3.3 Hindlimb incapacitance

Non-evoked joint pain was assessed by measuring differences in hindlimb weight bearing using a Dynamic Weight Bearing System (Bioseb, Vitrolles, France).

Mice were placed in a Plexiglas chamber (11.5cm long x 11.5cm wide x 20cm tall) with pressure sensor flooring (Bioseb DWB Mouse Sensor Pad). The animals were allowed to move freely around the chamber for 5min, during which a video was recorded using a ImagingSource DFK22AUC03 camera (ImagingSource, Charlotte, NC, USA), and weight bearing was continuously measured using the provided software (Bioseb Version 1.4.2.92). Hindlimb weight distribution was calculated and presented as the amount of weight borne by the ipsilateral hindlimb as a percentage of total weight borne by both hindlimbs. Weight-bearing was assessed 14 days after MIA injection.

2.3.4 Von Frey hair mechanosensitivity

Following incapacitance testing, the same animals underwent secondary allodynia testing as a behavioural measure of referred pain. Animals were placed in elevated Plexiglas chambers (30cm long x 9cm wide x 24cm tall) on metal mesh flooring, allowing access to the paws. After allowing the animal to acclimate until exploratory behaviour ceased, ipsilateral hindpaw mechanosensitivity was assessed by plantar application of von Frey hair filaments using a modification of the Dixon up-down method (Chaplan et al., 1994). A von Frey hair was applied perpendicular to the plantar surface of the hind paw (avoiding the toe pads) until it just bent, and then was held in place for 3 seconds. If there was a positive response (i.e. withdrawal, shake or lick of the hindpaw), the next lower strength hair was applied; if there was no response, the next higher strength hair was applied up to a maximum cut off level which corresponded to 4 grams of bending force. After the first difference in response was observed, four more measurements were made and the pattern of

responses was converted to a 50% withdrawal threshold calculated using the following formula: $10^{[Xf+k\delta]}/10{,}000$; where *Xf* = value (in log units) of the final von Frey hair used, *k* = tabular value for the pattern of the last 6 positive/negative responses, and δ = mean difference (in log units) between stimuli.

2.4 Materials

2.4.1 Drugs and reagents

Solutions of URB597 (0.27-27.0mM), AM251 (0.11mM), AM630 (0.12mM), RP67580 (0.2mM), and O-1918 (0.17mM) were prepared in DMSO: cremophor: saline vehicle (1:1:8) on day of use. Solutions of SP (1μM), CGRP (10μM), VIP (10μM), $CGRP_{8-37}$ (0.32 or 0.64mM), VIP_{6-28} (10μM), and SB366791 (8.6M) were prepared in saline. Rhodamine 6G (0.05%) was dissolved in saline and stored in the dark at 4°C. Physiological buffered saline (135mM NaCl, 20mM NaHCO3, 5mM KCl, 1mM MgSO4*7H2O, pH = 7.4) was prepared in house. Solutions of carrageenan (2%) and kaolin (2%) were dissolved in saline and stored at 4°C. MIA was dissolved in saline (0.3mg/10μl) on day of use.

Table 2.1 List of Reagents

Reagent	Description	Source
Carrageenan	• Sulphated polysaccharide • Inflammation inducer	Sigma Aldrich (St. Louis, Missouri, USA)
Cremophor	• Emulsifying solvent	Sigma Aldrich (St. Louis, Missouri, USA)
Dimethyl sulfoxide (DMSO)	• Polar aprotic solvent	Sigma Aldrich (St. Louis, Missouri, USA)
Kaolin	• Inorganic solid • Intra-articular irritant	Sigma Aldrich (St. Louis, Missouri, USA)
Rhodamine 6G	• Mitochondria binding fluorophore	Sigma Aldrich (St. Louis, Missouri, USA)
Sodium monoiodoacetate (MIA)	• GAPDH inhibitor • OA model inducer	Sigma Aldrich (St. Louis, Missouri, USA)

Table 2.2 List of Drugs

Drug	Description	Source
AM251	• CB1R receptor antagonist • 1-(2,4-dichlorophenyl)-5-(4-iodophenyl)-4-methyl-N-piperidin-1-ylpyrazole-3-carboxamide	Cayman Chemical (Ann Arbor, Michigan, USA)
AM630	• CB2R antagonist • 6-iodo-2-methyl-1-(2-morpholin-4-ylethyl)indol-3-yl]-(4-methoxyphenyl)methanone	Cayman Chemical (Ann Arbor, Michigan, USA)
Calcitonin gene related peptide (CGRP)	• Neuropeptide	Sigma Aldrich (St. Louis, Missouri, USA)
$CGRP_{8-37}$	• CGRP fragment/antagonist	California Peptide Research Inc. (Napa, California, USA)
O-1918	• GPR55 antagonist • 1,3-dimethoxy-5-methyl-2-[(1R,6R)-3-methyl-6-prop-1-en-2-ylcyclohex-2-en-1-yl]benzene	Tocris Bioscience (Bristol, United Kingdom)
RP67580	• NK1 (Substance P receptor) antagonist • 2-[1-imino-2-(2-methoxyphenyl)ethyl]-7,7-diphenyl-4-perhydroisoindolone (3aR, 7aR)	Tocris Bioscience (Bristol, United Kingdom)
SB366791	• TRPV1 antagonist • N-(3-methoxyphenyl)-4-chlorocinnamide	Sigma Aldrich (St. Louis, Missouri, USA)
Substance P	• Neuropeptide	Sigma Aldrich (St. Louis, Missouri, USA)
URB597	• FAAH inhibitor • [3-(3-carbamoylphenyl)phenyl] N-cyclohexylcarbamate	Cayman Chemical (Ann Arbor, Michigan, USA)
Urethane	• Anaesthetic • Ethyl carbamate	Sigma Aldrich (St. Louis, Missouri, USA)
Vasoactive intestinal peptide (VIP)	• Neuropeptide	Sigma Aldrich (St. Louis, Missouri, USA)
VIP_{6-28}	• VIP fragment/antagonist	California Peptide Research Inc. (Napa, California, USA)

2.4.2 Equipment

Table 2.3 Equipment List

Device	Model	Manufacturer
Blood Pressure Monitor	BP-1	World Precision Instruments (Sarasota, Florida, USA)
Temperature Control Monitor and Heating Pad	TC1000	CWE, Inc. (Ardmore, Pennsylvania, USA)
Electric Pulse Generator	SD9 Stimulator	Grass Technologies (Warwick, Rhode Island, USA)
Dissecting Microscope	SZ40	Olympus Canada Inc. Richmond Hill, Ontario, Canada
Microprocessor Controlled Waterbath	280 Series	Precision (Winchester, Virginia, USA)
Digital Weigh Scale	CP2202 S	Sartorius (Bohemia, New York, USA)
Digital Micrometer	62379-531	VWR (Friendswood, Texas, USA)
Micropipettes	20, 100 and 200µl	Eppendorf Research (Mississauga, Ontario, Canada)
Digital Balance	AL54	Mettler Toledo (Mississauga, Ontario, Canada)
Blood Perfusion Imager	PeriCam PSI *Normal Resolution* with PimSoft Software	Perimed Inc., (Ardmore, Pennsylvania, USA)
Advanced Dynamic Weight Bearing System	BIO-DWB-AUTO-M - For mice with DFK22AUC03 camera	DWB - Bioseb, (Vitrolles, France) Camera - ImagingSource, (Charlotte, North Carolina, USA)
Von Frey Hairs	Semmes Weinstein Microfilaments	North Coast Medical, (Gilroy, California, USA)

Table 2.4 Equipment List Continued		
Device	**Model**	**Manufacturer**
Intravital Microscope #1	Leica DM2500 microscope with a HCX APO L 20X objective and an HC Plan 10X eyepiece (final magnification 200X), with a BC-71 AVT camera	Microscope - Leica Microsystems Inc. (Concord, Ontario, Canada) Camera - Horn Imaging (Aalen, Germany)
Intravital Microscope #2	Leica DM5000B with an N-Plan 20x objective and an HC Plan 10x eyepiece (final magnification 200X), and a Hamamatsu EM-CCD camera	Microscope - Leica Microsystems Inc. (Concord, Ontario, Canada) Camera - Hamamatsu Phototonics (Hamamatsu City, Japan)
Intravital Microscope #3	Leica DM2500 microscope with a HCX APO L 20X objective and an HC Plan 10X eyepiece, and a Leica DFC 3000 camera (final magnification 200X).	Leica Microsystems Inc. (Concord, Ontario, Canada)

2.5 Statistical analyses and data presentation

All data were tested for normality using the Kolmogrov-Smirnov normality test. For each comparison, if all groups passed the normality test, then the appropriate parametric statistical test was used. If one or more groups were not normally distributed, then the appropriate non-parametric statistical test was used. Specific statistical analyses differed between each study, and are mentioned in the corresponding figure legend. All analyses were performed, and all graphs were generated, using Prism 6.0 by GraphPad (La Jolla, California, USA). A $P<0.05$ was considered statistically significant. For each comparison, n is equal to the number of

animal subjects in a each experimental group. All data are presented as the mean ± the standard error of the mean (SEM).

2.6 Figures

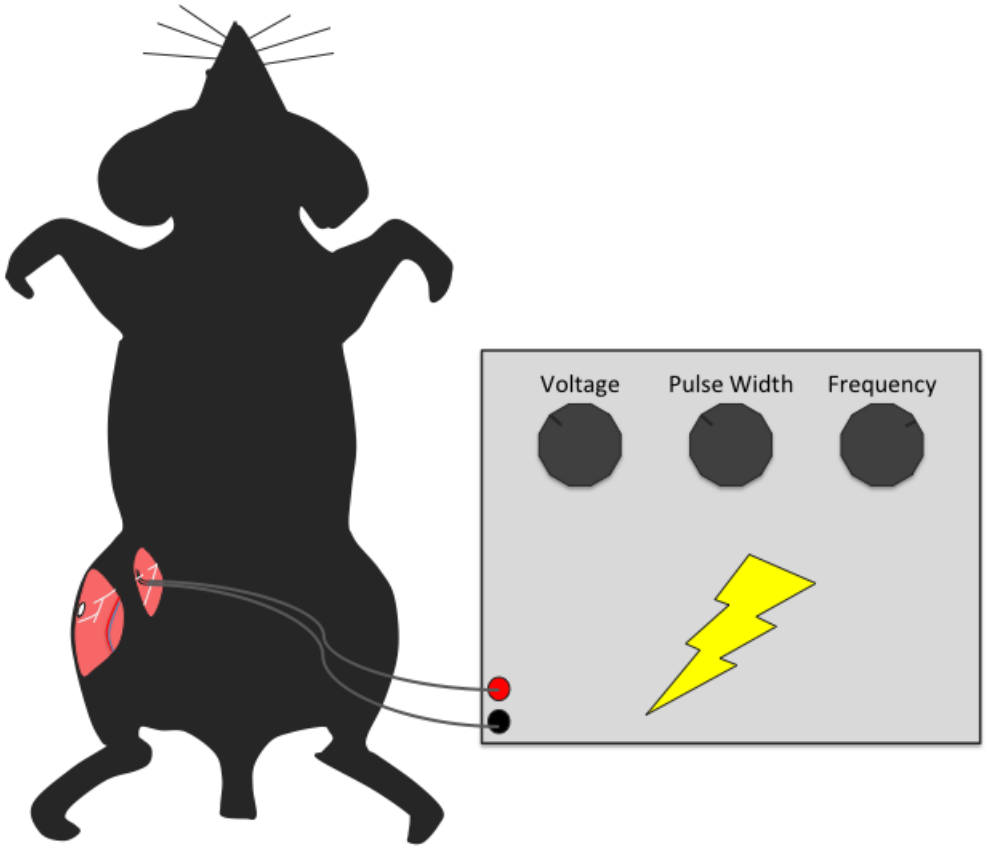

Figure 2.1 Visual representation of saphenous stimulation surgery and electrode placement.

Chapter 3: The Effects of FAAH Inhibition on Kaolin-Carrageenan-Induced Joint Inflammation

3.1 Background and hypotheses

Arthritis is a leading cause of disability worldwide, yet current therapies have sub-optimal safety and efficacy, such that the development of new, safer and more effective therapeutics is of the upmost importance. One family of molecules that have gained significant attention for their ability to decrease arthritic symptoms are the cannabinoids. The plant-derived cannabinoid Δ9-THC is capable of attenuating the development of experimental autoimmune arthritis (Sofia et al., 1973), and is anti-nociceptive in arthritic rats (Cox & Welch, 2004). Although cannabinoids were first discovered in plants, the mammalian body can also produce endocannabinoid molecules. These endocannabinoids are capable of exerting anti-arthritic effects, and inhibit the development of collagen-induced joint inflammation and pain (Kinsey et al., 2011). Furthermore, the knee joint possesses an elaborate endocannabinoid system. Both normal and diseased human knees express CB1Rs and CB2Rs, as well as FAAH; however, anandamide and 2-AG are only measurable in diseased joints (Richardson et al., 2008).

Given the anti-inflammatory and anti-nociceptive effects of endocannabinoids, these molecules likely play a role in dampening arthritic symptoms; however, the beneficial effects of endocannabinoids are limited due to rapid degradation by hydrolytic enzymes. Inhibiting the enzymes responsible for anandamide and 2-AG degradation is one strategy that has been employed to increase endocannabinoid levels *in vivo* (Kinsey et al., 2011). Anandamide is a substrate for FAAH, a

membrane bound hydrolyzing enzyme that converts anandamide into arachidonic acid and ethanolamine. This enzymatic process is essential in controlling anandamide activity, but also limits its beneficial effects. Several FAAH inhibitors have been developed for research and clinical trials, and these compounds increase circulating and tissue levels of anandamide, as well as the other fatty acid amides, OEA and PEA (Otrubova et al., 2011). One such inhibitor is URB597, which irreversibly binds FAAH and has anti-inflammatory, as well as anti-nociceptive, effects in experimental RA (Kinsey et al., 2011) and OA (Schuelert et al., 2011); however, the effects of locally administered URB597 have yet to be tested in the KC model of arthritic knee joint inflammation. The KC arthritis model produces a robust inflammatory response that peaks after several hours and is maintained for several days. KC-induced joint inflammation is characterized by joint swelling, increased leukocyte infiltration, hyperaemia, and increased nociceptive behaviours. In this study, KC was injected into the intra-articular space and inflammation was assessed in the presence or absence of URB597.

We hypothesized that local application of URB597, a potent and selective FAAH inhibitor, would decrease leukocyte-endothelial interactions and hyperaemia in KC-inflamed joints, and that this response would be mediated by cannabinoid receptors.

3.2 Effect of local URB597 on KC-induced inflammation

3.2.1 Methods

Kaolin (2%; 10µl in saline) and carrageenan (2%; 10µl in saline) were injected into the right knee joint of deeply anesthetised (isoflurane; 2-3%; 1L/min; O_2) male

C57Bl/6 mice (21-32g; 6-8 weeks old). After 24hrs, either leukocyte-endothelial interactions, or articular hyperaemia was assessed.

Before vascular assessment, the animals were deeply anaesthetised with urethane (25%; 2-3ml in saline) and surgically prepared (trachea, carotid artery and jugular vein cannulated; skin overlying inflamed knee removed). A baseline IVM or LASCA measure (1min) was taken, after which the mouse received one of the following treatments:

I. Vehicle (DMSO: cremophor: saline, 1:1:8; 100µl; topical onto exposed knee joint)

II. URB597 (0.3mg/kg; 100µl; topical onto exposed knee joint)

III. URB597 (3.0mg/kg; 100µl; topical onto exposed knee joint)

IV. URB597 (10.0mg/kg; 100µl; topical onto exposed knee joint)

V. URB597 (30.0mg/kg; 100µl; topical onto exposed knee joint)

Following treatment, 1min IVM or LASCA measures were recorded at 5, 10, 20, 30 and 60mins.

3.2.2 Results

3.2.2.1 Effects of URB597 on articular leukocyte-endothelial interactions

When compared to vehicle, URB597 0.3mg/kg, applied topically to the exposed knee joint, significantly decreased leukocyte rolling over the 1hr time course ($P<0.0001$; n=7-11; Figure 3.2). This effect peaked at 20mins; therefore, this time point was the focus of subsequent assessments. The lowest dose of URB597 (0.3mg/kg) decreased leukocyte rolling by 68.0 ± 6.8%, 20mins after drug application

($P<0.001$; n=11; Figure 3.1 and 3.2). Surprisingly, at higher doses (3.0-30.0mg/kg), the inhibitory effect of URB597 on leukocyte rolling was not maintained, and there was no change in leukocyte rolling when compared to vehicle ($P>0.05$; n=5-6; Figure 3.2). A similar effect was observed with leukocyte adherence, where low (0.3mg/kg) and medium (3.0mg/kg) doses of URB597 significantly decreased leukocyte adherence when compared to vehicle ($P<0.05$; n=6-11; Figure 3.2), but this effect was not observed at higher doses (10.0 and 30.0mg/kg) ($P>0.05$; n=5-7; Figure 3.2).

3.2.2.2 Effects of URB597 on articular hyperaemia

URB597 (3.0mg/kg; topical over exposed knee joint) significantly decreased articular blood flow over the 1hr time course when compared to vehicle control ($P<0.01$; n=6-10, Figure 3.4). This anti-hyperaemic effect was most profound 20min after drug administration, where URB597 decreased vascular perfusion by 19.6 ± 3.6% (n=7; Figure 3.3 and 3.4). Similar to the effects of URB597 on leukocyte-endothelial interactions, this anti-inflammatory effect was not maintained at higher doses of URB597 (10.0-30.0mg/kg), and hyperaemia was not changed when compared to vehicle ($P>0.05$; n=5-7; Figure 3.4); therefore, our dose response profile was U-shaped once again, insofar as there was an effect at the lowest dose tested but not at higher doses.

3.3 Contribution of CB1R and CB2R to the anti-inflammatory effects of URB597

3.3.1 Methods

Although U-shaped, the dose response curve did identify low-medium dose URB597 (0.3-3.0mg/kg) as capable of decreasing articular leukocyte recruitment and hyperaemia in this model of arthritis. Our next objective was to test which cannabinoid receptors were responsible for the inhibitory effects of URB597 on leukocyte-endothelial interactions and hyperaemia. To test this, the exposed inflamed knee was pre-treated topically with either the CB1R antagonist AM251 (0.2mg/kg) or the CB2R antagonist AM630 (0.2mg/kg), followed by URB597 10min later. The effects of antagonist treatment alone on leukocyte-endothelial interactions were also assessed; therefore, mice in these experiments received one of the following treatments:

I. Vehicle (DMSO: cremophor: saline, 1:1:8; 100µl; topical onto exposed knee joint)

II. URB597 (0.3 or 3.0 mg/kg; 100µl in vehicle; topical onto exposed knee joint) + AM251 (0.2mg/kg; 100µl in vehicle; topical onto exposed knee joint 10min before URB597)

III. URB597 (0.3 or 3.0mg/kg; 100µl in vehicle; topical onto exposed knee joint) + AM630 (0.2mg/kg; 100µl in vehicle; topical onto exposed knee joint 10min before URB597)

IV. AM630 alone (0.2mg/kg; 100µl in vehicle; topical onto exposed knee joint)

V. AM251 alone (0.2mg/kg; 100µl in vehicle; topical onto exposed knee joint)

IVM or LASCA was assessed before and 20min after drug treatment, and inflammatory scores were compared against either vehicle or URB597 alone.

3.3.2 Results

Both the CB1R antagonist AM251 (0.2mg/kg) and CB2R antagonist AM630 (0.2mg/kg) blocked the inhibitory effects of URB597 (0.3mg/kg) on leukocyte rolling ($P<0.01$; n=6; Figure 3.6 A). Interestingly, neither CB1R nor CB2R antagonism could block the effect of URB597 (0.3mg/kg) on leukocyte adherence ($P>0.05$; n=6; Figure 3.3). When administered alone, neither AM251 (0.2mg/kg) nor AM630 (0.2mg/kg) had an effect on leukocyte rolling or adherence ($P>0.05$; n=6-7; Figure 3.6 B).

Both the CB1R antagonist AM251 (0.2mg/kg), and the CB2R antagonist AM630 (0.2mg/kg) blocked the anti-hyperaemic effect of URB597 (3.0mg/kg) on KC-inflamed knee joints ($P<0.05$; n=5-11; Figure 3.4 C).

3.4 Involvement of TRPV1 in the loss of effect of URB597 at higher doses

3.4.1 Methods

Given the U-shaped dose response curve of URB597, we hypothesized that excessive endocannabinoid build-up in the joint was producing off-target effects which were counteracting the anti-inflammatory effects observed at lower doses. One possibility is that anandamide, acting through TPRV1, is producing a neurogenic inflammatory response; we used the TRPV1 antagonist SB366791 to test this hypothesis. Each mouse underwent the following protocol, which included three different treatments:

- First, the mouse was pre-treated with a systemic vehicle (2% DMSO, 1% cremophor, saline; i.p.), then, after 15min, a local vehicle (DMSO: cremophor: saline, 1:1:8; 100µl) was applied topically to the exposed knee joint.
- The next treatment was systemic SB366791 (500µg/kg in 2% DMSO, 1% cremophor, saline; 500µl; i.p.), then after 15min, local vehicle (DMSO: cremophor: saline, 1:1:8; 100µl) was applied topically to the exposed knee joint.
- The final treatment was systemic SB366791 (500µg/kg in 2% DMSO, 1% cremophor, saline; 500µl; i.p.), then, after 15min, local URB597 (30.0mg/kg; 100µl) was applied topically to the exposed knee joint.

Either an IVM or LASCA measure (1min) was recorded before and 20min after each local treatment. Using this protocol, we obtained three seperate baseline and test measures from each animal.

3.4.2 Results

Systemic SB366791 partially restored the anti-inflammatory effect of high dose URB597 (30.0mg/kg) on leukocyte rolling ($P<0.05$; n=5-12; Figure 3.7), but not leukocyte adherence ($P>0.05$; n=5-12; Figure 3.7).

SB366791 did not restore the anti-hyperaemic effect of URB597, as high dose URB597 (30.0mg/kg) failed to reduce articular blood flow in KC-inflamed knees ($P>0.05$; n=6-14; Figure 3.7).

3.5 Chapter summary

The results of this study suggest that the potent and selective FAAH inhibitor URB597 is capable of decreasing inflammatory leukocyte-endothelial interactions and hyperaemia in the KC knee joint arthritis model. Furthermore, the anti-inflammatory effects of URB597 on leukocyte rolling and hyperaemia were blocked by both CB1R and CB2R antagonism, while the effect on leukocyte adherence was mediated by a non-canonical endocannabinoid receptor. Interestingly, the anti-inflammatory effects of URB597 were only apparent at low to medium doses, and the dose response curve of this FAAH inhibitor was U-shaped. TRPV1 antagonism only partially restored the anti-inflammatory effect of high dose URB597 on leukocyte rolling, but had no effect on leukocyte adherence or hyperaemia.

3.6 Figures

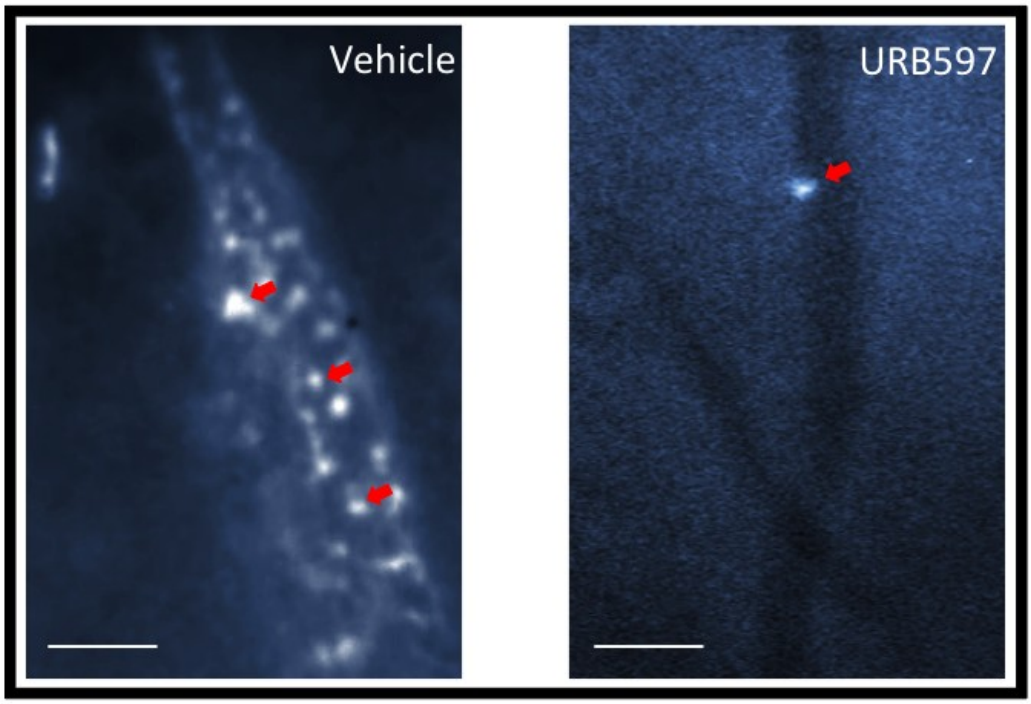

Figure 3.1 Intravital micrograph of the effect of URB597 on synovial leukocyte-endothelial interactions 20min after administration. Intraluminal white blood cells denoted by red arrows. Note the significant reduction in leukocytes 20min after URB597 treatment. Scale bar = 50μm. (Krustev et al., 2014).

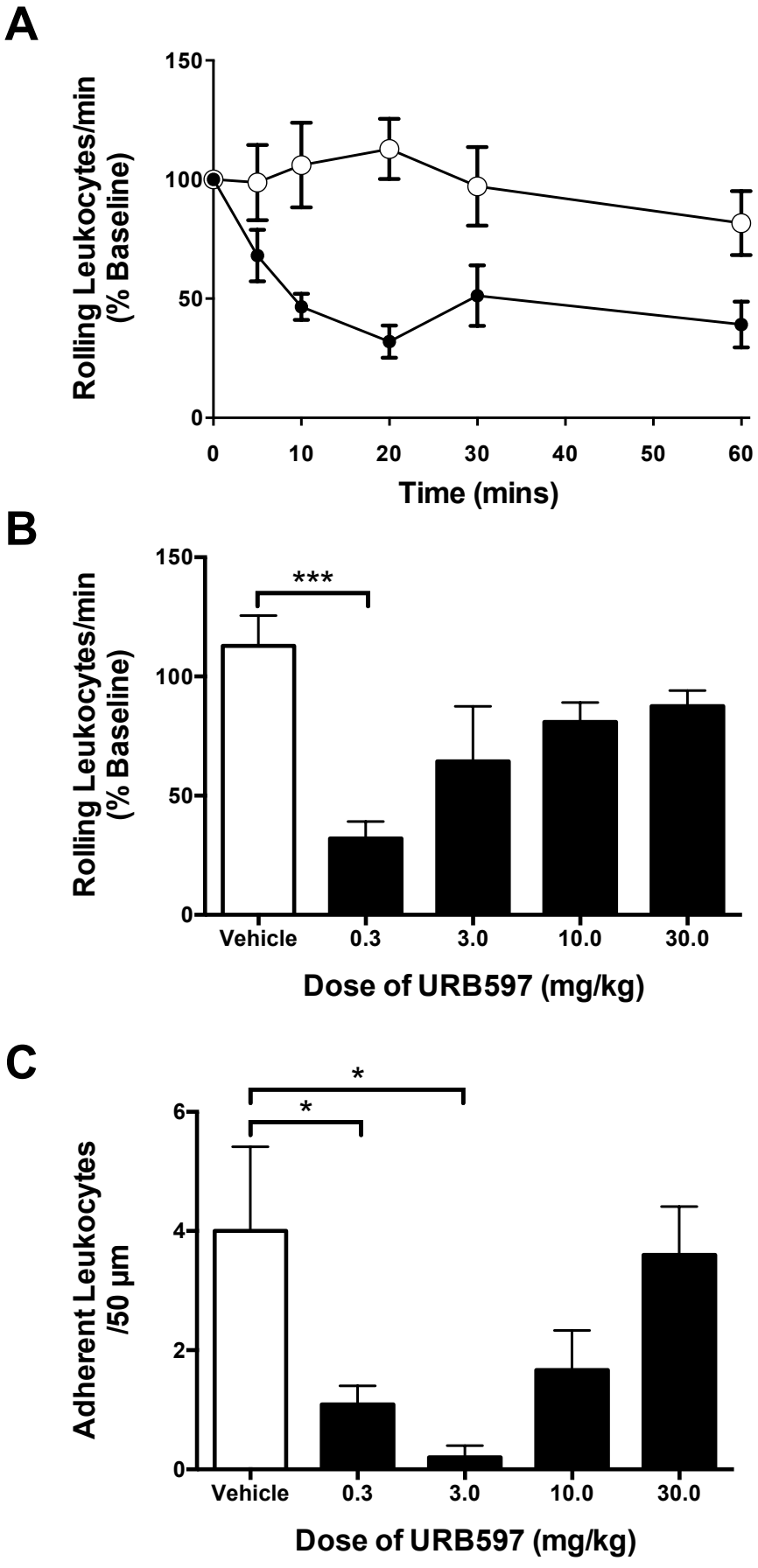
A
Rolling Leukocytes/min
(% Baseline)
150
100
50
0
0
10
20
30
40
50
60
Time (mins)
B
Rolling Leukocytes/min
(% Baseline)
150
100
50
0
***
Vehicle
0.3
3.0
10.0
30.0
Dose of URB597 (mg/kg)
C
Adherent Leukocytes
/50 µm
6
4
2
0
*
*
Vehicle
0.3
3.0
10.0
30.0
Dose of URB597 (mg/kg)

Figure 3.2 Effects of local URB597 on leukocyte-endothelial interactions in KC-inflamed mouse knee joints. **(A)** Time course (1hr) of the effect of URB597 (0.3mg/kg on exposed joint) on leukocyte rolling within the synovial microvasculature. URB597 (solid circles) significantly decreased leukocyte rolling when compared to vehicle (open circles)(two-way ANOVA; $P<0.0001$; n=7-11). **(B)** Dose response profile of the effect of URB597 (0.3 - 30.0mg/kg on exposed knee joint) on leukocyte rolling 20min after drug administration. Low dose URB597 (0.3mg/kg) significantly decreased leukocyte rolling (one-way ANOVA with Dunnett; $P<0.001$; n=11); however, there was no effect at higher doses (one-way ANOVA with Dunnett; $P>0.05$; n=5-7). **(C)** Dose response profile of the effect URB597 (0.3-30.0mg/kg on exposed knee joint) on leukocyte adherence 20min after drug administration. URB597 (0.3 and 3.0mg/kg) significantly decreased leukocyte adherence (one-way ANOVA with Dunnett; $P<0.05$; n=5-11), but higher doses of URB597 (10.0 and 30.0mg/kg) did not (one-way ANOVA with Dunnett; $P>0.05$; n=5-7) (Krustev et al., 2014).

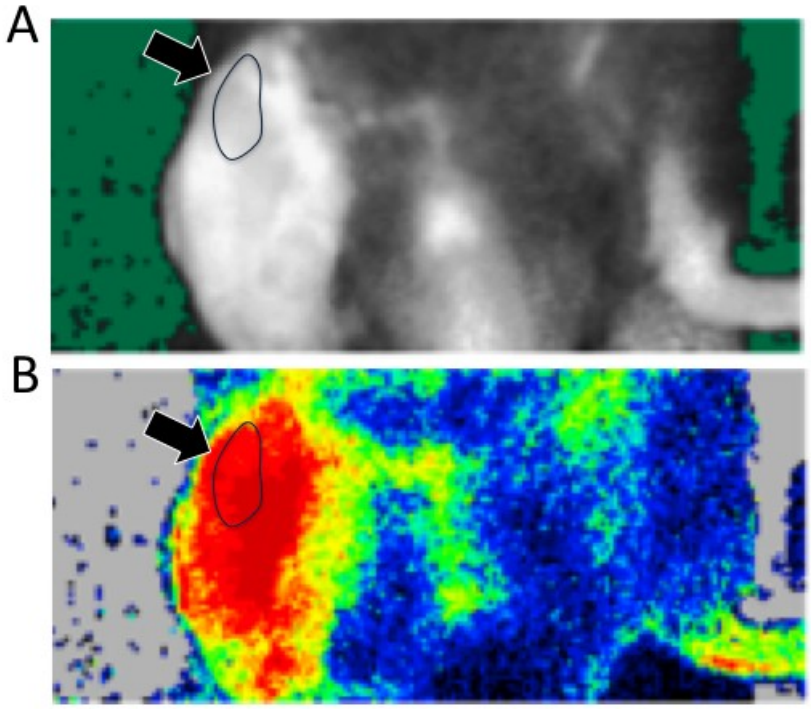

Figure 3.3 LASCA image of a KC inflamed knee. A) Reflected light intensity map of mouse inguinal region and lower limbs. This image is used for selecting the appropriate knee joint area for analysis. Knee joint is encircled and denoted by the black arrow. **B)** Corresponding vascular perfusion map of the inguinal region and lower limbs. A LASCA value is calculated for the selected knee joint, and then averaged over the 1min recording. Knee joint is encircled and denoted by the black arrow.

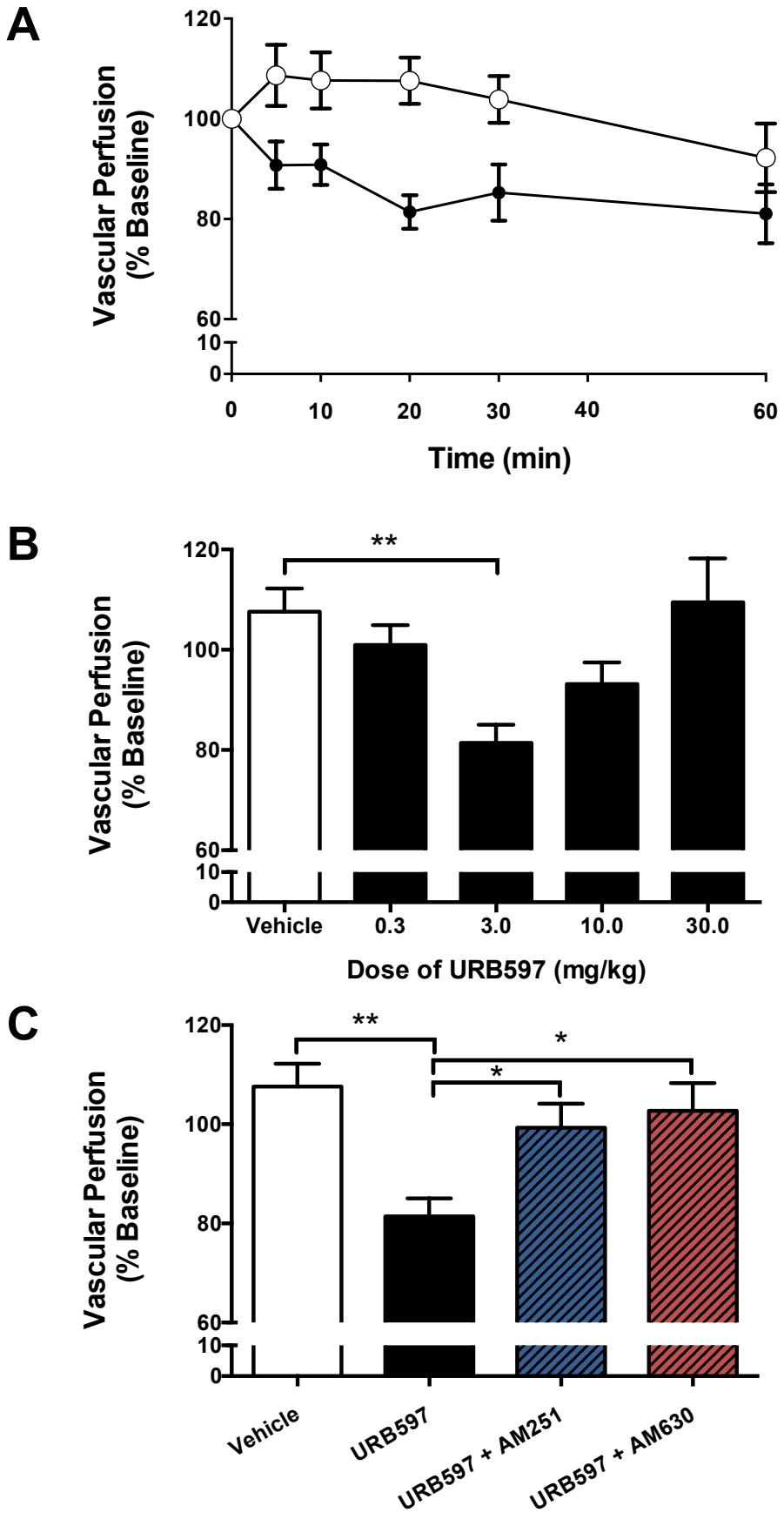
A
Vascular Perfusion (% Baseline)
120
100
80
60
10
0
0
10
20
30
40
60
Time (min)
B
**
Vascular Perfusion (% Baseline)
120
100
80
60
10
0
Vehicle
0.3
3.0
10.0
30.0
Dose of URB597 (mg/kg)
C
**
*
*
Vascular Perfusion (% Baseline)
120
100
80
60
10
0
Vehicle
URB597
URB597 + AM251
URB597 + AM630

Figure 3.4 Effect of URB597 on inflammatory hyperaemia in KC-inflamed mouse knee joints (A) Time course (1hr) of the effect of URB597 (3.0mg/kg on exposed knee joint) on vascular perfusion. When compared to vehicle (open circles), URB597 (solid circles) significantly decreased articular blood flow (two-way ANOVA; $P<0.0001$; n=6-7). **(B)** Dose response profile of the effects of URB597 (0.3-30.0mg/kg on exposed knee joint) on inflamed knee joint blood flow. Medium dose URB597 (3.0mg/kg) significantly decreased vascular perfusion (one-way ANOVA with Dunnett; $P<0.01$; n=6-7); however this effect was not maintained at higher doses (10.0 and 30.0mg/kg) (one-way ANOVA with Dunnett; $P>0.05$; n=5-7). **(C)** Effect of CB1R and CB2R antagonism on the anti-hyperaemic effect of URB597 (0.3mg/kg on exposed knee joint). Both AM251 (CB1R antagonist; 0.2mg/kg on exposed knee joint) and AM630 (CB2R antagonist; 0.2mg/kg on exposed knee joint) abolished the effect of URB597 on knee joint blood flow (one-way ANOVA with Bonferroni; $P<0.05$; n=6-8) (Krustev et al., 2014).

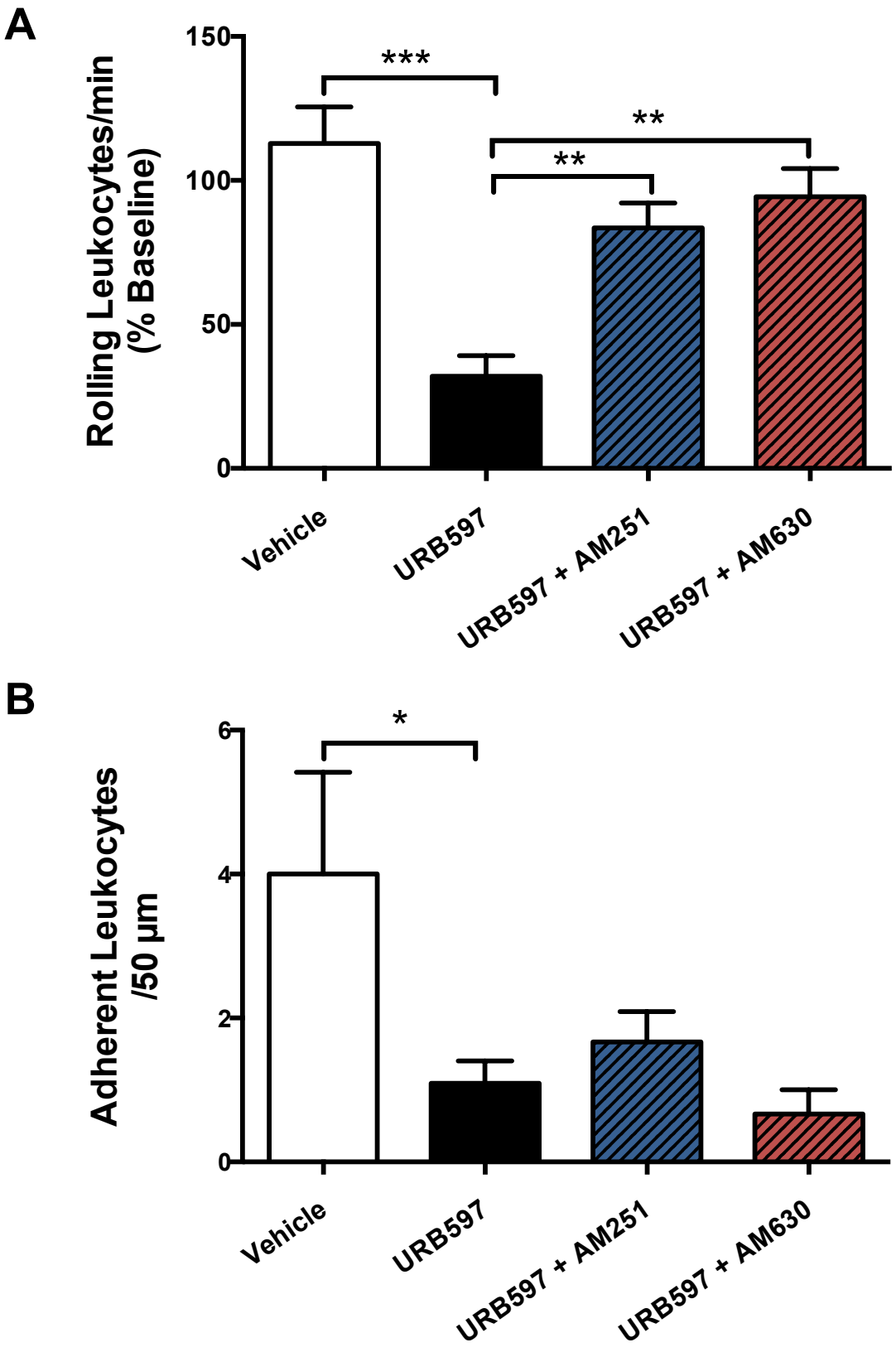
A
Rolling Leukocytes/min
(% Baseline)
150
100
50
0
***
**
**
Vehicle
URB597
URB597 + AM251
URB597 + AM630
B
Adherent Leukocytes
/50 µm
6
4
2
0
*
Vehicle
URB597
URB597 + AM251
URB597 + AM630

Figure 3.5 Involvement of cannabinoid receptors in the anti-inflammatory effects of URB597 on leukocyte-endothelial interactions. (A) Effect of CB1R and CB2R antagonism on the inhibitory effect of URB597 (0.3mg/kg on exposed knee joint) on leukocyte rolling. Both AM251 (0.2mg/kg on exposed knee joint) and AM630 (0.2mg/kg on exposed knee joint) blocked the effect of URB597 on leukocyte rolling (one-way ANOVA with Bonferroni; $P<0.01$; $n=6$). **(B)** Effect of CB1R and CB2R antagonism on the inhibitory effect of URB597 on leukocyte adherence. Neither CB1R nor CB2R antagonism blocked the effect of URB597 (0.3mg/kg on exposed knee joint) on leukocyte adherence (one-way ANOVA with Bonferroni; $P>0.05$; $n=6$) (Krustev et al., 2014).

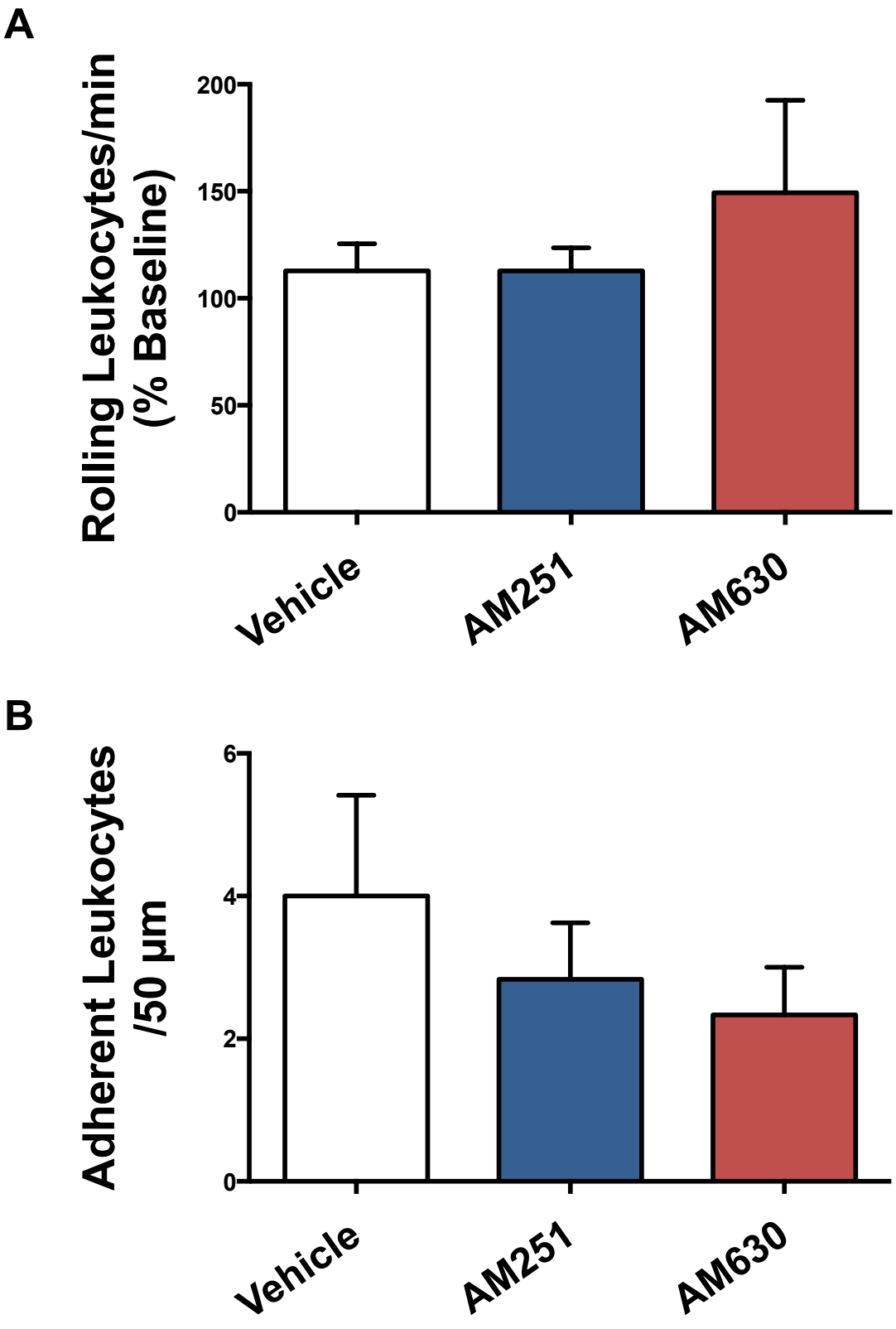
A
Rolling Leukocytes/min
(% Baseline)
200
150
100
50
0
Vehicle
AM251
AM630
B
Adherent Leukocytes
/50 µm
6
4
2
0
Vehicle
AM251
AM630

Figure 3.6 Effect of cannabinoid receptor antagonists when administered alone on leukocyte-endothelial interactions, 20mins after administration. A) Neither AM251 (0.2mg/kg on exposed knee joint) nor AM630 (0.2mg/kg on exposed knee joint) had an effect on leukocyte rolling 20min after administration (one-way ANOVA with Dunnett; $P>0.05$; n=6-12). **B)** Neither AM251 (0.2mg/kg on exposed knee joint) nor AM630 (0.2mg/kg on exposed knee joint) had an effect on leukocyte adherence 20min after administration (one-way ANOVA with Dunnett; $P>0.05$; n=6-12).

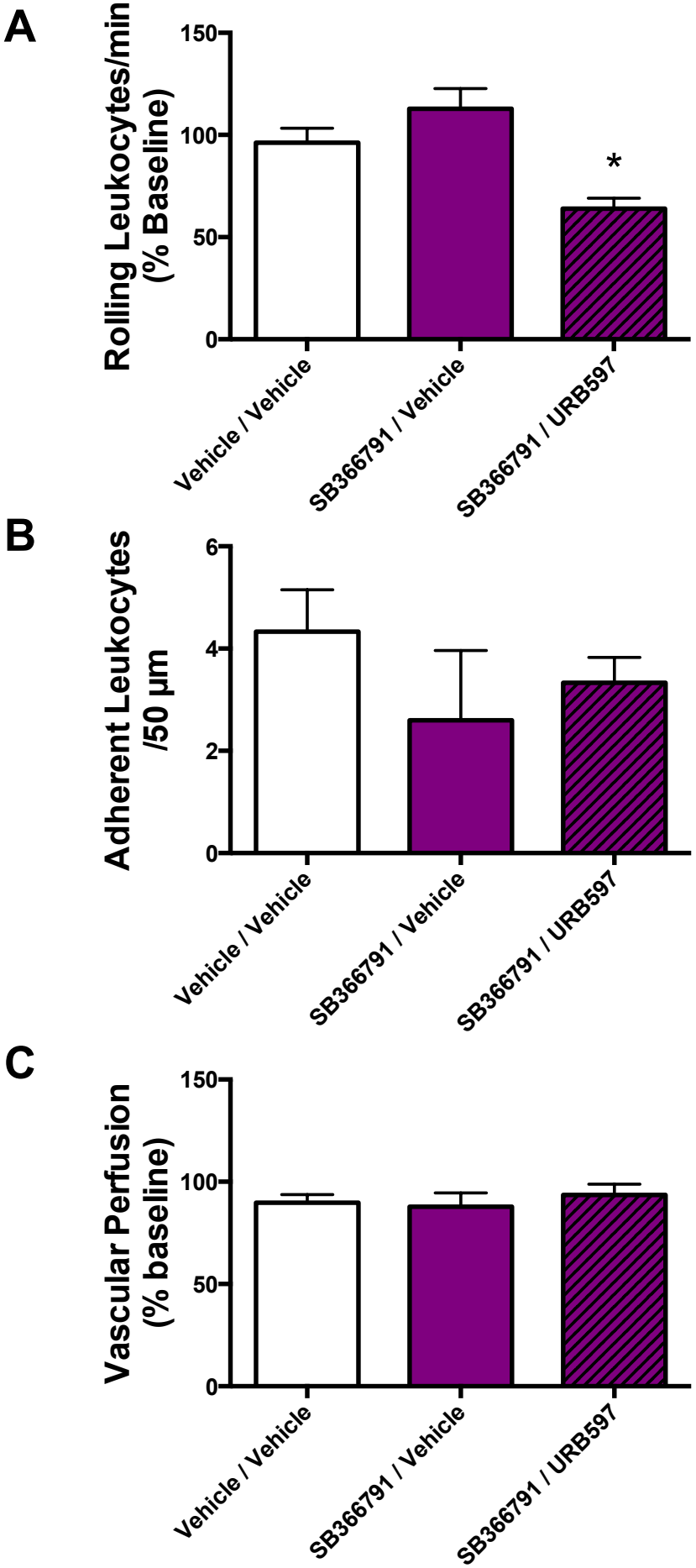
A
Rolling Leukocytes/min
(% Baseline)
150
100
50
0
*
Vehicle / Vehicle
SB366791 / Vehicle
SB366791 / URB597
B
Adherent Leukocytes
/50 µm
6
4
2
0
Vehicle / Vehicle
SB366791 / Vehicle
SB366791 / URB597
C
Vascular Perfusion
(% baseline)
150
100
50
0
Vehicle / Vehicle
SB366791 / Vehicle
SB366791 / URB597

Figure 3.7 Involvement of TRPV1 in attenuating the anti-inflammatory effects of URB597 at highest dose (30.0mg/kg). (A) Effect of locally administered high dose URB597 (30.0mg/kg on exposed knee joint) on leukocyte rolling, with TRPV1 antagonism (SB366791; 500μg/kg i.p.). When the mice were pre-treated with SB366791, high dose URB597 decreased leukocyte rolling (one-way ANOVA with Dunnett; $P<0.05$; n=6-12). On its own, SB366791 had no effect on leukocyte rolling ($P>0.05$; n=6-12). **(B)** Effect of locally administered high dose URB597 (30.0mg/kg) on leukocyte adherence with TRPV1 antagonism (SB366791; 500μg/kg i.p.). Neither SB366791, nor the combination of SB366791 with high dose URB597 (30.0mg/kg), had an effect on leukocyte adherence in KC-inflamed knees (one-way ANOVA with Dunnett; $P>0.05$; n=5-12). **(C)** Effect of locally-administered high dose URB597 (30.0mg/kg) on vascular hyperaemia, with or without TRPV1 antagonism (SB366791; 500μg/kg i.p.). Neither SB366791, nor the combination of SB366791 with high dose URB597, had an effect on blood flow in KC-inflamed knees (one-way ANOVA with Dunnett; $P>0.05$; n=5-12).

Chapter 4: Effect of URB597 on Articular Neurogenic Inflammation

4.1 Background and hypotheses

Neurogenic inflammation has been implicated as a contributing factor in a number of inflammatory diseases, including arthritis. Neurogenic inflammatory responses are elicited by the release of immunomodulatory neuropeptides from the peripheral terminals of small diameter afferents. SP, CGRP, and VIP are all stored in the peripheral terminals of articular C fibres, and released in response to antidromic signalling. Electrostimulation of articular nociceptors is capable of eliciting plasma extravasation in cat knee joints, and this effect is mediated by both SP (Ferrell & Russell, 1985) and CGRP (Karimian & Ferrell, 1994). CGRP also produces robust vasodilatation in rabbit knee joint ligaments (Ferrell et al., 1997). Similarly, topical application of VIP produces a dose-dependent increase in articular blood flow that does not involve synovial mast cells (McDougall & Barin, 2005). SP, CGRP and VIP are also capable of increasing leukocyte adherence to vascular endothelial cells *in vitro* (Zimmerman et al., 1992; de la Fuente et al., 1994), while selective nociceptor denervation attenuates arthritis-induced articular leukocyte accumulation *in vivo* (Hood et al., 2001).

CB1R is expressed on CGRP and SP containing neurons, and, when activated by anandamide, prevents CGRP release from skin preparations *ex vivo* (Engel et al., 2011). KC joint inflammation is known to have a neurogenic component; therefore, we hypothesized that the CB1R-mediated effects of URB597 on KC joint inflammation were due to endocannabinoid-mediated decreases in neurogenic inflammation. To test this hypothesis, we first identified the ideal electrostimulation

parameters for inducing neurogenic leukocyte-endothelial interactions within synovial venules, then tested the effects of URB597 on this response *in vivo*.

The following three hypotheses were tested in this study:

I. **Electrostimulation of the ipsilateral saphenous nerve would increase leukocyte rolling and adherence within the synovial microcirculation of the knee (Section 4.2), and this effect would be mediated by either SP, CGRP or VIP (Section 4.3).**
II. **Local application of exogenous SP, CGRP and VIP directly to the exposed knee joint would increase leukocyte-endothelial interactions within the synovial microcirculation (Section 4.4).**
III. **Local URB597 (0.3mg/kg) treatment would attenuate antidromic saphenous stimulation-induced neurogenic responses, and this effect would be CB1R dependent (Section 4.5).**

4.2 Frequency response profile of saphenous nerve stimulation-induced leukocyte-endothelial interactions

4.2.1 Methods

Although numerous studies have explored the effects of nerve stimulation on joint inflammation, none have specifically investigated how saphenous nerve stimulation affects leukocyte rolling and adherence within mouse knee joints; therefore, we tested a range of frequencies (0.5, 1.0, 2.0 and 5.0Hz), at a fixed voltage (10V) and pulse width (1ms), in order to find the ideal parameters for inducing this effect.

Male C57Bl/6 mice (21-37g; 6-10 weeks old) were deeply anaesthetised with urethane (2-3ml i.p.; 25% in saline), and surgically prepared for IVM and electrostimulation by cannulating the trachea, jugular vein and carotid artery. The saphenous nerve was isolated, cut centrally, and placed atop two stimulating electrodes. The skin overlying the knee joint was surgically removed, and R6G (0.05ml; 0.05% in saline) was injected via the jugular cannula. A baseline IVM measure was taken, followed by 5min of saphenous stimulation. Each mouse saphenous nerve received upwards of four rounds of stimulation, as we aimed to test each frequency in every subject. A mouse received less than four rounds if they died or if the viability of the knee joint preparation was compromised. The order in which each frequency was tested was randomized, and there was a 10min recovery period between each test. Leukocyte-endothelial interactions were recorded before and after (2min and 5min) electrostimulation.

For both leukocyte rolling and adherence, the effects of each frequency tested were analyzed using a one-sample t test, where the mean was compared back to a hypothetical value (rolling value = 100; adherence value = 0).

4.2.2 Results

Saphenous nerve stimulation at 0.5Hz for 2min had no effect on leukocyte rolling ($P>0.05$; n=8; Figure 4.1); however, 5min of 0.5Hz stimulation significantly decreased leukocyte rolling ($P<0.05$; n=7; Figure 4.1). Neither 2min nor 5min saphenous nerve stimulation at 1.0Hz had an effect on leukocyte rolling ($P>0.05$; n=9; Figure 4.1). Articular leukocyte rolling was increased following 2.0Hz stimulation with both 2min ($P<0.05$; n=9; Figure 4.1) and 5min ($P<0.05$; n=8; Figure

4.1) stimulation periods. 5Hz stimulation increased leukocyte rolling when the nerve was stimulated for 5min ($P<0.05$; n=6; Figure 4.1), but 2min stimulation had no effect ($P>0.05$; n=5; Figure 4.1). Saphenous nerve electrostimulation had no effect on leukocyte adherence at any of the frequencies or stimulation times tested ($P>0.05$; n=5-9; Figure 4.1).

4.3 The contribution of SP, CGRP and VIP to stimulation-induced rolling

4.3.1 Methods

Saphenous nerve electrostimulation for 5min produced the most distinct frequency response profile, and 2Hz stimulation had the greatest effect on leukocyte rolling at this time; therefore, 5mins of 2Hz stimulation was chosen for subsequent experiments. In order to discern which neuropeptides were responsible for inducing leukocyte rolling, the knee was pre-treated (5min before stimulation) with selective antagonists for SP (RP67580; 20nmol in 100µL of DMSO: cremophor: saline, 1:1:8 on exposed knee joint), CGRP ($CGRP_{8-37}$; 3.2nmol in 100µL saline on exposed knee joint), and VIP (VIP_{6-28}; 1nmol in 100µL saline on exposed knee joint).

4.3.2 Results

When compared to the surgery control, where the saphenous was isolated but not electrostimulated, 2Hz stimulation significantly increased leukocyte rolling in both groups of vehicle-treated knees ($P<0.001$; n=15; Figure 4.2 A). When compared to saline-treated knees, SP antagonism had no effect on stimulation-induced leukocyte rolling when compared to vehicle control ($P>0.05$; n=8-15; Figure 4.2 A). CGRP antagonism also had no effect on saphenous stimulation-induced leukocyte rolling

(P>0.05; n=6; Figure 4.2 A). Stimulation-induced rolling was completely abolished when the knee was pre-treated with the VIP antagonist VIP_{6-28} (P<0.05; n=6; Figure 4.2 A).

Saphenous stimulation once again had no effect on leukocyte adherence, and neuropeptide antagonism did not change this (P>0.05; n=6-8; Figure 4.2 B)

4.4 Effect of neuropeptides on articular leukocyte-endothelial interactions

4.4.1 Methods

The following experiments were conducted in order to test the effects of exogenously administered neuropeptides on leukocyte-kinetics in naïve mouse knee joints. For each mouse, the trachea, carotid artery and jugular vein were cannulated, and R6G was injected (0.05%; 0.05ml i.v.). The skin overlying both knees was removed, and, for each knee, three baseline IVM videos were recorded. Following this, a 100µl bolus of saline (0.9%) was applied topically to the exposed knee joint. After 10min three more IVM videos were recorded for each knee. Following this, a 100µl bolus of either SP (0.1nmol; saline), CGRP (1.0nmol; saline) or VIP (1.0nmol; saline) was applied topically atop both exposed knee joints. Ten minutes after bolus application, three more test videos were recorded. Leukocyte rolling and adherence were quantified and averaged between the three test videos from each time point, and then compared back to baseline (the three videos obtained immediately before the last bolus application). By using this procedure, each mouse provided a vehicle measure and a neuropeptide treatment measure.

4.4.2 Results

When compared to saline control, SP (0.1nmol; saline) significantly increased leukocyte rolling 10min after administration ($P<0.05$; n=6-12; Figure 4.3). Neither CGRP (1.0nmol; saline), nor VIP (1.0nmol; saline) had an effect on leukocyte rolling in naïve mouse knee joints ($P<0.05$; n=6-12; Figure 4.3).

SP (0.1nmol; saline) also increased leukocyte adherence in naïve mouse knee joints, when compared to saline control ($P<0.05$; n=6-12; Figure 4.3). Interestingly, VIP increased leukocyte adherence when compared to saline control ($P<0.001$; n=7-12; Figure 4.3). CGRP had no effect on leukocyte adherence when compared to saline control ($P>0.05$; n=6-12; Figure 4.3).

4.5 Effect of URB597 on saphenous nerve stimulation-induced leukocyte rolling

4.5.1 Methods

Having established that saphenous nerve stimulation increases synovial leukocyte rolling through a VIP-dependent mechanism,we wanted to test if URB597 treatment could inhibit this effect. Knees were pre-treated with URB597 (0.3mg/kg on exposed knee joint; 20min before saphenous stimulation) and leukocyte rolling was measured before and after stimulation (10V, 2Hz, 1ms pulse width, 5min). This dose of URB597 had the most profound effect on leukocyte rolling in previous studies. In separate groups of mice, knees were pre-treated (10min before URB597) with either AM251 (CB1R antagonist; 0.2mg/kg; 100µl DMSO: cremophor: saline), AM630 (CB2R antagonist; 0.2mg/kg; 100µl DMSO: cremophor: saline), or O-1918

(GPR55 antagonist; 0.17mg/kg; 100µl DMSO: cremophor: saline), in order to test the contribution of CB1R, CB2R, and GPR55, respectively.

4.5.2 Results

The pro-rolling effect of saphenous nerve stimulation was completely abolished when the knee was pre-treated with URB597, and this effect was significant when compared to vehicle ($P<0.001$; $n=6$). In order to test whether this effect was mediated by CB1R or CB2R, knees were pre-treated with either AM251 (0.2mg/kg on exposed knee joint) or AM630 (0.2mg/kg on exposed knee joint), followed by URB597 (0.3mg/kg on exposed knee joint), and the saphenous nerve was electrostimulated. Interestingly, neither CB1R nor CB2R antagonism could block the inhibitory effect of URB597 on saphenous stimulation-induced leukocyte rolling ($P>0.05$; $n=5$-6). Since CB1R and CB2R antagonism was ineffective, it was hypothesized that GPR55 may be responsible for the inhibitory effect of URB597 on stimulation-induced rolling; therefore, the knee was pre-treated with the GPR55 antagonist O-1918 (0.17mg/kg on exposed knee joint), followed by URB597 and electrostimulation. GPR55 antagonism not only blocked the anti-inflammatory effect of URB597 on leukocyte rolling ($P<0.001$; $n=5$), but exacerbated the pro-inflammatory response of saphenous nerve stimulation on leukocyte rolling when compared to vehicle ($P<0.05$; $n=5$).

4.6 Chapter summary

Based on the frequency response profile presented in this study, it appears that 0.5Hz stimulation of the saphenous nerve decreases leukocyte rolling within synovial post-capillary venules, while 2.0Hz and 5.0Hz stimulation increases leukocyte rolling.

Furthermore, at the parameters used in this study, saphenous nerve stimulation had no effect on leukocyte adherence. The pro-rolling effect of 2Hz stimulation was completely blocked by VIP antagonism, suggesting an involvement of this neuropeptide in this response. When SP and VIP were applied exogenously to the exposed knee joint, both neuropeptides increased leukocyte-endothelial interactions, while CGRP did not. Lastly, locally administered URB597 also abolished the effect of saphenous nerve stimulation on leukocyte rolling, and this effect was blocked by GPR55 antagonism.

4.7 Figures

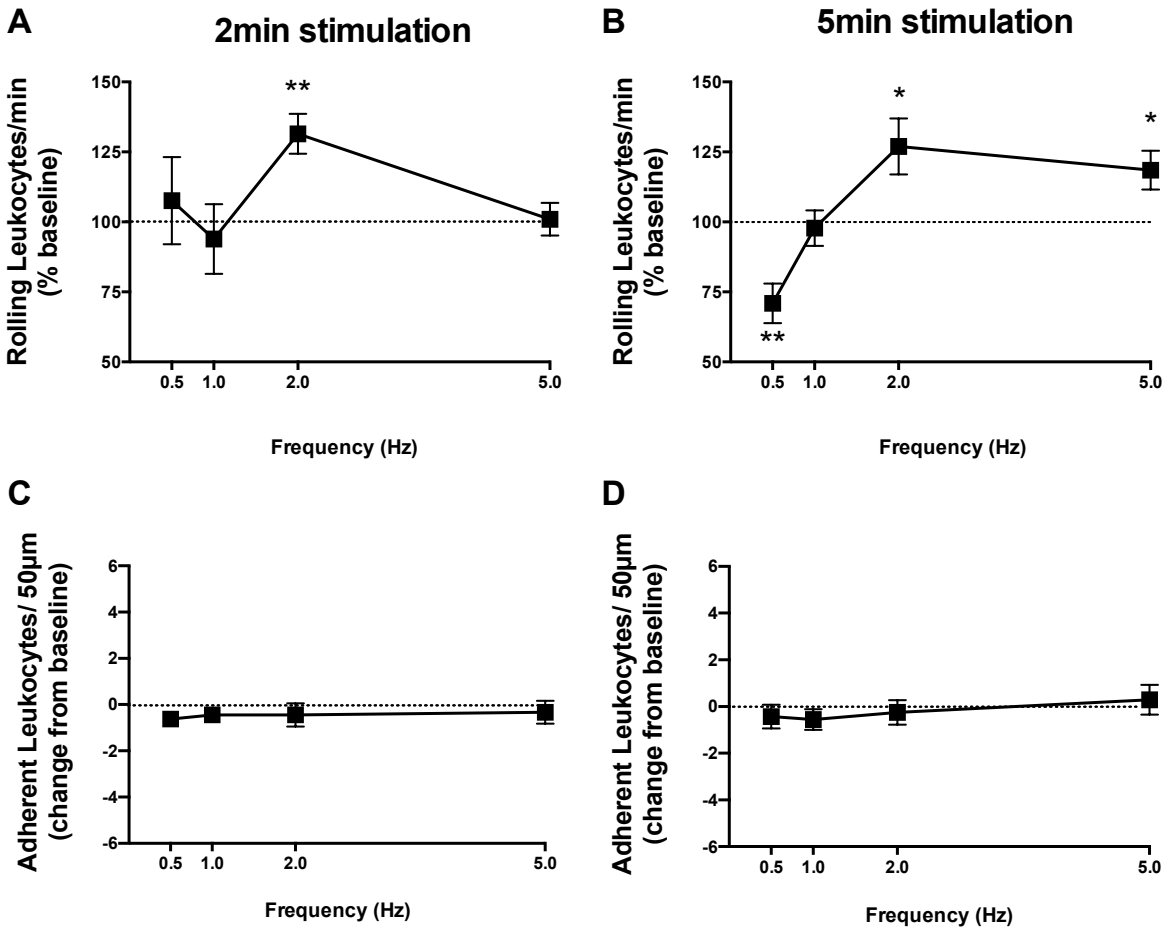
A
2min stimulation
Rolling Leukocytes/min (% baseline)
150
125
100
75
50
**
0.5
1.0
2.0
5.0
Frequency (Hz)
B
5min stimulation
Rolling Leukocytes/min (% baseline)
150
125
100
75
50
*
*
**
0.5
1.0
2.0
5.0
Frequency (Hz)
C
Adherent Leukocytes/ 50µm (change from baseline)
6
4
2
0
-2
-4
-6
0.5
1.0
2.0
5.0
Frequency (Hz)
D
Adherent Leukocytes/ 50µm (change from baseline)
6
4
2
0
-2
-4
-6
0.5
1.0
2.0
5.0
Frequency (Hz)

Figure 4.1 Frequency response profiles of the effects of saphenous nerve stimulation on leukocyte-endothelial interactions. (A) Effect of 2min saphenous nerve stimulation on leukocyte rolling within the microvasculature of the knee. Following 2min of electrostimulation, 2Hz stimulation significantly increased leukocyte rolling (one-sample t-test; $P<0.01$; n=9), while 0.5Hz, 1.0Hz and 5.0Hz had no effect (one-sample t-test; $P>0.05$; n=5-8). **(B)** Effect of 5min saphenous nerve electrostimulation on leukocyte rolling within the microvasculature of the knee. Following 5min of electrostimulation, 0.5Hz stimulation significantly decreased leukocyte rolling (one-sample t-test; $P<0.01$; n=7), 1.0Hz stimulation had no effect on leukocyte rolling (one-sample t-test; $P>0.05$; n=9), and both 2.0Hz and 5.0Hz stimulation increased leukocyte rolling (one-sample t-test; $P<0.05$; n=6-8). **(C)** Effect of 2min stimulation on leukocyte adherence within the knee joint microvasculature. Leukocyte adherence was not affected by saphenous nerve stimulation at any of the frequencies tested (one-sample t-test; $P>0.05$; n=6-9). **(D)** Effect of 5min saphenous nerve stimulation on leukocyte adherence within the knee joint microvasculature. There was no effect on leukocyte adherence with any of the stimulation frequencies tested (one-sample t-test; $P>0.05$; n=7-9).

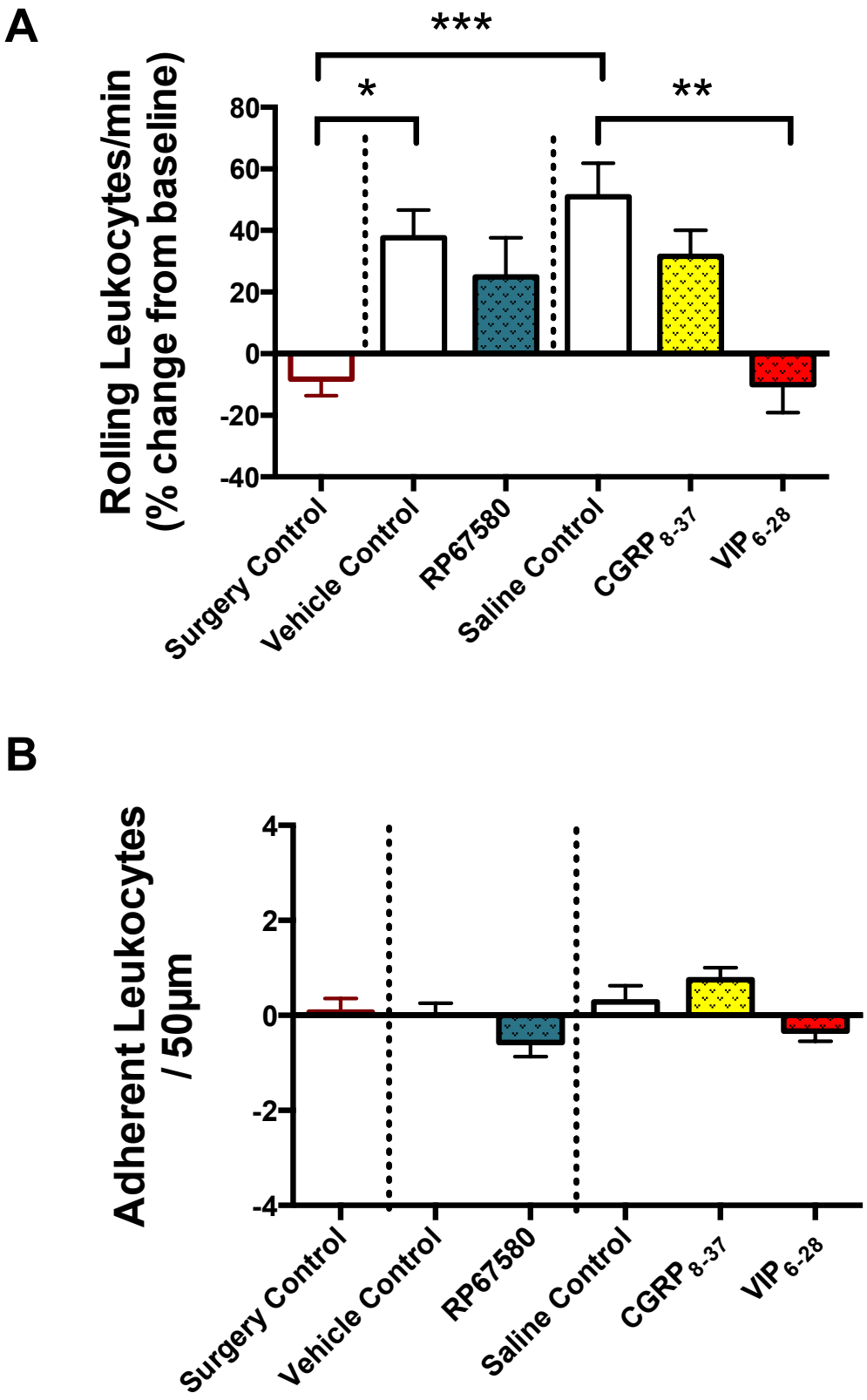
A
***
*
**
Rolling Leukocytes/min
(% change from baseline)
80
60
40
20
0
-20
-40
Surgery Control
Vehicle Control
RP67580
Saline Control
CGRP 8-37
VIP 6-28
B
Adherent Leukocytes
/ 50µm
4
2
0
-2
-4
Surgery Control
Vehicle Control
RP67580
Saline Control
CGRP 8-37
VIP 6-28

Figure 4.2 Involvement of SP, CGRP, and VIP in saphenous nerve stimulation-induced leukocyte-trafficking in mouse knee joints. (A) Effect of neuropeptides on leukocyte-rolling. When compared to surgery control (n=15), leukocyte rolling was significantly increased following saphenous nerve stimulation when knees were treated with either vehicle control (DMSO: cremophor: saline, 1:1:8; 100µl) (unpaired two-tailed t test; $P<0.05$; n=6), or saline (0.9%) control (unpaired two-tailed t-test; $P<0.01$; n=15). The SP antagonist RP67580 had no effect on stimulation-induced leukocyte rolling when compared to its respective control (DMSO: cremophor: saline, 1:1:8) (unpaired two-tailed t-test; $P>0.05$; n=8). The CGRP antagonist $CGRP_{8-37}$ had no effect on saphenous stimulation-induced leukocyte rolling when compared to its respective control (saline) (one-way ANOVA with Dunnett; $P>0.05$; n=6). The VIP antagonist VIP_{6-28} completely blocked the effect of saphenous nerve stimulation on knee joint leukocyte rolling when compared to its respective control (saline) (one-way ANOVA with Dunnett; $P<0.01$; n=6), **(B)** 2Hz stimulation with or without neuropeptide antagonism had no effect on leukocyte adherence (one way ANOVA with Dunnett; $P>0.05$; n=6-15).

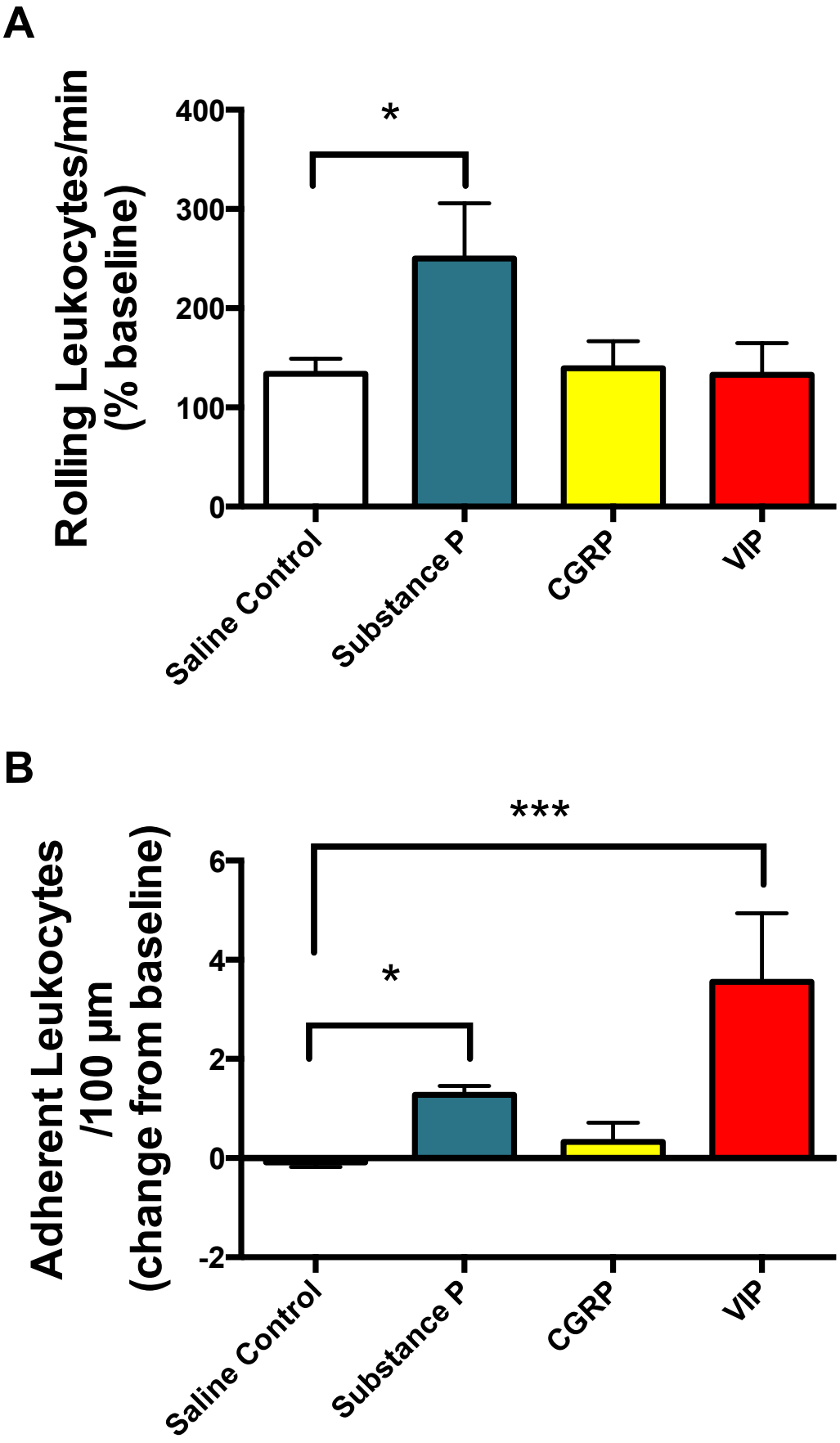
A
Rolling Leukocytes/min
(% baseline)
400
300
200
100
0
*
Saline Control
Substance P
CGRP
VIP
B
Adherent Leukocytes
/100 µm
(change from baseline)
6
4
2
0
-2
***
*
Saline Control
Substance P
CGRP
VIP

Figure 4.3 Effect of exogenous neuropeptides on synovial leukocyte-endothelial interactions in mouse knee joints. (A) Effect of neuropeptides on leukocyte rolling when applied topically to exposed knee joint. SP (0.1nmol; 100µl saline) significantly increased leukocyte rolling when compared to saline control (one-way ANOVA with Dunnett; $P<0.05$; n=6-12). Neither CGRP (3.2nmol; 100µl saline), nor VIP (1.0nmol; 100µl saline), had an effect on leukocyte rolling (one-way ANOVA with Dunnett; $P>0.05$; n=6-12). **(B)** Effect of neuropeptides on leukocyte adherence when applied topically to the exposed knee joint. When compared to saline control, leukocyte adherence was significantly increased by both SP (0.1nmol; 100µl saline) (one-way ANOVA with Dunnett; $P<0.05$; n=6-12), and VIP (1.0nmol; 100µl saline) (one-way ANOVA with Dunnett; $P<0.001$; n=7-12). CGRP (3.2nmol; 100µl saline) had no effect on leukocyte adherence when compared to saline (one-way ANOVA with Dunnett; $P>0.05$; n=6-12).

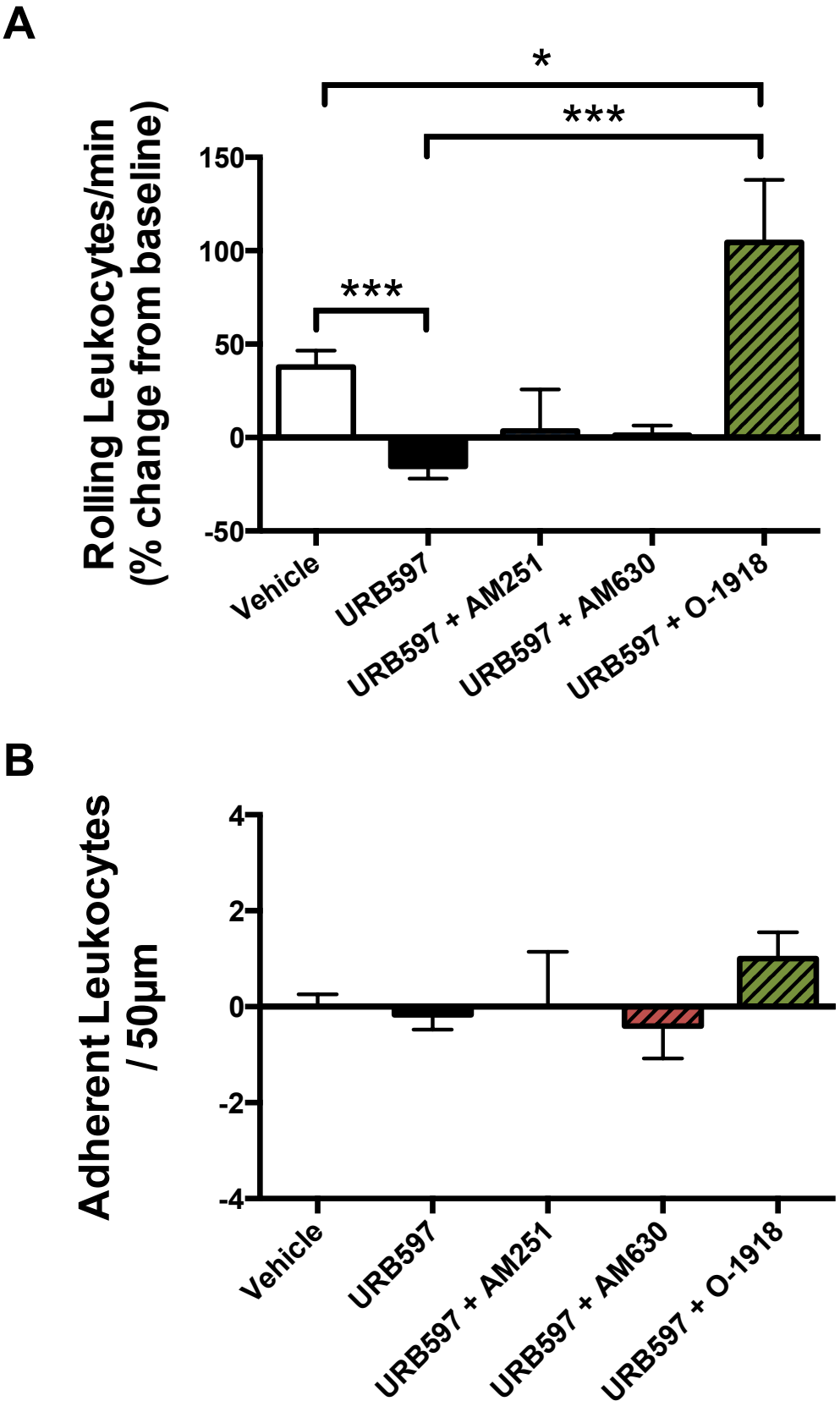
A
Rolling Leukocytes/min
(% change from baseline)
*
***
***
150
100
50
0
-50
Vehicle
URB597
URB597 + AM251
URB597 + AM630
URB597 + O-1918
B
Adherent Leukocytes
/ 50µm
4
2
0
-2
-4
Vehicle
URB597
URB597 + AM251
URB597 + AM630
URB597 + O-1918

Figure 4.4 Effect of URB597 on saphenous nerve stimulation-induced leukocyte-endothelial interactions, and the involvement of endocannabinoid receptors in this effect. (A) Topically applied URB597 (0.3mg/kg) completely abolished the effect of 2Hz saphenous nerve stimulation on leukocyte rolling within the knee joint microvasculature (unpaired two tailed t-test; $P<0.001$; n=6). Neither the CB1R antagonist AM251 (0.2mg/kg), nor the CB2R antagonist AM630 (0.2mg/kg) blocked the anti-rolling effect of URB597 (one-way ANOVA with Bonferroni; $P>0.05$; n=5-6). The GPR55 antagonist O-1918 (0.17mg/kg) blocked the anti-rolling effect of URB597 on saphenous nerve stimulation-induced neurogenic inflammation (one-way ANOVA with Bonferroni; $P<0.002$; n=5-6). **(B)** 2Hz stimulation had no effect on leukocyte adherence (unpaired two tailed t-test; $P>0.05$; n=6-15), with or without drug treatment (one-way ANOVA with Dunnett; $P>0.05$; n=6-15).

Chapter 5: The Effect of URB597 on the Development of Pain in the Sodium Monoiodoacetate Osteoarthritis Model

5.1 Background and hypotheses

For years, many of those working in the OA field believed that abnormal joint usage and dysregulated cartilage remodelling were the sole contributors to joint damage. Additionally, inflammation was simply thought of as a product of joint damage, playing little to no role in disease progression; however, in recent years, there has been a paradigm shift in how clinicians and scientists think of OA inflammation, and how it may contribute to the progression of joint damage and subsequent pain in OA (Liu-Bryan & Terkeltaub, 2014). In OA, inflammation is the product of many different pro-inflammatory molecules, including, but not limited to, cytokines, the complement system, alarmins and neuropeptides. The contribution of complement activation and alarmin signalling to joint damage has been thoroughly investigated in terms of OA pathogenesis (Wang et al., 2011; van Lent et al., 2012;); however, one avenue that has been underexplored is the possible contribution of neurogenic factors to early OA pathogenesis. Immunomodulatory neuropeptides like SP, CGRP and VIP have all been implicated in clinical and experimental synovitis (Levine et al., 1984, 1985; Saito & Koshino, 2000; Saito, 2003). As shown in the previous chapter, saphenous nerve stimulation can increase leukocyte-endothelial interactions within the microcirculation of the knee, and this effect is primarily mediated by VIP. Furthermore, when applied exogenously, SP and VIP increased leukocyte adherence within synovial post-capillary venules. As for the role of neurogenic inflammation in experimental models, inhibition of global nociceptor activity using capsaicin (s.c.) decreased swelling in a rat model of polyarthritis (Cruwys et al., 1995) and leukocyte infiltration in a guinea pig model of

monoarthritis (Hood et al., 2001); however, neuropeptidergic control of early inflammation in the MIA mouse model of OA has yet to be investigated.

Intra-articular injection of MIA, a highly chondrotoxic agent, is frequently used to induce OA-like symptoms in rodents. In most studies, at least 14 days is given after MIA injection before testing the animals, because the most profound joint damage is present after this time point. Although OA symptoms are found 14 days after injection, there is evidence of an early inflammatory phase in this model, at 1-3 days after injection of MIA (Bove et al., 2003). Furthermore, an ongoing study from our laboratory has found that joint diameter, leukocyte rolling, leukocyte adherence, and articular blood flow are all increased 1 day after injection of MIA, and all of these measures subsided after 3 days (Figure 5.1; unpublished data). One aim of this study was to characterize this inflammatory phase, and, more specifically, identify the role of neurogenic inflammation in the early inflammatory phase of the MIA model.

Given the anti-inflammatory effects of endocannabinoid modulation, we hypothesized that URB597 would be capable of decreasing inflammation during the early inflammatory phase of the MIA model. As shown in the previous chapters, the FAAH inhibitor URBB597 decreased KC-induced inflammation, as well as saphenous nerve stimulation-induced neurogenic inflammation. The anti-inflammatory effects of URB597 in the KC model were CB1R and CB2R mediated, while its effects on neurogenic inflammation involved GPR55. The second aim of this study was to test the effects of local URB597 administration on MIA-induced inflammation at day 1, and determine if the endocannabinoid system could be a viable target for decreasing inflammation in early OA.

Our reason for characterizing the early inflammatory phase of the MIA model, and the effects URB597 on this response, was the possibility to attenuate the development of pain in this model. Mice overexpressing CB2R receptors are protected against the development of MIA-induced joint pain (La Porta et al., 2013); therefore, the final aim of this study was to test if prophylactic URB597 treatment could decrease the development of pain 14 days after MIA injection.

Three hypotheses were tested in this study.

I. **MIA-induced inflammation is driven at least in part by neurogenic mechanisms, and, therefore, neuropeptide antagonism would decrease leukocyte-endothelial interactions and hyperaemia at day 1 in this model (Section 5.2).**
II. **Local administration of the FAAH inhibitor URB597 would decrease acute (day 1) inflammation in MIA-injected knees (Section 5.3).**
III. **Prophylactic URB597, before MIA injection and throughout the early inflammatory phase, would inhibit the development of nociceptive behaviours at day 14 (Section 5.4).**

5.2 Neurogenic component of MIA-induced inflammation

5.2.1 Methods

C57Bl/6 mice were deeply anaesthetised with isoflurane (2-3%; 1L/min; 100% O_2), after which MIA (0.3mg; 10µl saline) was injected into the intra-articular space of the right knee joint. This dose was based on a previous pilot study from our laboratory, where this dose was the most effective for inducing nociceptive behaviours in mice 14 days after injection. Following injection of MIA, mice were returned to their cages for

24hrs, after which inflammation was assessed with or without neuropeptide inhibition. This time point was chosen based on previous experiments from our lab (Figure 5.1; unpublished data), as well as others (Bove et al., 2003; Guzman et al., 2003), where the most robust inflammation was observed 24hrs after MIA injection.

Before assessing inflammation, the trachea was cannulated to provide an open airway, and the right carotid artery and jugular vein were cannulated to measure mean arterial pressure and allow venous access, respectively. R6G (0.05%; 0.05ml saline), which fluorescently labels circulating leukocytes, was administered via the jugular cannula, and the skin overlying the joint was surgically removed, exposing the synovial microcirculation. For each mouse, three 1min baseline IVM videos were recorded, and a 1min LASCA baseline was taken. Subsequently a 100µl bolus of either RP67580 (SP antagonist; 20nmol; DMSO: cremophor: saline, 1:1:8), $CGRP_{8-37}$ (CGRP antagonist; 1nmol; saline) or VIP_{6-28} (VIP antagonist; 1nmol; saline), or their respective vehicle was applied topically over the exposed joint. IVM and LASCA inflammatory measures were then reassessed 10min after drug administration.

5.2.2 Results

5.2.2.1 Effects of neuropeptide antagonism on MIA-induced leukocyte-endothelial interactions

When compared to vehicle control (DMSO: cremophor: saline, 1:1:8), RP67580 (20nmol) significantly decreased MIA-induced leukocyte rolling 10min after drug administration ($P<0.05$; n=5-8; Figure 5.2 A). $CGRP_{8-37}$ (6.4nmol) also significantly decreased leukocyte rolling, when compared to saline vehicle ($P<0.05$; n=6-8; Figure 5.2

A). When compared to saline vehicle, VIP_{6-28} trended towards a decrease, but this effect was not significant (P>0.05; n=5-8; Figure 5.2 A).

Similar to its effect on leukocyte rolling, RP67580 significantly decreased leukocyte adherence when compared to vehicle (unpaired two-tailed t test; P<0.05; n=5-8; Figure 5.2 B). Neither $CGRP_{8-37}$, nor VIP_{6-28}, had an effect on day 1 MIA-induced leukocyte adherence when compared to saline control (P>0.05; n=5-8; Figure 5.2 B).

5.2.2.2 Effect of neuropeptide antagonism on MIA-induced articular hyperaemia

When compared to their respective vehicle controls, RP67580 (P>0.05; n=5-8; Figure 5.2 C), $CGRP_{8-37}$ (P>0.05; n=6-8; Figure 5.2 C), or VIP_{6-28} (P>0.05; n=5-8; Figure 5.2 C) all failed to decrease day 1 MIA-induced hyperaemia.

5.3 Effect of URB597 on day 1 MIA-induced knee joint inflammation

5.3.1 Methods

The next goal of this study was to investigate if URB597 could decrease day 1 MIA-induced inflammation. To test this, MIA (0.3mg; 10µl saline) was injected into the right knee joint of deeply anaesthetised C57Bl/6 mice (isoflurane; 2-3%; 1L/min; 100% O_2), after which the mice were returned to their cages. After 24hrs, the mice were anaesthetised with urethane (25%; 0.3-0.4ml; saline), and prepared for articular vascular analysis. Three 1min baseline IVM videos were recorded, followed by a 1min LASCA measurement. Following baseline, a 100µl bolus of either vehicle (DMSO: cremophor: saline, 1:1:8), low-dose URB597 (0.3mg/kg), or medium-dose URB597 (3.0mg/kg) was applied topically to the exposed knee joint. After 20min, IVM and LASCA measures were reassessed.

5.3.2 Results

When compared to vehicle control, low dose URB597 (0.3mg/kg) had no effect on leukocyte rolling ($P>0.05$; n=6-8; Figure 5.3 A), but significantly decreased leukocyte adherence ($P<0.05$; n=6-8; Figure 5.3 B) during the early inflammatory phase of the MIA model. The higher dose of URB597 (3.0mg/kg) had no effect on leukocyte rolling ($P>0.05$; n=6-8) or adherence ($P>0.05$; n=6-8; Figure 5.3 AB).

When the effects of URB597 on MIA-induced hyperaemia were assessed, the lower dose (0.3mg/kg) significantly decreased articular blood flow ($P<0.05$; n=6-8; Figure 5.3 C), while the higher dose (3.0mg/kg) had no effect ($P>0.05$; n=6-8; Figure 5.3 C).

5.4 Prophylactic effect of URB597 (0.3mg/kg) on the development of MIA-induced joint pain

5.4.1 Methods

Based on the results from the previous section, low-dose URB597 (0.3mg/kg) is capable of decreasing inflammation during day 1 of the MIA OA model; therefore, we set investigated if this anti-inflammatory effect could inhibit the development of pain in MIA-treated joints. For this study, all mice received an intra-articular injection of MIA (0.3mg; 10µl; saline) into the right knee joint, expect for one group, which received an intra-articular injection of saline (0.9%; 10µl). The MIA-injected mice were further subdivided into five groups, making six groups in total:

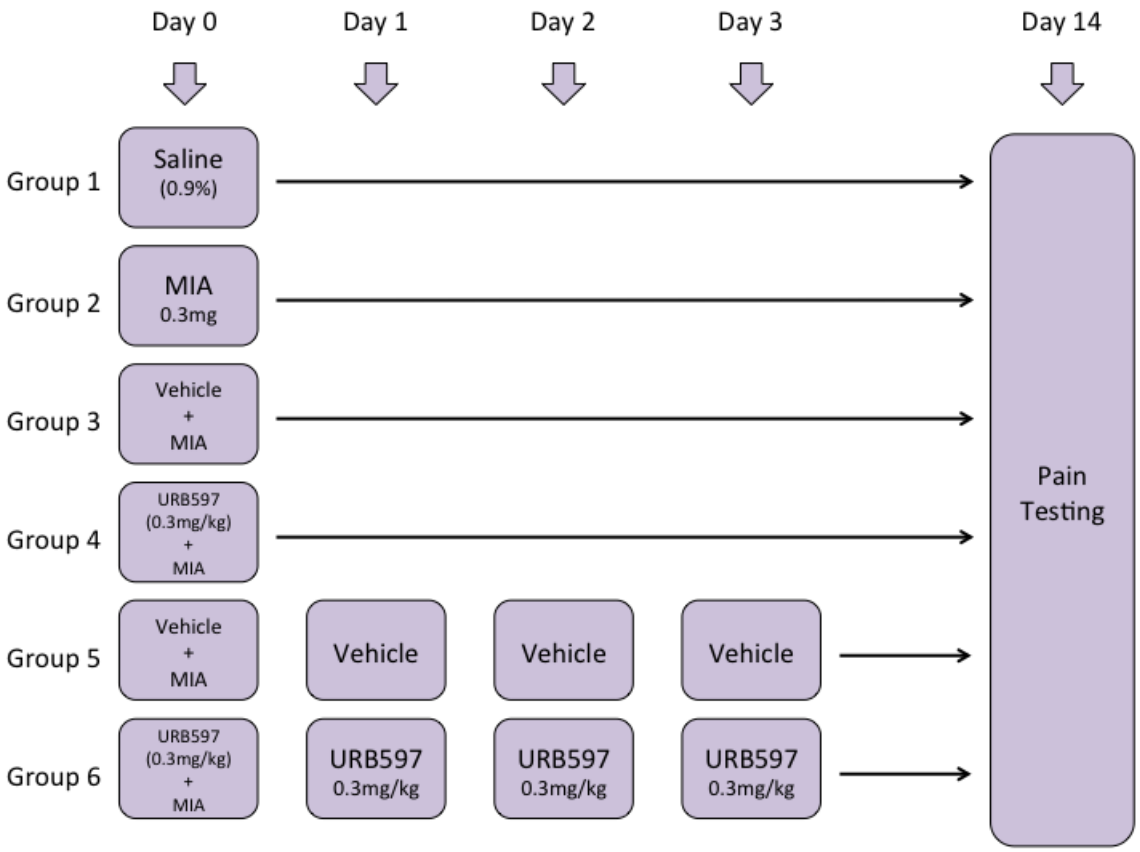

All drug or vehicle treatments were administered locally to the affected knee joint as a 10µl bolus (s.c.). Hindlimb incapacitance and von Frey hair algesiometry were assessed on day 14. Each mouse underwent von Frey hair testing, and was then placed in the dynamic hindlimb weight bearing apparatus. Weight bearing was measured for 5mins.

5.4.2 Results

5.4.2.1 Hindlimb incapacitance

Although intra-articular MIA normally reduces weight bearing on the affected hindlimb, this effect was not observed in this study, and there was no-difference in hindlimb weight bearing between saline injected (0.9%; intra-articular) and MIA-injected (0.3mg; intra-articular) mice ($P>0.05$; n=5-9; Figure 5.4). Furthermore, when

compared to their vehicle controls, neither single-dose URB597 (0.3mg/kg 30min before MIA), nor repeated-dose URB597 (0.3mg/kg x4), had any effect on hindlimb weight bearing in MIA-injected mice ($P>0.05$; n=6-10; Figure 5.4).

5.4.2.2 Von Frey hair algesiometry

When compared to saline-injected controls, intra-articular MIA (0.3mg) significantly reduced von Frey hair tactile sensitivity 14 days after injection ($P<0.05$; n=5-9; Figure 5.4). Prophylactic single-dose URB597 (0.3mg/kg) had no effect on MIA-induced tactile allodynia, when compared to vehicle control ($P>0.05$; n=6-9; Figure 5.4). When compared to vehicle control, repeated treatments with URB597 (0.3mg/kg x4) completely abolished the development MIA-induced hypersensitivity ($P<0.05$; n=8-9; Figure 5.4).

5.5 Chapter summary

5.5.1 MIA-induced inflammation has a neurogenic component

The results presented in section 5.3 would suggest that inflammatory neuropeptides do play a role in MIA-induced inflammation. Both SP and CGRP antagonism reduced leukocyte rolling 1day after MIA injection. Furthermore, RP67580, the SP receptor (NK1) antagonist, was also capable of decreasing leukocyte adherence during this early inflammatory phase. Interestingly, despite playing a role in leukocyte-endothelial interactions, immunomodulatory neuropeptide antagonism had no effect on inflammatory hyperaemia during day 1 MIA-induced inflammation.

5.5.2 URB597 decreases MIA-induced inflammation

When applied locally to the MIA-injected knee, the lower-dose of URB597 (0.3mg/kg) significantly decreased inflammatory leukocyte adherence and hyperaemia, while having no effect on leukocyte rolling. Interestingly, although only two doses were tested, it would appear that this anti-inflammatory effect is lost with higher-doses of URB597, which corroborates the findings presented in Chapter 3, where URB597 had a U-shaped dose response curve when tested against KC-induced joint inflammation.

5.5.3 URB597 inhibits the development of MIA-induced joint pain

In this study, our goal was to test if URB597 treatment during the early inflammatory phase of the MIA OA model could decrease the development of pain at day 14. Based on the results presented in Section 5.5, the multiple dosing regimen of URB597 (0.3mg/kg; once before MIA, then daily for 3 days) significantly attenuated the development of von Frey hair tactile allodynia.

5.6 Figures

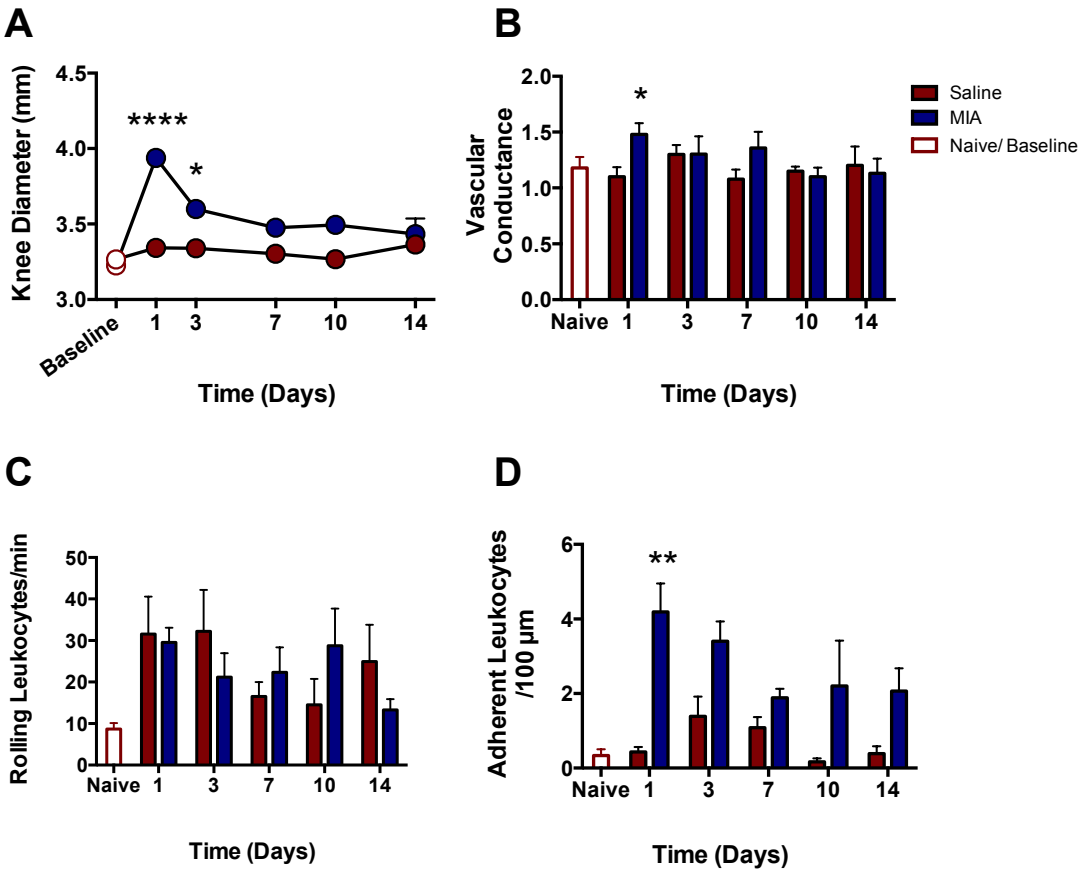
A
Knee Diameter (mm)
4.5
4.0
3.5
3.0
****
*
Baseline
1
3
7
10
14
Time (Days)
B
Vascular Conductance
2.0
1.5
1.0
0.5
0.0
*
Naive
1
3
7
10
14
Time (Days)
Saline
MIA
Naive/ Baseline
C
Rolling Leukocytes/min
50
40
30
20
10
0
Naive
1
3
7
10
14
Time (Days)
D
Adherent Leukocytes /100 µm
6
4
2
0
**
Naive
1
3
7
10
14
Time (Days)

Figure 5.1 Time-course of MIA-induced articular inflammation in mice. (A) Effect of intra-articular MIA on knee joint diameter. When compared to saline control, knee joint diameter was significantly increased 1 day ($P<0.0001$; n=9-30), and 3 days ($P<0.05$; n=6), after MIA injection. Knee joint diameter was not significantly different between MIA- and saline-injected knees on days 7, 10 or 14 ($P>0.05$; n=5-6). **(B)** Effect of intra-articular MIA on synovial inflammatory hyperaemia. When compared to saline injected controls, intra-articular MIA significantly increased knee joint blood flow 1day after injection ($P<0.05$; n=10-27), but not on subsequent days ($P>0.05$; n=4-6). **(C)** Effect of intra-articular MIA on leukocyte rolling within the synovial microcirculation. When compared to saline control, MIA had no effect on leukocyte rolling *in vivo* ($P>0.05$; n=4-27). **(D)** Effect of intra-articular MIA on leukocyte adherence within synovial post capillary venules. When compared to saline vehicle, leukocyte adherence was significantly increased 1day after MIA injection ($P<0.05$; n=9-27), but not at later time-points ($P>0.05$; n=4-6).

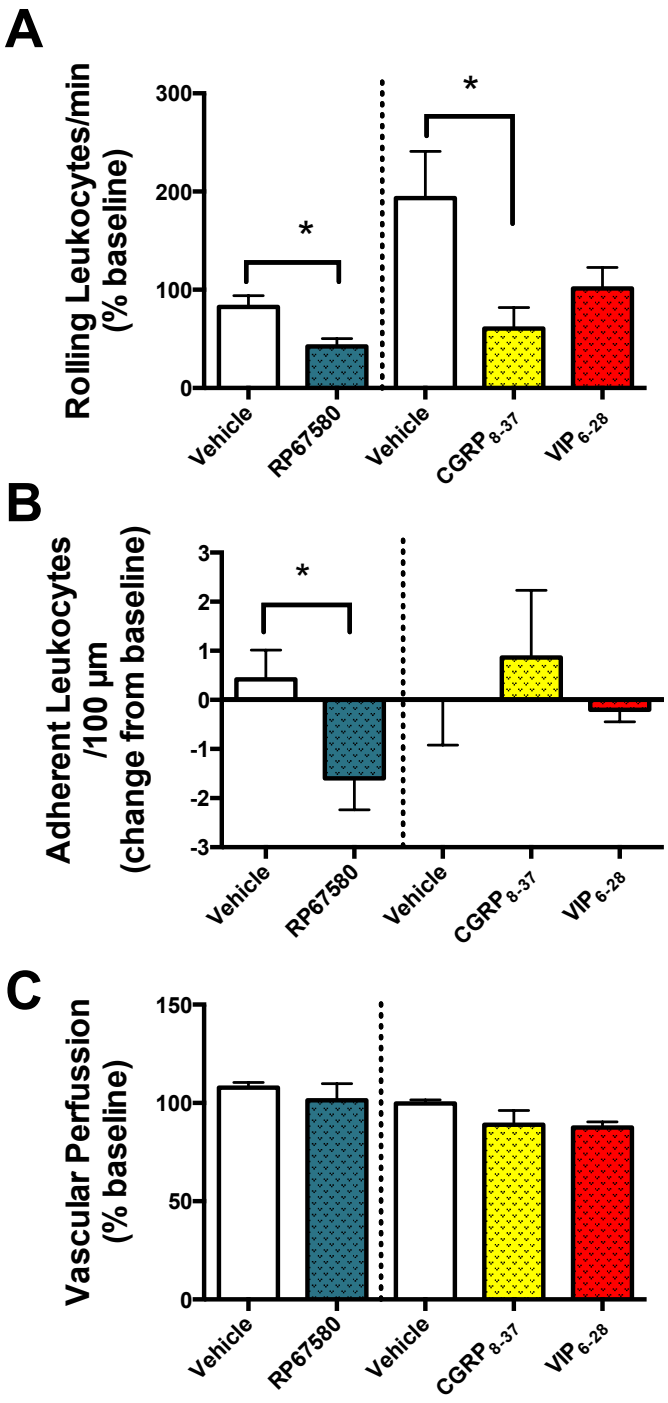
A
Rolling Leukocytes/min
(% baseline)
300
200
100
0
*
*
Vehicle
RP67580
Vehicle
CGRP 8-37
VIP 6-28
B
Adherent Leukocytes
/100 µm
(change from baseline)
3
2
1
0
-1
-2
-3
*
Vehicle
RP67580
Vehicle
CGRP 8-37
VIP 6-28
C
Vascular Perfussion
(% baseline)
150
100
50
0
Vehicle
RP67580
Vehicle
CGRP 8-37
VIP 6-28

Figure 5.2 Neurogenic component of day 1 MIA-induced inflammation. (A) Effect of neuropeptide antagonism on leukocyte rolling within the synovial microcirculation. When compared to vehicle control (DMSO: cremophor: saline, 1:1:8), RP67580 (20nmol) significantly decreased leukocyte rolling 10mins after drug administration (unpaired two-tailed t test; $P<0.05$; n=5-8). $CGRP_{8-37}$ (6.4nmol) also decreased leukocyte rolling when compared to control (0.9% saline) (one-way ANOVA with Dunnett; $P<0.05$; 6-8), while VIP_{6-28} (1.0nmol) did not (one-way ANOVA with Dunnett; $P>0.05$; n=5-8). **(B)** Effect of neuropeptide antagonism on leukocyte adherence within the synovial microcirculation. When compared to vehicle control (DMSO: cremophor: saline, 1:1:8), RP67580 (20nmol) significantly reduced the number of adherent leukocytes within 100μm of vessel (unpaired two-tailed t test; $P<0.05$; n=5-8). Neither $CGRP_{8-37}$ (6.4nmol), nor VIP_{6-28} (1.0nmol), had an effect on leukocyte adherence within the synovial microcirculation of MIA-injected knees (Kruskal Wallis test with Dunn; $P>0.05$; n=5-8). **(C)** Effect of neuropeptide antagonism on articular blood flow. There was no change in articular blood flow when the knees were treated with RP67580 (unpaired two-tailed t test; $P>0.05$; n=5-8), $CGRP_{8–37}$ (Kruskal Wallis test with Dunn; $P>0.05$; n=5-8), or VIP_{6-28} (Kruskal Wallis test with Dunn; $P>0.05$; n=5-8).

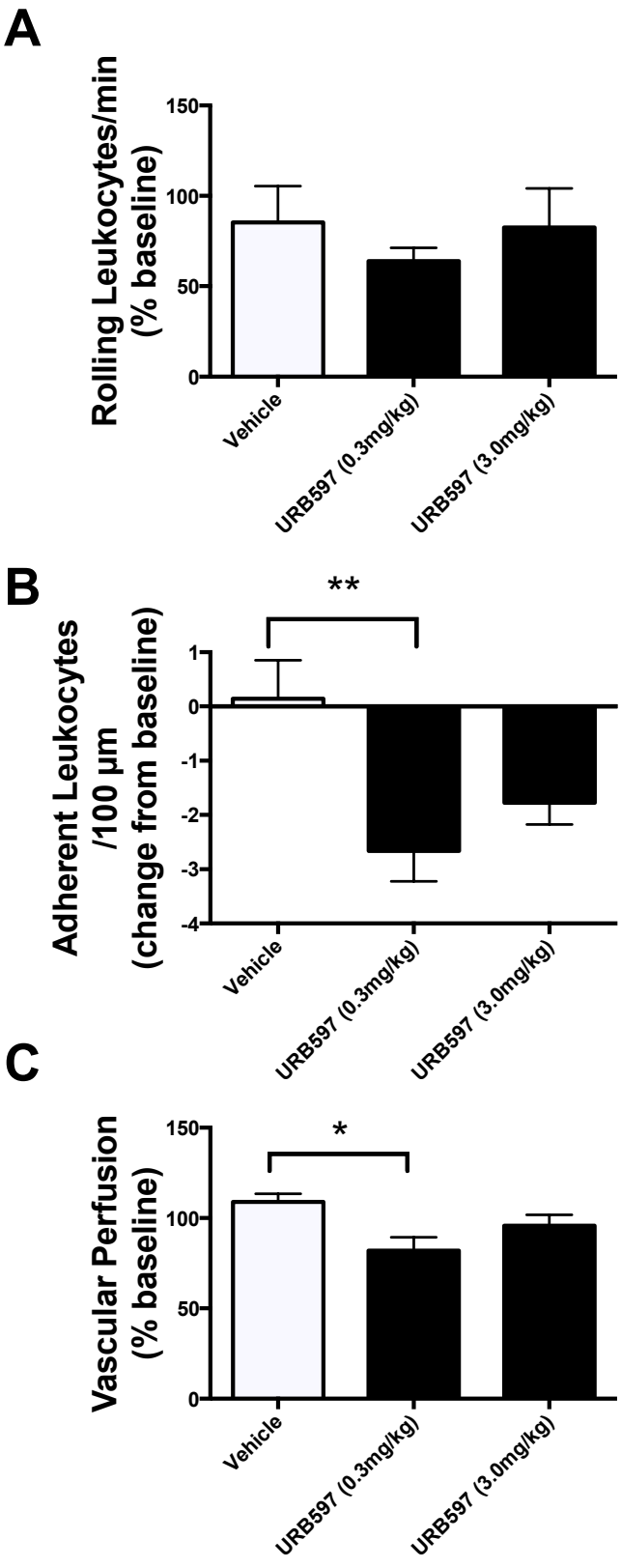
A
Rolling Leukocytes/min
(% baseline)
150
100
50
0
Vehicle
URB597 (0.3mg/kg)
URB597 (3.0mg/kg)
B
**
Adherent Leukocytes
/100 µm
(change from baseline)
1
0
-1
-2
-3
-4
Vehicle
URB597 (0.3mg/kg)
URB597 (3.0mg/kg)
C
*
Vascular Perfusion
(% baseline)
150
100
50
0
Vehicle
URB597 (0.3mg/kg)
URB597 (3.0mg/kg)

Figure 5.3 Effect of URB597 on day 1 MIA-induced inflammation. (A) Effect of locally administered URB597 on leukocyte rolling within the synovial microcirculation of MIA-injected knees. Neither low-dose URB597 (0.3mg/kg), nor the higher-dose (3.0mg/kg), had an effect on leukocyte rolling when compared to vehicle (DMSO: cremophor: saline, 1:1:8) (one-way ANOVA with Dunnett; $P>0.05$; n=6-8). **(B)** Effect of local URB597 on leukocyte adherence within synovial post-capillary venules. The lower dose of URB597 (0.3mg/kg) significantly decreased leukocyte adherence when compared to vehicle (DMSO: cremophor: saline, 1:1:8) (Kruskal Wallis test with Dunn; $P<0.01$; n=6-8), while the higher dose of URB597 had no effect (Kruskal Wallis test with Dunn; $P>0.05$; n=5-8). **(C)** Effect of URB597 on MIA-induced inflammatory hyperaemia. Low-dose URB597 (0.3mg/kg) significantly decreased knee joint blood flow when compared to vehicle (DMSO: cremophor saline, 1:1:8) (one-way ANOVA with Dunnett; $P<0.05$; n=6-8), while the higher dose had no effect (one-way ANOVA with Dunnett; $P>0.05$; n=5-8).

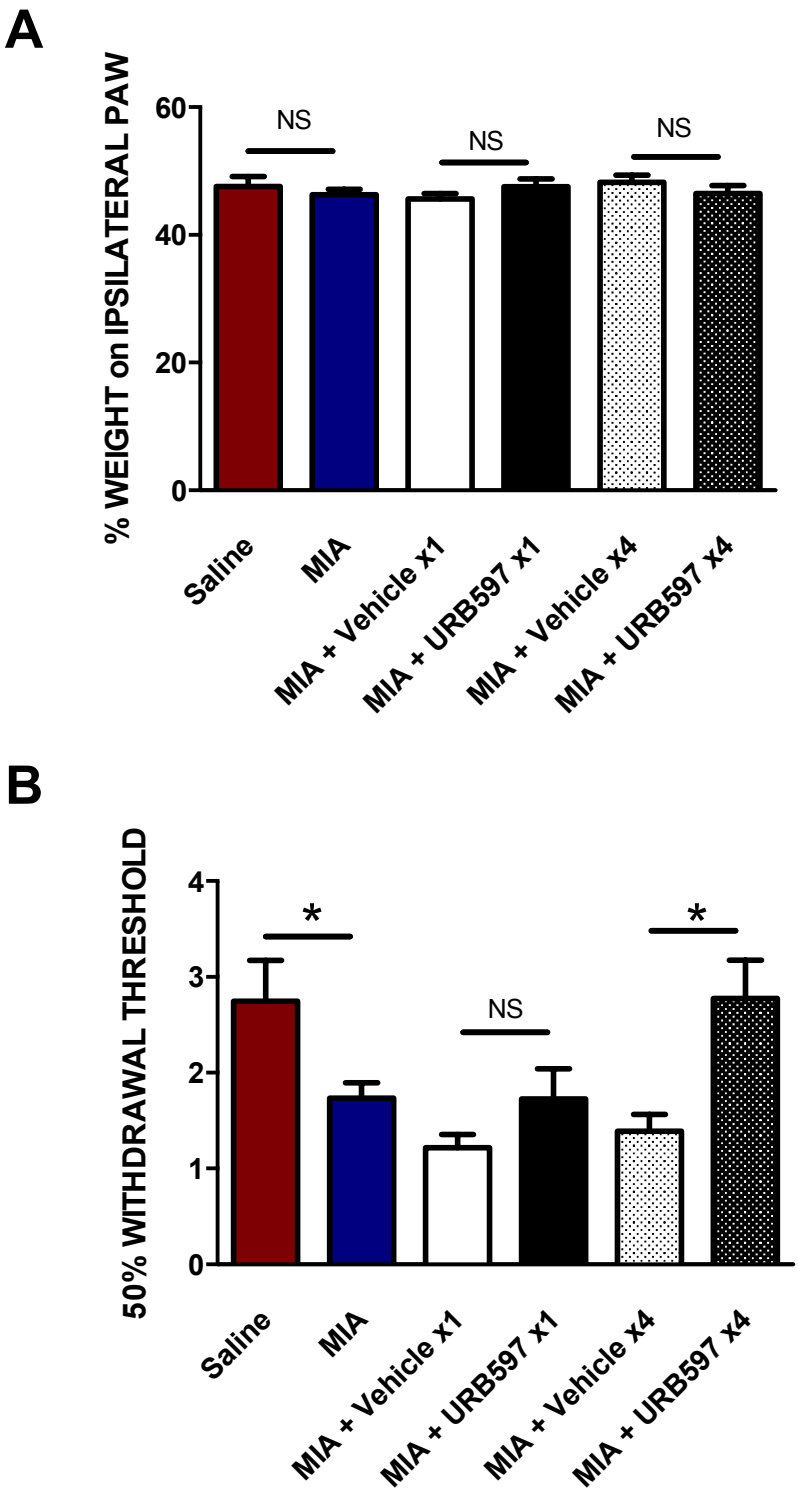
A
% WEIGHT on IPSILATERAL PAW
60
40
20
0
NS
NS
NS
Saline
MIA
MIA + Vehicle x1
MIA + URB597 x1
MIA + Vehicle x4
MIA + URB597 x4
B
50% WITHDRAWAL THRESHOLD
4
3
2
1
0
*
NS
*
Saline
MIA
MIA + Vehicle x1
MIA + URB597 x1
MIA + Vehicle x4
MIA + URB597 x4

Figure 5.4 Effect of prophylactic URB597 treatment on the development of nociceptive behaviours 14 days after MIA injection. (A) Effect of URB597 on hindlimb weight bearing. Intra-articular injection of MIA had no effect on hindlimb weight bearing when compared to saline-injected controls (unpaired two-tailed t test; $P>0.05$; n=9-14). Neither single-dose URB597 (0.3mg/kg x1; s.c. atop knee before MIA injection), nor multi-dose URB597 (0.3mg/kg x4; s.c. atop MIA-injected knee), had an effect on hindlimb weight bearing in MIA-injected mice, when compared to their respective controls (unpaired two-tailed t test; $P>0.05$; n=6-10). **(B)** Effect of URB597 on von Frey hair tactile sensitivity. Intra-articular MIA significantly reduced von Frey hair withdrawal thresholds 14 days after injection (unpaired two-tailed t test; $P<0.05$; n=9-14). Single dose URB597 had no effect on MIA-induced tactile sensitivity (0.3mg/kg x1; s.c. atop knee before MIA injection), when compared to vehicle control (DMSO: cremophor: saline, 1:1:8) (unpaired two-tailed t test; $P>0.05$; n=6-9). Multi-dose URB597 (0.3mg/kg x4; s.c. atop MIA-injected knee) abolished MIA-induced von Frey hair hypersensitivity on day 14 (unpaired two-tailed t test; $P<0.05$; n=8-10).

Chapter 6: Discussion

The results presented here further confirm a role for neurogenic inflammation in joint inflammation, and implicate SP, VIP and CGRP as all playing a role in modulating murine synovitis. Furthermore, the ability of endocannabinoid modulation to decrease inflammation was shown in three separate models of knee joint inflammation, and a role for CB1R, CB2R and GPR55 was identified.

6.1 Articular Neurogenic Inflammation

There is evidence suggesting that neurogenic factors contribute to inflammation in a number of different organs. In his seminal paper on the subject, William Bayliss described the effect of small diameter afferent electrostimulation on blood flow in the hindlimbs of dogs (Bayliss, 1901). Plasma extravasation, and subsequent joint oedema, can also be induced by stimulating the posterior articular nerve of cats (Ferrell & Russell, 1985; 1986). The results presented in Chapter 4 suggest that electrostimulation of the saphenous nerve can increase or decrease leukocyte rolling within the synovial microcirculation, depending on the stimulation frequency. When the nerve was stimulated at higher frequencies (2Hz and 5Hz) there was a significant increase in the number of rolling leukocytes, while a significant reduction was observed following low-frequency stimulation (0.5Hz). These results suggest that antidromic stimulation of the articular innervation can have both pro-inflammatory and anti-inflammatory effects, with higher frequency stimulation promoting leukocyte trafficking, and lower frequency stimulation reducing leukocyte-endothelial interactions.

6.1.1 Contribution of neuropeptides to acute synovitis

Numerous immunomodulatory neuropeptides have been implicated in neurogenic inflammation; however, of these signalling molecules, SP has undoubtedly garnered the most attention. In sensory neurons, SP is synthesized within the soma and transported bidirectionally, towards the CNS and periphery (MacLean, 1987). In the periphery, SP is stored within nociceptive free nerve endings and modulates local inflammatory responses upon release (Larsson et al., 1976; Gamse et al., 1980; Noguchi et al., 1990). When administered directly to the knee joint, SP causes vasodilation and plasma extravasation in normal joints, but shows virtually no response in inflamed joints (McDougall et al., 1994). Furthermore, the SP fragment (D-Pro^{4}, DTrp^{7,9,10})-SP$_{4\text{-}11}$, which is an NK (NK$_1$ - NK$_3$) receptor antagonist, is capable of decreasing antidromic stimulation-induced plasma extravasation *in vivo* (Ferrell & Russell, 1985). As shown in Chapter 4, local application of SP to naïve mouse knee joints is also capable of increasing leukocyte rolling and adherence within the synovial microcirculation. Our results are in agreement with a previous study, where incubation with SP promoted the expression of CAMs on isolated endothelial cells *in vitro*, suggesting a direct action of SP on endothelial cells (Vishwanath & Mukherjee, 1996). Another possible mechanism for SP-induced leukocyte rolling and adherence involves the release of histamine from mast cells. In a previous study, the pro-inflammatory effects of SP were partially mediated by histamine, and SP-induced vasodilation and plasma extravasation were blocked by histamine antagonism and mast cell depletion (Lembeck & Holzer, 1979); therefore,

it is likely that the effects of SP on leukocyte kinetics presented in Chapter 4 involve direct action on endothelial cells, as well as mast-cells.

The results presented in Chapter 4 also implicate VIP as having pro-inflammatory effects in mouse knee joints. VIP antagonism blocked saphenous stimulation (2Hz)-induced leukocyte rolling and, when exogenous VIP was applied directly to the joint, it promoted leukocyte adherence within synovial post-capillary venules. These results corroborate a previous finding, where VIP was chemotactic and promoted macrophage adherence *in vitro* (de la Fuente et al., 1994; Ahmed et al., 1998). It is possible that VIP is playing a pro-inflammatory role in the joint, and promoting synovitis by recruiting immune cells. Interestingly, VIP has recently gained significant attention for its anti-inflammatory effects in multiple inflammatory pathologies, including the rheumatic diseases (reviewed Gonzalez-Rey et al., 2007); therefore, another possibility is that VIP-induced leukocyte recruitment may actually be part of an anti-inflammatory mechanism. Increased leukocyte recruitment is normally considered pro-inflammatory, because, for the most part, infiltrating leukocytes promote local inflammatory processes; however, the recruitment of certain leukocyte subtypes can actually be anti-inflammatory. Some monocyte and macrophage phenotypes synthesize and release endogenous opioids, and actually have anti-nociceptive and anti-inflammatory effects in the tissues they infiltrate (reviewed Iwaszkiewicz et al., 2013). Given that VIP has been shown to promote the resolution of inflammation, it is possible that VIP-mediated leukocyte recruitment may actually serve a similar purpose.

Another interesting observation presented in Chapter 4 was that low frequency saphenous stimulation (0.5Hz) decreased leukocyte rolling. One possibility is that this effect is also VIP-mediated, and, at lower concentrations, VIP decreases leukocyte rolling, while promoting it at higher concentrations. In addition to VIP, somatostatin and endomorphin-1 are two other neuropeptides that have gained significant attention for their anti-inflammatory effects. Somatostatin was originally discovered in the hypothalamus, where it has numerous signalling functions (Ling et al., 1973). In the periphery, somatostatin is expressed in DRG neurons (Hökfelt et al., 1976), and transported down the axon towards the peripheral nerve endings (Rasool et al., 1981). *In vitro,* somatostatin decreases leukocyte migration towards the potent chemokine stromal cell-derived factor 1-α (Talme et al., 2004), as well as SP (Kolasinski et al., 1992). Furthermore, somatostatin reduces histamine release from human basophils *in vitro* (Goetzl & Payan, 1984). *In vivo*, systemic administration of somatostatin analogue TT-232 decreased oedema in a model of adjuvant-induced arthritis, while somatostatin antagonism exacerbated symptoms in this model (Helyes et al., 2004). Endomorphin-1 is also stored in the peripheral terminals of joint nociceptors, and decreases blood flow in normal and acutely inflamed joints, but not during chronic joint inflammation (McDougall et al., 2004a; McDougall et al., 2004b). It is therefore possible that somatostatin or endomorphin-1 may play a role in the inhibitory effect of low frequency (0.5Hz) saphenous stimulation on leukocyte rolling.

6.1.2 Involvement of neuropeptides in joint disease

Based on the results of numerous pre-clinical and clinical studies, it appears that neurogenic mechanisms contribute to inflammation in a number of different

arthropathies. SP antagonism is capable of reducing carrageenan-induced joint inflammation by 44%; therefore, suggesting a neurogenic component to this model (Lam & Ferrell, 1989). Furthermore, in a model of gouty arthritis, where monosodium urate (MSU) crystals are injected directly into the intra-articular space, researchers observed immediate SP release from articular nociceptors following MSU injection (Lunam & Gentle, 2004). This finding is corroborated by clinical evidence, where SP and CGRP levels were significantly higher in the synovial fluid of gout patients, when compared to patients with degenerative arthritis (Hernanz et al., 1993). Furthermore, in a model of adjuvant-induced arthritis, the ankle developed more severe arthritis when compared to the knee, and it was hypothesized that this was due to the fact that the ankle has a higher degree of SP positive innervation than the knee (Levine et al., 1985). Additionally, nociceptor specific denervation, using capsaicin, protects the joint from swelling and pain, as well as histological and radiographic scores of joint damage in adjuvant-induced arthritis (Cruwys et al., 1995).

Previous results from our laboratory have shown that joint oedema, leukocyte trafficking and blood flow are all increased on day 1 in the MIA model. The results presented in Chapter 5 suggest for the first time that neurogenic inflammation contributes to this early inflammatory response that occurs 1day after intra-articular MIA injection. Based on the results presented here, it appears that SP plays a role in both leukocyte rolling and adherence, while hyperaemia is not mediated by neurogenic mechanisms. These results are in agreement with those presented in Chapter 4, where locally applied SP increased both leukocyte rolling and adherence within the synovial microcirculation, as well as a previous study from our laboratory

where RP67580 decreased leukocyte rolling and adherence in PAR2-induced joint inflammation (Russell et al., 2012). Interestingly, VIP does not appear to be involved in MIA-induced leukocyte-endothelial interactions, despite showing activity in stimulation-induced leukocyte rolling, and promoting adherence when administered topically to naïve knee joints. It is, therefore, possible that VIP only increases leukocyte-recruitment during the very acute phase of joint inflammation, but is not involved in a more developed inflammatory response, like that observed 24hrs after MIA injection. In addition to SP, CGRP antagonism also decreased MIA-induced leukocyte rolling, when compared to vehicle control. This result is in agreement with a previous finding where $CGRP_{8-37}$ blocked ischemia/reperfusion-induced leukocyte rolling, but not adherence, in the gut (Yusof et al., 2007); however, this finding should be interpreted with caution, as the saline control in this group produced an increase in leukocyte rolling on its own, which undoubtedly skewed the significance of the CGRP effect.

Interestingly, none of the neuropeptide antagonists had an effect on MIA-induced hyperaemia. This finding is intriguing, because the involvement of SP and CGRP in MIA-induced leukocyte-endothelial interactions would suggest that these neuropeptides are released in this model. Furthermore, numerous other studies have shown that both these peptides are capable of promoting articular hyperaemia (Lam & Ferrell, 1993; McDougall et al., 1999). There are several possible reasons why SP and CGRP antagonism only decreased leukocyte-endothelial interactions, but not blood flow, in the MIA model at day 1. The first possibility is that local concentrations of SP and CGRP are high enough to induce leukocyte-endothelial interactions, but not

hyperaemia. The second possibility is that the doses of antagonists used in this study were adequate for blocking the effects of SP and CGRP and on leukocyte-endothelial interactions, but insufficient at blocking hyperaemia. Regardless, future studies should aim to uncover which inflammatory mediators are driving MIA-induced hyperaemia.

What cannot be deduced from these results is whether or not inflammation promotes disease progression in this model. Although we did show that URB597 is anti-inflammatory, and that it does reduce the development of pain in this model (which will be discussed in more detail below), these two effects may be entirely unrelated. Future studies should further investigate the role of neurogenic inflammation in the MIA model, and the role it plays in disease progression.

6.2 Targeting the endocannabinoid system in arthritis

Targeting the endocannabinoid system for the treatment of rheumatic conditions is not a new concept. Arthritis sufferers are the most prevalent users of medicinal cannabis, and records of cannabis use amongst arthritis patients go back as far as ancient Egyptian manuscripts (Zias et al., 1993). A relatively newer concept, however, is modulating endocannabinoid levels to treat arthritic inflammation and pain. One strategy that has proven successful in pre-clinical models has been inhibiting FAAH, the enzyme responsible for anandamide hydrolysis. FAAH is expressed throughout the CNS (Egertová et al., 1998; Füllhase et al., 2013), as well as the periphery, including the knee joints of arthritic patients (Richardson et al., 2008). The results presented in Chapter 1 suggest that local FAAH inhibition is capable of decreasing leukocyte rolling and adherence, as well as hyperaemia, during acute KC-

induced synovitis. Similar results were observed when the effects of synthetic cannabinoids were tested on leukocyte rolling and adherence within the cerebral (Ni et al., 2004; M. Zhang et al., 2007) and ocular (Toguri et al., 2014) microcirculation during inflammation.

Although low to medium doses of URB597 (0.3 and 3.0mg/kg) reduced KC-induced inflammation, this effect was not observed at higher doses. We hypothesized that off-target TRPV1 activation may be involved in this loss of effect at higher doses, but the anti-inflammatory effects of URB597 were not fully restored by pre-treating the mice with SB366791, a TRPV1 antagonist; therefore, some other mechanism must be responsible for the lack of effect of URB597 at higher doses. One possibility is that increased anandamide signalling is causing receptor down-regulation, as this effect has been shown *in vitro* (Martini et al., 2007). An interesting future study would be to quantify the difference in membrane expressed CB1R and CB2R between inflamed knee joints treated with a range of doses of URB597. A second possibility is that FAAH inhibition may be promoting the conversion of anandamide into pro-inflammatory prostamides. Although FAAH-mediated hydrolysis is the primary endogenous mechanism for attenuating anandamide signalling, anandamide can also be oxidized by COX2, and this reaction produces prostaglandin-ethanolamides (prostamides) (Yu et al., 1997). As their full-name suggests, prostamides are prostaglandin derivatives, and although their formation stops anandamide signalling, their pharmacology is by no means inert (Woodward et al., 2008). Intrathecal administration of prostamide F2α increases nociceptive behaviours during knee joint arthritis (Gatta et al., 2012), while prostamide F2α

antagonism decreases capsaicin-induced ocular pain (Woodward et al., 2013). The effects of prostamides on synovitis have yet to be explored; however, given their pro-nociceptive effects, as well as their structural similarities to their prostaglandin analogues, it is possible that they have pro-inflammatory effects in the joint. One laboratory has already identified several prostamide F2α antagonists that are also capable of inhibiting FAAH activity (Ligresti et al., 2014). These dual action compounds are capable of inhibiting anandamide breakdown, while blocking the adverse bioactivity of its COX2 metabolites (Ligresti et al., 2014); therefore, possibly circumventing the dose limiting effects of pure FAAH inhibition.

Despite having a U-shaped dose response curve, low and medium dose URB597 (0.3mg/kg and 3.0mg/kg) was effective at decreasing KC-induced synovitis. When we investigated the involvement of cannabinoid receptors in this response, we observed that CB1R and CB2R antagonism abolished the effect of URB597 on leukocyte rolling and hyperaemia, but not leukocyte adherence. This result is in agreement with *in vitro* evidence showing that 2-AG is capable of increasing endothelial cell membrane expression of P- and E-selectin, and this effect was mediated by both CB1R and CB2R (Gasperi et al., 2014). Interestingly, when the effects of the non-selective cannabinoid receptor agonist WIN 55212-2 were tested on CNS inflammation, leukocyte rolling was decreased, but this effect only involved CB2R, not CB1R (Ni et al., 2004). This difference between the effects of the cannabinoid system on leukocyte rolling within the CNS and the knee may be the result of the different drugs used, or may reflect differences in inflammatory mechanisms between both systems.

6.2.1 Effect of endocannabinoid modulation of neurogenic synovitis

The contribution of CB1R to the inhibitory effect of URB597 on KC-induced leukocyte rolling and hyperaemia led us to hypothesize that endocannabinoid modulation may be decreasing the neurogenic component of KC-induced inflammation via CB1R activation. CB1R is expressed on nociceptive free nerve endings (McDougall, 2009), and CB1R activation has been shown to inhibit CGRP release *in vitro* (Engel et al., 2011); therefore, we decided to test URB597 (0.3mg/kg) against saphenous nerve stimulation-induced leukocyte rolling. When we pre-treated the knee with URB597 (0.3mg/kg), we observed that the pro-rolling effect of saphenous nerve stimulation was completely abolished in the presence of the FAAH inhibitor. We hypothesized that this effect would be CB1R mediated, but AM251 had no effect on this response. Interestingly, the CB2R antagonist AM630 also did not restore saphenous stimulation-induced neurogenic rolling in URB597-treated knees. Since neither CB1R nor CB2R appeared to be involved in the effect of URB597 on synovial neurogenic leukocyte rolling, we hypothesized that the non-canonical cannabinoid receptor GPR55 may be involved. When we pre-treated the knee with O-1918, a GPR55 antagonist, followed by URB597, not only was the pro-rolling effect restored, but is also appeared to be greatly exacerbated.

The literature surrounding GPR55 seems to be in disagreement concerning its role in inflammation. Several studies have shown GPR55 to be anti-inflammatory in a number of diseases, as well as pro-inflammatory under particular conditions. The GPR55 agonist O-1602 significantly inhibited the expression of pro-inflammatory cytokines in a mouse pancreatitis model (Li et al., 2013), and decreased movement-

induced C fibre responses during KC-induced joint inflammation (Schuelert & McDougall, 2011). Furthermore, PEA, a fatty acid amide and GPR55 agonist, decreased cytokine expression and histological changes in a colitis model, and GPR55 antagonism blocked this effect (Borrelli et al., 2015). Conversely, GPR55 increases pro-inflammatory cytokine expression in foam cells (obese macrophages) (Lanuti et al., 2015), monocytes and natural killer cells (Chiurchiù et al., 2015), as well as promotes nociceptor sensitization when activated by lysophosphatidylinositol (Gangadharan et al., 2013). Furthermore, GPR55 knockout mice are protected against adjuvant-induced arthritis (Staton et al., 2008). It is therefore possible that the GPR55-mediated inhibitory effect of URB597 on leukocyte rolling could be either pro-inflammatory or anti-inflammatory, and future studies should investigate the phenotypes of the leukocytes being recruited.

6.2.2 Effect of URB597 on MIA-induced pain and inflammation

Similar to its effects on KC-induced inflammation, URB597 also decreased leukocyte adherence and hyperaemia during the early inflammatory phase of the MIA OA model. Once again, this effect was evident with the lowest dose tested, while the higher dose did not produce a statistically significant effect. Furthermore, when URB597 was administered before MIA injection and then daily for three days, the development of pain on day 14 was significantly reduced. This effect is in concert with a previous finding, where CB2R overexpression also decreased the development of MIA-induced pain (La Porta et al., 2013). Interestingly, the fact that repeated-dose URB597 was efficacious, while single dose URB597 was not, is in contrast to another previous study, where a single pre-treatment with URB597, but not pre-treatment

daily for 3 days, before injection of carrageenan decreased the development of carrageenan-induced inflammatory pain (Okine et al., 2012). The authors of this study concluded that chronic pre-treatment with URB597 altered the spinal endocannabinoid system in such a way that the analgesic effects of acute endocannabinoid modulation were negated. One difference between our study and theirs, is that here URB597 was administered locally to joint, while Okine and colleagues administered the FAAH inhibitor systemically. Furthermore, Okine et al., were investigating the development of acute carrageenan-induced inflammatory pain, while we were interested in the development of pain in an OA model. These differences likely contributed to the differences in results between studies.

Our interest in URB597 comes from several pre-clinical studies, which have shown anti-inflammatory and analgesic effects of FAAH inhibition in a number of disease models, including arthritis (Kinsey et al., 2011; Schuelert et al., 2011; Füllhase et al., 2013). Although FAAH inhibition has had success in animal models, its clinical effectiveness in OA has been less than promising. In a clinical trial involving OA patients, the FAAH inhibitor PF-04457845 blocked systemic FAAH activity by >96% and significantly increased systemic fatty acid amide levels, but provided no significant amount of pain relief for the subjects in this trial (Huggins et al., 2012). There are several reasons as to why FAAH inhibition may have failed in this particular study. Firstly, a heterogeneous patient population was used, where no effort was made to identify the source of pain for each subject (*i.e.* inflammatory and/or neuropathic). Given the anti-inflammatory effects of FAAH inhibition, it is possible that a population with more inflammatory-mediated pain would obtain

greater benefit from FAAH inhibition. Secondly, the near complete FAAH inhibition observed in this study may have resulted in an over-accumulation of anandamide, which may have led to off-target effects (Gauldie et al., 2001) or COX-2 metabolites (Yu et al., 1997). Lastly, our results show that FAAH inhibition can attenuate the development of OA pain, while Huggins et al. were trying to treat already established joint pain. Future studies involving FAAH inhibitors should aim to 1) stratify their subject populations, so as to identify patients that would benefit the most from this therapeutic strategy, 2) test the effects of lower doses, 3) test the effects of co-treatment with a COX-2 inhibitor, and 4) test the effects of FAAH inhibition on the development of pain in early OA patients, as well as patients who may be at risk of developing the disease.

6.3 Limitations

6.3.1 Surgery-induced inflammation

The majority of data presented in this study were based on vascular assessment of synovitis, which requires several invasive surgical procedures. The trachea needed to be cannulated to ensure a clear airway throughout the experiment, the carotid artery was cannulated so that MAP could be recorded, and the jugular vein was cannulated to allow venous access. In addition to the aforementioned cannulations, the skin overlying the knee joint of interest was surgically removed in order to expose the synovial microvasculature. Furthermore, an even more invasive procedure was required to isolate the saphenous nerve during the electrostimulation experiments. Due to these surgical procedures, there was a degree of injury-induced inflammation added to each of our models, as well as to our "naïve" groups; therefore, when

interpreting the IVM and LASCA results one should keep in mind that any anti-inflammatory effects may be the effect of a drug on acute injury-induced inflammation, rather than on inflammation induced purely by the model in question. Furthermore, when interpreting our results concerning the effects of electrostimulation and exogenous neuropeptides on synovial leukocyte kinetics, it should be noted that all knees had an underlying degree of inflammation, and that the same results may not occur in unoperated mouse knee joints.

6.3.2 Non-specific rhodamine staining

One limitation of our IVM protocol is that rhodamine 6G stains all circulating leukocytes equally, which prevents us from differentiating between leukocyte lineages and inflammatory phenotypes. This prevents us from being able to tell if rolling and adherent leukocytes have pro-inflammatory or anti-inflammatory phenotypes. This limitation was most evident when trying to interpret our VIP-mediated saphenous nerve stimulation results. Because we are unable to differentiate leukocyte phenotypes using our technique, we do not know whether the leukocytes recruited by VIP would promote or resolve inflammation.

6.3.3 Adherence calculations

Throughout this manuscript, adherence was calculated as the number of adherent leukocytes per unit length of the vessel of interest. While this protocol has been standard for our laboratory, other groups have reported leukocyte adherence as a measure of total adherent leukocytes per area of vessel. When compared to this latter

method, our technique is less precise, as it does not take into account differences in vessel diameters.

6.3.4 Animal models of arthritis

No animal model is perfect, and that is the case in any *in vivo* study; however, the degree to which a model approximates the true symptoms of a human disorder defines the usefulness of the results obtained from it. Three different mouse models were used in this project, each having their own pros and cons.

KC-induced joint inflammation is widely used for studying arthritic inflammation and pain. Kaolin acts as an irritant, and causes significant joint damage. Although kaolin-induced joint damage resembles that observed in OA, a 24hr onset period cannot adequately replicate the subchondral and neuropathic components of human OA, which develop over a substantially longer period of time. Furthermore, inflammation in RA is T cell driven, while OA inflammation involves multiple PRRs, only one of which is TLR4. Conversely, carrageenan produces an innate immune response by first activating TLR4, and therefore, differing substantially from RA inflammation, and failing to capture the entire profile of OA inflammation.

There is evidence to suggest that neurogenic inflammation is a component in multiple arthropathies, but is by no means the only mechanism involved. Therefore, our stimulation-induced neurogenic inflammation model only accounts for one of many inflammatory mechanisms involved in arthritis.

Intra-articular injection of MIA produces significant joint damage and pain, which resembles that observed in OA; however, these changes occur over 14 days, unlike the chronic timeframe of human OA. Treatment with URB597 during the early

inflammatory phase of the MIA model attenuated the development of pain at day 14; however, the relevance of this finding is confounded by the lack of similarity between this model and human disease. Future studies should investigate the effects of early FAAH inhibition in more clinically relevant models of OA development, like the MCL transection model.

6.3.5 Drugs

Aside from URB597, many of the drug doses chosen were based on results from previous studies. It should therefore be noted that a negative result does not necessarily mean that the compound of interest has no effect in that particular model, but rather that the compound at that particular dose was ineffective.

Furthermore, our drug choices were based on an assessment of the literature concerning each compound, its selectivity for the target of interest, and previous use in our laboratory. Despite our best efforts, the selectivity of several of the compounds used in this project are less than ideal. AM251, which was chosen as a CB1R antagonist, is actually an inverse agonist at CB1R, has agonist activity at GPR55 (Kapur et al., 2009), has antagonist activity at μ-opioid receptors (Seely et al., 2012), and also acts as an inverse agonist at the estrogen-related receptor α (ERRα) (Fiori et al., 2011); therefore, non-CB1R-mediated off-target effects may be responsible for the effects of AM251 in this study. O-1918, which was used as a GPR55 antagonist, can also act as an agonist at GPR18 (Console-Bram et al., 2014). All of these off-target receptors have potential inflammatory activity; therefore, it is possible that potential off-target effects may have confounded our interpretations of the results.

6.4 Future directions

6.4.1 Mechanism for effect of URB597 on leukocyte adherence

The mechanism responsible for the inhibitory effect of URB597 (0.3 and 3.0mg/kg) on leukocyte adherence still needs to be elucidated. Given that GPR55 was involved in the effect of URB597 on neurogenic leukocyte rolling, it would be an ideal candidate. Another possibility is that anandamide is working through GPR18, which has been shown to increase pro-resolution inflammatory molecule expression in human embryonic kidney cells (Burstein et al., 2011), and decrease microglial inflammatory measures *in vitro* (Malek et al., 2015).

6.4.2 Hormetic response of URB597

The mechanism responsible for the loss of effect of URB597 on KC-induced inflammation still needs to be uncovered. Based on our results, TRPV1 activation does not seem to be entirely responsible for this effect. This still leaves the possibility that receptor down-regulation or prostamide formation may be involved. Future studies should test the effects on synovitis of co-treatment with high dose URB597 and a prostamide antagonist. Furthermore, CB1R and CB2R expression should be compared between low-dose and high-dose URB597-treated mouse knee joints.

6.4.3 The role of VIP-mediated leukocyte-endothelial interactions

Whether VIP-mediated neurogenic rolling is driving or attenuating inflammation also needs to be further investigated. Although we normally associate leukocyte recruitment with pro-inflammatory mechanisms, the recruitment of particular leukocyte phenotypes may actually contribute to the resolution of inflammation.

Given that VIP has both pro-inflammatory and anti-inflammatory effects, it would be interesting to try and delineate the types of leukocytes that are recruited by VIP and what their effect is on articular inflammation.

6.4.4 Mechanism of URB597 on development of MIA-induced pain

The receptors responsible for the effect of URB597 on MIA-induced inflammation were not tested, and should be the subject of future studies; however, based on the results presented in Chapters 3 and 4, CB1R, CB2R and GPR55 are all possible candidates.

Additionally, although the development of pain was inhibited by prophylactic URB597 treatment, the mechanism by which URB597 exerts this anti-nociceptive effect is still unknown. One possibility, is that the anti-inflammatory effects of URB597 are responsible for this effect. Cytokines released from infiltrating immune cells are capable of inducing the expression of MMPs, which promote the breakdown of joint constituents. By inhibiting inflammation early in this model, it is possible that URB597 is decreasing the expression of cartilage degrading enzymes, and subsequent joint damage. Another possibility is that endocannabinoid modulation is having a neuroprotective effect, which is attenuating the development of MIA-induced neuropathic pain. Future experiments should aim to uncover if URB597 is actually protecting against joint destruction, having anti-neuropathic effects, or if this effect is simply a persistent anti-inflammatory effect.

6.4.5 Cannabinoids and arthritis

The results presented in this study focused on one small aspect of the endocannabinoid system. FAAH and its substrates have been popular targets in decreasing arthritic pain in pre-clinical studies; however, many studies have also focused on targeting numerous other aspects of the endocannabinoid system for the treatment of OA and RA. MAGL is another enzyme involved in endocannabinoid degradation, and inhibition results in increased 2-AG levels. This enzyme has been the subject of several other studies, but has received substantially less attention when compared to FAAH. Future studies should aim to further investigate the potential of MAGL inhibition in decreasing the development of pain and inflammation in models of arthritis. Furthermore, the results presented here highlight the fact that non-canonical cannabinoid receptors (non-CB1R/CB2R) play a role in joint inflammation. Future studies should aim at identifying other cannabinoid targets, as well as their role and therapeutic potential in joint pathology.

6.5 Conclusions

The results presented here provide further evidence that neurogenic factors contribute to joint inflammation, and suggest that neurogenic mechanisms are also involved in the early inflammatory phase of OA. Furthermore, FAAH inhibition was shown to have an anti-inflammatory effect in multiple models of arthritis, and to attenuate the development of pain in a model of OA. These results corroborate numerous findings, where targeting the endocannabinoid system has been beneficial in treating experimental arthritis, as well as the clinical evidence that medicinal cannabis, its active compounds, and their derivatives decrease symptoms in patients

with rheumatic diseases. Whether or not endocannabinoid-based therapies will be employed for treating disease progression in arthritis is still unknown; however, based on the results presented here, this system is a viable target for attenuating disease progression and treating symptoms.

References

Ahmed, A. A., Wahbi, A., Nordlind, K., Kharazmi, A., Sundqvist, K. G., Mutt, V., & Lidén, S. (1998). In vitro Leishmania major promastigote-induced macrophage migration is modulated by sensory and autonomic neuropeptides. *Scand. J. Immunol.*, *48*(1), 79–85.

Aletaha, D., Neogi, T., Silman, A. J., Funovits, J., Felson, D. T., Bingham, C. O., Birnbaum, N. S., Burmester, G. R., Bykerk, V. P., Cohen, M. D., Combe, B., Costenbader, K. H., Dougados, M., Emery, P., Ferraccioli, G., Hazes, J. M. W., Hobbs, K., Huizinga, T. W. J., Kavanaugh, A., Kay, J., Kvien, T. K., Laing, T., Mease, P., Ménard, H. A., Moreland, L. W., Naden, R. L., Pincus, T., Smolen, J. S., Stanislawska-Biernat, E., Symmons, D., Tak, P. P., Upchurch, K. S., Vencovský, J., Wolfe, F., & Hawker, G. (2010). 2010 Rheumatoid arthritis classification criteria: an American College of Rheumatology/European League Against Rheumatism collaborative initiative. *Arthritis Rheum.*, *62*(9), 2569–81.

Alexander, S. P. H. (2012). So what do we call GPR18 now? *Br. J. Pharmacol.*, *165*(8), 2411–3.

Andruski, B., McCafferty, D. M., Ignacy, T., Millen, B., & McDougall, J. J. (2008). Leukocyte trafficking and pain behavioral responses to a hydrogen sulfide donor in acute monoarthritis. *Am J Physiol Regul Integr Comp Physiol*, *295*(3), R814–20.

Applequist, S. E., Wallin, R. P. A., & Ljunggren, H.-G. (2002). Variable expression of Toll-like receptor in murine innate and adaptive immune cell lines. *Int. Immunol.*, *14*(9), 1065–74.

Azzolina, A., Bongiovanni, A., & Lampiasi, N. (2003). Substance P induces TNF-alpha and IL-6 production through NF kappa B in peritoneal mast cells. *Biochim. Biophys. Acta*, *1643*(1-3), 75–83.

Baatz, H., Steinbauer, M., Harris, A. G., & Krombach, F. (1995). Kinetics of White Blood Cell Staining by Intravascular Administration of Rhodamine 6G. *Int. J. Microcirc.*, *15*(2), 85–91.

Bär, K.-J., Schurigt, U., Scholze, A., Segond Von Banchet, G., Stopfel, N., Bräuer, R., Halbhuber, K.-J., & Schaible, H.-G. (2004). The expression and localization of somatostatin receptors in dorsal root ganglion neurons of normal and monoarthritic rats. *Neuroscience*, *127*(1), 197–206.

Barbezat, G. O., & Grossman, M. I. (1971). Intestinal secretion: stimulation by peptides. *Science*, *174*(4007), 422–4.

Bayliss, W. M. (1901). On the origin from the spinal cord of the vaso-dilator fibres of the hind-limb, and on the nature of these fibres. *J. Physiol.*, *26*(3-4), 173–209.

Bhattacharyya, S., Gill, R., Chen, M. L., Zhang, F., Linhardt, R. J., Dudeja, P. K., & Tobacman, J. K. (2008). Toll-like receptor 4 mediates induction of the Bcl10-NFkappaB-interleukin-8 inflammatory pathway by carrageenan in human intestinal epithelial cells. *J. Biol. Chem.*, *283*(16), 10550–8.

Birder, L. A., & Perl, E. R. (1999). Expression of alpha2-adrenergic receptors in rat primary afferent neurones after peripheral nerve injury or inflammation. *J. Physiol.*, *515 (Pt 2)*, 533–42.

Boas, D. A., & Dunn, A. K. (2010). Laser speckle contrast imaging in biomedical optics. *J. Biomed. Opt.*, *15*(1), 011109.

Borrelli, F., Romano, B., Petrosino, S., Pagano, E., Capasso, R., Coppola, D., Battista, G., Orlando, P., Di Marzo, V., & Izzo, A. A. (2015). Palmitoylethanolamide, a naturally occurring lipid, is an orally effective intestinal anti-inflammatory agent. *Br. J. Pharmacol.*, *172*(1), 142–158.

Boucher, R. C., Ranga, V., Pare, P. D., Inoue, S., Moroz, L. A., & Hogg, J. C. (1978). Effect of histamine and methacholine on guinea pig tracheal permeability to HRP. *J Appl Physiol*, *45*(6), 939–948.

Bove, S. E., Calcaterra, S. L., Brooker, R. M., Huber, C. M., Guzman, R. E., Juneau, P. L., Schrier, D. J., & Kilgore, K. S. (2003). Weight bearing as a measure of disease progression and efficacy of anti-inflammatory compounds in a model of monosodium iodoacetate-induced osteoarthritis. *Osteoarthritis Cartilage*, *11*(11), 821–30.

Brackmann, U. (1986). Lambdachrome laser dyes. *Goettingen Lambda Phys. GmbH, 1986*, *1*.

Brain, S. D., Williams, T. J., Tippins, J. R., Morris, H. R., & MacIntyre, I. (1985). Calcitonin gene-related peptide is a potent vasodilator. *Nature*, *313*(5997), 54–6.

Bruce, A. N. (1913). Vaso-dilator axon-reflexes. *Q J Exp Physiol*, *6*(4), 339–354.

Buckley, T. L., Brain, S. D., Collins, P. D., & Williams, T. J. (1991). Inflammatory edema induced by interactions between IL-1 and the neuropeptide calcitonin gene-related peptide. *J. Immunol.*, *146*(10), 3424–30.

Burstein, S. H., McQuain, C. A., Ross, A. H., Salmonsen, R. A., & Zurier, R. E. (2011). Resolution of inflammation by N-arachidonoylglycine. *J. Cell. Biochem.*, *112*(11), 3227–33.

Camu, F., Shi, L., & Vanlersberghe, C. (2003). The role of COX-2 inhibitors in pain modulation. *Drugs*, *63 (1)*, 1–7.

Carlton, S. M., Du, J., Davidson, E., Zhou, S., & Coggeshall, R. E. (2001). Somatostatin receptors on peripheral primary afferent terminals: inhibition of sensitized nociceptors. *Pain*, *90*(3), 233–244.

Catre, M. G., & Salo, P. T. (1999). Quantitative analysis of the sympathetic innervation of the rat knee joint. *J. Anat.*, *194 (2)*, 233–9.

Chaplan, S. R., Bach, F. W., Pogrel, J. W., Chung, J. M., & Yaksh, T. L. (1994). Quantitative assessment of tactile allodynia in the rat paw. *J Neurosci Methods*, *53*(1), 55–63.

Chiurchiù, V., Lanuti, M., De Bardi, M., Battistini, L., & Maccarrone, M. (2015). The differential characterization of GPR55 receptor in human peripheral blood reveals a distinctive expression in monocytes and NK cells and a proinflammatory role in these innate cells. *Int. Immunol.*, *27*(3), 153–60.

Codreanu, C., & Damjanov, N. (2015). Safety of biologics in rheumatoid arthritis: data from randomized controlled trials and registries. *Biologics*, *9*, 1–6.

Console-Bram, L., Brailoiu, E., Brailoiu, G. C., Sharir, H., & Abood, M. E. (2014). Activation of GPR18 by cannabinoid compounds: a tale of biased agonism. *Br. J. Pharmacol.*, *171*(16), 3908–17.

Costenbader, K. H., & Karlson, E. W. (2006). Epstein-Barr virus and rheumatoid arthritis: is there a link? *Arthritis Res. Ther.*, *8*(1), 204.

Cox, M. L., & Welch, S. P. (2004). The antinociceptive effect of Delta9-tetrahydrocannabinol in the arthritic rat. *Eur. J. Pharmacol.*, *493*(1-3), 65–74.

Cravatt, B. F., Giang, D. K., Mayfield, S. P., Boger, D. L., Lerner, R. a, & Gilula, N. B. (1996). Molecular characterization of an enzyme that degrades neuromodulatory fatty-acid amides. *Nature*, *384*, 83–87.

Cross, M., Smith, E., Hoy, D., Nolte, S., Ackerman, I., Fransen, M., Bridgett, L., Williams, S., Guillemin, F., Hill, C. L., Laslett, L. L., Jones, G., Cicuttini, F., Osborne, R., Vos, T., Buchbinder, R., Woolf, A., & March, L. (2014). The global burden of hip and knee osteoarthritis: estimates from the global burden of disease 2010 study. *Ann. Rheum. Dis.*, *73*(7), 1323–30.

Cruwys, S. C., Garrett, N. E., & Kidd, B. L. (1995). Sensory denervation with capsaicin attenuates inflammation and nociception in arthritic rats. *Neurosci. Lett.*, *193*(3), 205–207.

Cuello, A. C., Del Fiacco, M., & Paxinos, G. (1978). The central and peripheral ends of the substance P-containing sensory neurones in the rat trigeminal system. *Brain Res.*, *152*(3), 499–500.

Curtis, J. R., Chastek, B., Becker, L., Quach, C., Harrison, D. J., Yun, H., Joseph, G. J., & Collier, D. H. (2015). Cost and effectiveness of biologics for rheumatoid arthritis in a commercially insured population. *J. Manag. Care Spec. Pharm.*, *21*(4), 318–29.

Dawson, W. R. (1934). Studies in the Egyptian Medical Texts: III (Continued). *J. Egypt. Arch.*, 41-46.

De la Fuente, M., Delgado, M., del Rio, M., Garrido, E., Leceta, J., Hernanz, A., & Gomariz, R. P. (1994). Vasoactive intestinal peptide modulation of adherence and mobility in rat peritoneal lymphocytes and macrophages. *Peptides*, *15*(7), 1157–63.

De Petrocellis, L., Harrison, S., Bisogno, T., Tognetto, M., Brandi, I., Smith, G. D., Creminon, C., Davis, J. B., Geppetti, P., & Di Marzo, V. (2001). The vanilloid receptor (VR1)-mediated effects of anandamide are potently enhanced by the cAMP-dependent protein kinase. *J. Neurochem.*, *77*(6), 1660–1663.

Delgado, M., & Ganea, D. (2003). Vasoactive intestinal peptide inhibits IL-8 production in human monocytes. *Biochem. Biophys. Res. Commun.*, *301*(4), 825–32.

Demuth, D. G., & Molleman, A. (2006). Cannabinoid signalling. *Life Sci.*, *78*(6), 549–63.

Devane, W. A., Hanus, L., Breuer, A., Pertwee, R. G., Stevenson, L. A., Griffin, G., Gibson, D., Mandelbaum, A., Etinger, A., & Mechoulam, R. (1992). Isolation and structure of a brain constituent that binds to the cannabinoid receptor. *Science 258*(5090), 1946–1949.

Dinh, T. P., Carpenter, D., Leslie, F. M., Freund, T. F., Katona, I., Sensi, S. L., Kathuria, S., & Piomelli, D. (2002). Brain monoglyceride lipase participating in endocannabinoid inactivation. *Proc. Natl. Acad. Sci. U. S. A.*, *99*(16), 10819–24.

Diogenes, A., Ferraz, C. C. R., Akopian, A. N., Henry, M. A., & Hargreaves, K. M. (2011). LPS sensitizes TRPV1 via activation of TLR4 in trigeminal sensory neurons. *J. Dent. Res.*, *90*(6), 759–64.

Dole, V. S., Bergmeier, W., Mitchell, H. A., Eichenberger, S. C., & Wagner, D. D. (2005). Activated platelets induce Weibel-Palade-body secretion and leukocyte rolling in vivo: role of P-selectin. *Blood*, *106*(7), 2334–9.

Dreier, R., Wallace, S., Fuchs, S., Bruckner, P., & Grässel, S. (2001). Paracrine interactions of chondrocytes and macrophages in cartilage degradation: articular chondrocytes provide factors that activate macrophage-derived pro-gelatinase B (pro-MMP-9). *J. Cell Sci.*, *114*(21), 3813–22.

Dustin, M. L. (1988). Lymphocyte function-associated antigen-1 (LFA-1) interaction with intercellular adhesion molecule-1 (ICAM-1) is one of at least three mechanisms for lymphocyte adhesion to cultured endothelial cells. *J. Cell Biol.*, *107*(1), 321–331.

Ebbinghaus, M., Uhlig, B., Richter, F., von Banchet, G. S., Gajda, M., Bräuer, R., & Schaible, H.-G. (2012). The role of interleukin-1β in arthritic pain: main involvement in thermal, but not mechanical, hyperalgesia in rat antigen-induced arthritis. *Arthritis Rheum.*, *64*(12), 3897–907.

Ebnet, K., & Vestweber, D. (1999). Robert Feulgen Lecture 1998. *Histochem. Cell Biol.*, *112*(1), 1–23.

Eccles, J. C., Schimdt, R., & Willis, W. D. (1963). Pharmacological studies on presynaptic inhibition. *J. Physiol.*, *168*, 500–30.

Egertová, M., Giang, D. K., Cravatt, B. F., & Elphick, M. R. (1998). A new perspective on cannabinoid signalling: complementary localization of fatty acid amide hydrolase and the CB1 receptor in rat brain. *Proc. Biol. Sci.*, *265*(1410), 2081–5.

Engel, M. A., Izydorczyk, I., Mueller-Tribbensee, S. M., Becker, C., Neurath, M. F., & Reeh, P. W. (2011). Inhibitory CB1 and activating/desensitizing TRPV1-mediated cannabinoid actions on CGRP release in rodent skin. *Neuropeptides*, *45*(3), 229–37.

Escott, K. J., & Brain, S. D. (1993). Effect of a calcitonin gene-related peptide antagonist (CGRP8-37) on skin vasodilatation and oedema induced by stimulation of the rat saphenous nerve. *Br. J. Pharmacol.*, *110*(2), 772–776.

Evans, R. H., & Long, S. K. (1989). Primary afferent depolarization in the rat spinal cord is mediated by pathways utilising NMDA and non-NMDA receptors. *Neurosci. Lett.*, *100*(1-3), 231–6.

Fagan, S. G., & Campbell, V. A. (2014). The influence of cannabinoids on generic traits of neurodegeneration. *Br. J. Pharmacol.*, *171*(6), 1347–60.

Farahat, M. N., Yanni, G., Poston, R., & Panayi, G. S. (1993). Cytokine expression in synovial membranes of patients with rheumatoid arthritis and osteoarthritis. *Ann. Rheum. Dis.*, *52*(12), 870–75.

Favalli, E. G., Biggioggero, M., & Meroni, P. L. (2014). Methotrexate for the treatment of rheumatoid arthritis in the biologic era: still an ‘anchor’ drug? *Autoimmun. Rev.*, *13*(11), 1102–8.

Felson, D. T. (2000). Osteoarthritis: New Insights. Part 2: Treatment Approaches. *Ann. Intern. Med.*, *133*(9), 726.

Fernández-Moreno, M., Rego, I., Carreira-Garcia, V., & Blanco, F. J. (2008). Genetics in osteoarthritis. *Curr. Genomics*, *9*(8), 542–7.

Ferrell, W. R., McDougall, J. J., & Bray, R. C. (1997). Spatial heterogeneity of the effects of calcitonin gene-related peptide (CGRP) on the microvasculature of ligaments in the rabbit knee joint. *Br. J. Pharmacol.*, *121*(7), 1397–405.

Ferrell, W. R., & Russell, N. J. (1985). Plasma extravasation in the cat knee-joint induced by antidromic articular nerve stimulation. *Pflugers Arch.*, *404*(1), 91–3.

Ferrell, W. R., & Russell, N. J. (1986). Extravasation in the knee induced by antidromic stimulation of articular C fibre afferents of the anaesthetized cat. *J. Physiol.*, *379*, 407–16.

Fiori, J. L., Sanghvi, M., O’Connell, M. P., Krzysik-Walker, S. M., Moaddel, R., & Bernier, M. (2011). The cannabinoid receptor inverse agonist AM251 regulates the expression of the EGF receptor and its ligands via destabilization of oestrogen-related receptor α protein. *Br. J. Pharmacol.*, *164*(3), 1026–40.

Fiscus, R. R. (1988). Molecular mechanisms of endothelium-mediated vasodilation. *Semin. Thromb. Hemost.*, *14 Suppl*, 12–22.

Fitzner, N., Clauberg, S., Essmann, F., Liebmann, J., & Kolb-Bachofen, V. (2008). Human skin endothelial cells can express all 10 TLR genes and respond to respective ligands. *Clin. Vaccine Immunol.*, *15*(1), 138–46.

Flynn, S. B., & Owen, D. A. (1979). Histamine H1- and H2- receptor antagonists reduce histamine-induced increases in vascular permeability and oedema formation in cat skeletal muscle. *Agents Actions*, *9*(5-6), 450–4.

Foster, C. A., Mandak, B., Kromer, E., & Rot, A. (1992). Calcitonin gene-related peptide is chemotactic for human T lymphocytes. *Ann N Y Acad Sci*, *657*, 397–404.

Foxall, D. L., Brindle, K. M., Campbell, I. D., & Simpson, R. J. (1984). The inhibition of erythrocyte glyceraldehyde-3-phosphate dehydrogenase. In situ PMR studies. *Biochim. Biophys. Acta*, *804*(2), 209–15.

Freeman, M. A., & Wyke, B. (1967). The innervation of the knee joint. An anatomical and histological study in the cat. *J. Anat.*, *101*(Pt 3), 505–32.

Fukuda, H., Abe, T., & Yoshihara, S. (2010). The cannabinoid receptor agonist WIN 55,212-2 inhibits antigen-induced plasma extravasation in guinea pig airways. *Int. Arch. Allergy Immunol.*, *152*(3), 295–300.

Füllhase, C., Russo, A., Castiglione, F., Benigni, F., Campeau, L., Montorsi, F., Gratzke, C., Bettiga, A., Stief, C., Andersson, K.-E., & Hedlund, P. (2013). Spinal cord FAAH in normal micturition control and bladder overactivity in awake rats. *J. Urol.*, *189*(6), 2364–70.

Galli, S. J., Gordon, J. R., & Wershil, B. K. (1991). Cytokine production by mast cells and basophils. *Curr. Opin. Immunol.*, *3*(6), 865–873.

Gamse, R., Holzer, P., & Lembeck, F. (1980). Decrease of substance P in primary afferent neurones and impairment of neurogenic plasma extravasation by capsaicin. *Br. J. Pharmacol.*, *68*(2), 207–13.

Gangadharan, V., Selvaraj, D., Kurejova, M., Njoo, C., Gritsch, S., Škoricová, D., Horstmann, H., Offermanns, S., Brown, A. J., Kuner, T., Tappe-Theodor, A., & Kuner, R. (2013). A novel biological role for the phospholipid lysophosphatidylinositol in nociceptive sensitization via activation of diverse G-protein signalling pathways in sensory nerves in vivo. *Pain*, *154*(12), 2801–12.

Gaoni, Y., & Mechoulam, R. (1964). Isolation, Structure, and Partial Synthesis of an Active Constituent of Hashish. *J. Am. Chem. Soc.*, *86*(8), 1646–1647.

Gasperi, V., Evangelista, D., Chiurchiù, V., Florenzano, F., Savini, I., Oddi, S., Avigliano, L., Catani, M. V., & Maccarrone, M. (2014). 2-Arachidonoylglycerol modulates human endothelial cell/leukocyte interactions by controlling selectin expression through CB1 and CB2 receptors. *Int. J. Biochem. Cell Biol.*, *51*, 79–88.

Gatta, L., Piscitelli, F., Giordano, C., Boccella, S., Lichtman, A., Maione, S., & Di Marzo, V. (2012). Discovery of prostamide F2α and its role in inflammatory pain and dorsal horn nociceptive neuron hyperexcitability. *PLoS One*, *7*(2), e31111.

Gauldie, S. D., McQueen, D. S., Pertwee, R., & Chessell, I. P. (2001). Anandamide activates peripheral nociceptors in normal and arthritic rat knee joints. *Br. J. Pharmacol.*, *132*(3), 617–21.

Gear, A. R. (1974). Rhodamine 6G. A potent inhibitor of mitochondrial oxidative phosphorylation. *J. Biol. Chem.*, *249*(11), 3628–37.

Gierse, J. K., McDonald, J. J., Hauser, S. D., Rangwala, S. H., Koboldt, C. M., & Seibert, K. (1996). A single amino acid difference between cyclooxygenase-1 (COX-1) and -2 (COX-2) reverses the selectivity of COX-2 specific inhibitors. *J. Biol. Chem.*, *271*(26), 15810–4.

Goetzl, E. J., & Payan, D. G. (1984). Inhibition by somatostatin of the release of mediators from human basophils and rat leukemic basophils. *J. Immunol.*, *133*(6), 3255–9.

Gold, M. S., Levine, J. D., & Correa, A. M. (1998). Modulation of TTX-R INa by PKC and PKA and their role in PGE2-induced sensitization of rat sensory neurons in vitro. *J. Neurosci.*, *18*(24), 10345–55.

Gonzalez-Rey, E., Varela, N., Chorny, A., & Delgado, M. (2007). Therapeutical approaches of vasoactive intestinal peptide as a pleiotropic immunomodulator. *Curr. Pharm. Des.*, *13*(11), 1113–39.

Gray, H. (1989). *Gray's anatomy*. (P. L. Williams & H. Gray, Eds.) (37th ed.). Edinburgh, Scotland: Churchill Livingston.

Greene, E. C. (1968). *Anatomy of the rat.* New York, New York: Hafner Pub. Co.

Griffioen, M. A., Dernetz, V. H., Yang, G. S., Griffith, K. A., Dorsey, S. G., & Renn, C. L. (2015). Evaluation of dynamic weight bearing for measuring nonevoked inflammatory hyperalgesia in mice. *Nurs. Res.*, *64*(2), 81–7.

Groetzner, P., & Weidner, C. (2010). The human vasodilator axon reflex - an exclusively peripheral phenomenon? *Pain*, *149*(1), 71–5.

Guzman, R. E., Evans, M. G., Bove, S., Morenko, B., & Kilgore, K. (2003). Mono-iodoacetate-induced histologic changes in subchondral bone and articular cartilage of rat femorotibial joints: an animal model of osteoarthritis. *Toxicol. Pathol.*, *31*(6), 619–24.

Han, J. S., & Neugebauer, V. (2005). mGluR1 and mGluR5 antagonists in the amygdala inhibit different components of audible and ultrasonic vocalizations in a model of arthritic pain. *Pain*, *113*(1-2), 211–22.

Helyes, Z., Szabó, A., Németh, J., Jakab, B., Pintér, E., Bánvölgyi, A., Kereskai, L., Kéri, G., & Szolcsányi, J. (2004). Antiinflammatory and analgesic effects of somatostatin released from capsaicin-sensitive sensory nerve terminals in a Freund's adjuvant-induced chronic arthritis model in the rat. *Arthritis Rheum.*, *50*(5), 1677–85.

Hensellek, S., Brell, P., Schaible, H.-G., Bräuer, R., & Segond von Banchet, G. (2007). The cytokine TNFalpha increases the proportion of DRG neurones expressing the TRPV1 receptor via the TNFR1 receptor and ERK activation. *Mol. Cell. Neurosci.*, *36*(3), 381–91.

Heppelmann, B., & Schaible, H. G. (1990). Origin of sympathetic innervation of the knee joint in the cat: a retrograde tracing study with horseradish peroxidase. *Neurosci. Lett.*, *108*(1-2), 71–5.

Hernanz, A., De Miguel, E., Romera, N., Perez-Ayala, C., Gijon, J., & Arnalich, F. (1993). Calcitonin gene-related peptide II, substance P and vasoactive intestinal peptide in plasma and synovial fluid from patients with inflammatory joint disease. *Br. J. Rheumatol.*, *32*(1), 31–5.

Hohmann, A. G., & Herkenham, M. (1999). Localization of central cannabinoid CB1 receptor messenger RNA in neuronal subpopulations of rat dorsal root ganglia: a double-label in situ hybridization study. *Neuroscience*, *90*(3), 923–31.

Hökfelt, T., Elde, R., Johansson, O., Luft, R., Nilsson, G., & Arimura, A. (1976). Immunohistochemical evidence for separate populations of somatostatin-containing and substance P-containing primary afferent neurons in the rat. *Neuroscience*, *1*(2), 131–6.

Hökfelt, T., Kellerth, J. O., Nilsson, G., & Pernow, B. (1975). Substance p: localization in the central nervous system and in some primary sensory neurons. *Science*, *190*(4217), 889–90.

Hood, V. C., Cruwys, S. C., Urban, L., & Kidd, B. L. (2001). The neurogenic contribution to synovial leucocyte infiltration and other outcome measures in a guinea pig model of arthritis. *Neurosci. Lett.*, *299*(3), 201–4.

Huggins, J. P., Smart, T. S., Langman, S., Taylor, L., & Young, T. (2012). An efficient randomised, placebo-controlled clinical trial with the irreversible fatty acid amide hydrolase-1 inhibitor PF-04457845, which modulates endocannabinoids but fails to induce effective analgesia in patients with pain due to osteoarthritis of th. *Pain*, *153*(9), 1837–46.

Hui, A. Y., McCarty, W. J., Masuda, K., Firestein, G. S., & Sah, R. L. (2012). A systems biology approach to synovial joint lubrication in health, injury, and disease. *Wiley Interdiscip. Rev. Syst. Biol. Med.*, *4*(1), 15–37.

Hunt, L., & Emery, P. (2014). Defining populations at risk of rheumatoid arthritis: the first steps to prevention. *Nat. Rev. Rheumatol.*, *10*(9), 521–30.

Iwaszkiewicz, K. S., Schneider, J. J., & Hua, S. (2013). Targeting peripheral opioid receptors to promote analgesic and anti-inflammatory actions. *Front. Pharmacol.*, *4*, 132.

Jancsó, N., Jancsó-Gábor, A., & Szolcsányi, J. (1967). Direct evidence for neurogenic inflammation and its prevention by denervation and by pretreatment with capsaicin. *Br. J. Pharmacol. Chemother.*, *31*(1), 138–51.

Johnston, J. A., Taub, D. D., Lloyd, A. R., Conlon, K., Oppenheim, J. J., & Kevlin, D. J. (1994). Human T lymphocyte chemotaxis and adhesion induced by vasoactive intestinal peptide. *J. Immunol.*, *153*(4), 1762–8.

Kapur, A., Zhao, P., Sharir, H., Bai, Y., Caron, M. G., Barak, L. S., & Abood, M. E. (2009). Atypical responsiveness of the orphan receptor GPR55 to cannabinoid ligands. *J. Biol. Chem.*, *284*(43), 29817–27.

Karimian, M., & Ferrell, W. R. (1994). Plasma protein extravasation into the rat knee joint induced by calcitonin gene-related peptide. *Neurosci. Lett.*, *166*(1), 39–42.

Kawabata, A., Kawao, N., Kuroda, R., Tanaka, A., & Shimada, C. (2002). The PAR-1-activating peptide attenuates carrageenan-induced hyperalgesia in rats. *Peptides*, *23*(6), 1181–3.

Kawai, T., & Akira, S. (2010). The role of pattern-recognition receptors in innate immunity: update on Toll-like receptors. *Nat. Immunol.*, *11*(5), 373–84.

Kidd, B. L., & Urban, L. A. (2001). Mechanisms of inflammatory pain. *Br. J. Anaesth.*, *87*(1), 3–11.

Kinsey, S. G., Naidu, P. S., Cravatt, B. F., Dudley, D. T., & Lichtman, A. H. (2011). Fatty acid amide hydrolase blockade attenuates the development of collagen-induced arthritis and related thermal hyperalgesia in mice. *Pharmacol. Biochem. Behav.*, *99*(4), 718–25.

Kobayashi, K., Imaizumi, R., Sumichika, H., Tanaka, H., Goda, M., Fukunari, A., & Komatsu, H. (2003). Sodium iodoacetate-induced experimental osteoarthritis and associated pain model in rats. *J. Vet. Med. Sci.*, *65*(11), 1195–9.

Kolasinski, S. L., Haines, K. A., Siegel, E. L., Cronstein, B. N., & Abramson, S. B. (1992). Neuropeptides and inflammation. A somatostatin analog as a selective antagonist of neutrophil activation by substance P. *Arthritis Rheum.*, *35*(4), 369–75.

Kozak, K. R., Crews, B. C., Morrow, J. D., Wang, L.-H., Ma, Y. H., Weinander, R., Jakobsson, P.-J., & Marnett, L. J. (2002). Metabolism of the endocannabinoids, 2-arachidonylglycerol and anandamide, into prostaglandin, thromboxane, and prostacyclin glycerol esters and ethanolamides. *J. Biol. Chem.*, *277*(47), 44877–85.

Krustev, E., Reid, A., & McDougall, J. J. (2014). Tapping into the endocannabinoid system to ameliorate acute inflammatory flares and associated pain in mouse knee joints. *Arthritis Res. Ther.*, *16*(5), 437.

Krustev, E., Rioux, D., & McDougall, J. J. (2015). Mechanisms and Mediators That Drive Arthritis Pain. *Curr. Osteoporos. Rep.*, *13*(4), 216–24.

La Porta, C., Bura, S. A., Aracil-Fernández, A., Manzanares, J., & Maldonado, R. (2013). Role of CB1 and CB2 cannabinoid receptors in the development of joint pain induced by monosodium iodoacetate. *Pain*, *154*(1), 160–74.

Lahiri, M., Morgan, C., Symmons, D. P. M., & Bruce, I. N. (2012). Modifiable risk factors for RA: prevention, better than cure? *Rheumatology*, *51*(3), 499–512.

Lam, F. Y., & Ferrell, W. R. (1989). Inhibition of carrageenan induced inflammation in the rat knee joint by substance P antagonist. *Ann. Rheum. Dis.*, *48*(11), 928–932.

Lanuti, M., Talamonti, E., Maccarrone, M., & Chiurchiù, V. (2015). Activation of GPR55 Receptors Exacerbates oxLDL-Induced Lipid Accumulation and Inflammatory Responses, while Reducing Cholesterol Efflux from Human Macrophages. *PLoS One*, *10*(5), e0126839.

Larsson, L. I., Fahrenkrug, J., Schaffalitzky De Muckadell, O., Sundler, F., Håkanson, R., & Rehfeld, J. R. (1976). Localization of vasoactive intestinal polypeptide (VIP) to central and peripheral neurons. *Proc. Natl. Acad. Sci. U. S. A.*, *73*(9), 3197–200.

Laszik, Z., Jansen, P. J., Cummings, R. D., Tedder, T. F., McEver, R. P., & Moore, K. L. (1996). P-selectin glycoprotein ligand-1 is broadly expressed in cells of myeloid, lymphoid, and dendritic lineage and in some nonhematopoietic cells. *Blood*, *88*(8), 3010–21.

Lauckner, J. E., Jensen, J. B., Chen, H.-Y., Lu, H.-C., Hille, B., & Mackie, K. (2008). GPR55 is a cannabinoid receptor that increases intracellular calcium and inhibits M current. *Proc. Natl. Acad. Sci. U. S. A.*, *105*(7), 2699–704.

Lawrence, T., Willoughby, D. A., & Gilroy, D. W. (2002). Anti-inflammatory lipid mediators and insights into the resolution of inflammation. *Nat. Rev. Immunol.*, *2*(10), 787–95.

Lembeck, F., Donnerer, J., & Barthó, L. (1982). Inhibition of neurogenic vasodilation and plasma extravasation by substance P antagonists, somatostatin and [D-Met2, Pro5]enkephalinamide. *Eur. J. Pharmacol.*, *85*(2), 171–6.

Lembeck, F., & Holzer, P. (1979). Substance P as neurogenic mediator of antidromic vasodilation and neurogenic plasma extravasation. *Naunyn. Schmiedebergs. Arch. Pharmacol.*, *310*(2), 175–83.

Levine, J. D., Clark, R., Devor, M., Helms, C., Moskowitz, M. A., & Basbaum, A. I. (1984). Intraneuronal substance P contributes to the severity of experimental arthritis. *Science*, *226*(4674), 547–9.

Levine, J. D., Moskowitz, M. A., & Basbaum, A. I. (1985). The contribution of neurogenic inflammation in experimental arthritis. *J. Immunol.*, *135*(2 Suppl), 843s–847s.

Lewthwaite, J., Blake, S., Hardingham, T., Foulkes, R., Stephens, S., Chaplin, L., Emtage, S., Catterall, C., Short, S., & Nesbitt, A. (1995). Role of TNF alpha in the induction of antigen induced arthritis in the rabbit and the anti-arthritic effect of species specific TNF alpha neutralising monoclonal antibodies. *Ann. Rheum. Dis.*, *54*(5), 366–74.

Ley, K. (1996). Molecular mechanisms of leukocyte recruitment in the inflammatory process. *Cardiovasc. Res.*, *32*(4), 733–42.

Li, K., Feng, J., Li, Y., Yuece, B., Lin, X., Yu, L., Li, Y., Feng, Y., & Storr, M. (2013). Anti-inflammatory role of cannabidiol and O-1602 in cerulein-induced acute pancreatitis in mice. *Pancreas*, *42*(1), 123–9.

Li, Z., Proud, D., Zhang, C., Wiehler, S., & McDougall, J. J. (2005). Chronic arthritis down-regulates peripheral mu-opioid receptor expression with concomitant loss of endomorphin 1 antinociception. *Arthritis Rheum.*, *52*(10), 3210–9.

Ligresti, A., Martos, J., Wang, J., Guida, F., Allarà, M., Palmieri, V., Luongo, L., Woodward, D., & Di Marzo, V. (2014). Prostamide F(2) α receptor antagonism combined with inhibition of FAAH may block the pro-inflammatory mediators formed following selective FAAH inhibition. *Br. J. Pharmacol.*, *171*(6), 1408–19.

Lin, Q., Wu, J., & Willis, W. D. (1999). Dorsal root reflexes and cutaneous neurogenic inflammation after intradermal injection of capsaicin in rats. *J. Neurophysiol.*, *82*(5), 2602–11.

Ling, N., Burgus, R., Rivier, J., Vale, W., & Brazeau, P. (1973). The use of mass spectrometry in deducing the sequence of somatostatin--a hypothalamic polypeptide that inhibits the secretion of growth hormone. *Biochem. Biophys. Res. Commun.*, *50*(1), 127–33.

Litvack, M. L., & Palaniyar, N. (2010). Review: Soluble innate immune pattern-recognition proteins for clearing dying cells and cellular components: implications on exacerbating or resolving inflammation. *Innate Immun.*, *16*(3), 191–200.

Liu-Bryan, R., & Terkeltaub, R. (2014). Emerging regulators of the inflammatory process in osteoarthritis. *Nat. Rev. Rheumatol., 11(1),* 35-44.

Lunam, C. A., & Gentle, M. J. (2004). Substance P immunoreactive nerve fibres in the domestic chick ankle joint before and after acute urate arthritis. *Neurosci. Lett.*, *354*(2), 87–90.

Luo, Z. D., Chaplan, S. R., Higuera, E. S., Sorkin, L. S., Stauderman, K. A., Williams, M. E., & Yaksh, T. L. (2001). Upregulation of dorsal root ganglion (alpha)2(delta) calcium channel subunit and its correlation with allodynia in spinal nerve-injured rats. *J. Neurosci.*, *21*(6), 1868–75.

Maccarrone, M., Bab, I., Bíró, T., Cabral, G. A., Dey, S. K., Di Marzo, V., Konje, J. C., Kunos, G., Mechoulam, R., Pacher, P., Sharkey, K. A., & Zimmer, A. (2015). Endocannabinoid signaling at the periphery: 50 years after THC. *Trends Pharmacol. Sci., 36(5),* 277-296.

Mack, A. (2001). *Marijuana as medicine? : the science beyond the controversy*. (J. E Joy, Ed.). Washington, D.C.: National Academy Press.

MacLean, D. B. (1987). Substance P synthesis and transport in explants of nodose ganglion/vagus nerve: effects of double ligation, 2-deoxyglucose, veratridine, and ouabain. *J. Neurochem.*, *48*(6), 1794–803.

Malaviya, R., & Abraham, S. N. (2000). Role of mast cell leukotrienes in neutrophil recruitment and bacterial clearance in infectious peritonitis. *J. Leukoc. Biol.*, *67*(6), 841–6.

Malek, N., Popiolek-Barczyk, K., Mika, J., Przewlocka, B., & Starowicz, K. (2015). Anandamide, Acting via CB2 Receptors, Alleviates LPS-Induced Neuroinflammation in Rat Primary Microglial Cultures. *Neural Plast.*, *2015*, 130639.

March, L., Smith, E. U. R., Hoy, D. G., Cross, M. J., Sanchez-Riera, L., Blyth, F., Buchbinder, R., Vos, T., & Woolf, A. D. (2014). Burden of disability due to musculoskeletal (MSK) disorders. *Best Pract. Res. Clin. Rheumatol.*, *28*(3), 353–366.

Martini, L., Waldhoer, M., Pusch, M., Kharazia, V., Fong, J., Lee, J. H., Freissmuth, C., & Whistler, J. L. (2007). Ligand-induced down-regulation of the cannabinoid 1 receptor is mediated by the G-protein-coupled receptor-associated sorting protein GASP1. *FASEB J.*, *21*(3), 802–11.

Masini, E., Giannella, E., Bani-Sacchi, T., Fantozzi, R., Palmerani, B., & Mannaioni, P. F. (1987). Histamine release from serosal mast cells by intermediate products of arachidonic acid metabolism. *Agents Actions*, *20*(3-4), 202–5.

Matsuda, L. A., Lolait, S. J., Brownstein, M. J., Young, A. C., & Bonner, T. I. (1990). Structure of a cannabinoid receptor and functional expression of the cloned cDNA. *Nature*, *346*(6284), 561–4.

Mayadas, T. N., Johnson, R. C., Rayburn, H., Hynes, R. O., & Wagner, D. D. (1993). Leukocyte rolling and extravasation are severely compromised in P selectin-deficient mice. *Cell*, *74*(3), 541–554.

McDougall, J. J. (2001). Abrogation of alpha-adrenergic vasoactivity in chronically inflamed rat knee joints. *Am. J. Physiol. Regul. Integr. Comp. Physiol.*, *281*(3), R821–7.

McDougall, J. J. (2009). Cannabinoids and Pain Control in the Periphery. (B. E. Cainrs ed.), *Peripher. Recept. Targets Analg.* (1st ed,). Hoboken, New Jersey: Wiley & Sons., 325–346.

McDougall, J. J., Baker, C. L., & Hermann, P. M. (2004a). Attenuation of knee joint inflammation by peripherally administered endomorphin-1. *J. Mol. Neurosci.*, *22*(1-2), 125–37.

McDougall, J. J., & Barin, A. K. (2005). The role of joint nerves and mast cells in the alteration of vasoactive intestinal peptide (VIP) sensitivity during inflammation progression in rats. *Br. J. Pharmacol.*, *145*(1), 104–13.

McDougall, J. J., Barin, A. K., & McDougall, C. M. (2004b). Loss of vasomotor responsiveness to the mu-opioid receptor ligand endomorphin-1 in adjuvant monoarthritic rat knee joints. *Am. J. Physiol. Regul. Integr. Comp. Physiol.*, *286*(4), R634–41.

McDougall, J. J., Ferrell, W. R., & Bray, R. C. (1999). Neurogenic origin of articular hyperemia in early degenerative joint disease. *Am. J. Physiol.*, *276*(Pt 2), R745–52.

McDougall, J. J., Karimian, S. M., & Ferrell, W. R. (1994). Alteration of substance P-mediated vasodilatation and sympathetic vasoconstriction in the rat knee joint by adjuvant-induced inflammation. *Neurosci. Lett.*, *174*(2), 127–9.

McDougall, J. J., Karimian, S. M., & Ferrell, W. R. (1995). Prolonged alteration of vasoconstrictor and vasodilator responses in rat knee joints by adjuvant monoarthritis. *Exp. Physiol.*, *80*(3), 349–57.

McDougall, J. J., & Schuelert, N. (2007). Age alters the ability of substance P to sensitize joint nociceptors in guinea pigs. *J. Mol. Neurosci.*, *31*(3), 289–96.

McDougall, J. J., Watkins, L., & Li, Z. (2006). Vasoactive intestinal peptide (VIP) is a modulator of joint pain in a rat model of osteoarthritis. *Pain*, *123*(1-2), 98–105.

McDougall, J. J., Zhang, C., Cellars, L., Joubert, E., Dixon, C. M., & Vergnolle, N. (2009). Triggering of proteinase-activated receptor 4 leads to joint pain and inflammation in mice. *Arthritis Rheum.*, *60*(3), 728–37.

McInnes, I. B., & Schett, G. (2007). Cytokines in the pathogenesis of rheumatoid arthritis. *Nat. Rev. Immunol.*, *7*(6), 429–42.

McKinney, M. K., & Cravatt, B. F. (2005). Structure and function of fatty acid amide hydrolase. *Annu. Rev. Biochem.*, *74*, 411–32.

Mechoulam, R., Ben-Shabat, S., Hanus, L., Ligumsky, M., Kaminski, N. E., Schatz, A. R., Gopher, A., Almog, S., Martin, B. R., & Compton, D. R. (1995). Identification of an endogenous 2-monoglyceride, present in canine gut, that binds to cannabinoid receptors. *Biochem. Pharmacol.*, *50*(1), 83–90.

Melrose, J., Fuller, E. S., Roughley, P. J., Smith, M. M., Kerr, B., Hughes, C. E., Caterson, B., & Little, C. B. (2008). Fragmentation of decorin, biglycan, lumican and keratocan is elevated in degenerate human meniscus, knee and hip articular cartilages compared with age-matched macroscopically normal and control tissues. *Arthritis Res. Ther.*, *10*(4), R79.

Menétrey, D., & Besson, J. M. (1982). Electrophysiological characteristics of dorsal horn cells in rats with cutaneous inflammation resulting from chronic arthritis. *Pain*, *13*(4), 343–64.

Montecucco, F., Burger, F., Mach, F., & Steffens, S. (2008). CB2 cannabinoid receptor agonist JWH-015 modulates human monocyte migration through defined intracellular signaling pathways. *Am. J. Physiol. Heart Circ. Physiol.*, *294*(3), H1145–55.

Morris, H. R., Panico, M., Etienne, T., Tippins, J., Girgis, S. I., & MacIntyre, I. (1984). Isolation and characterization of human calcitonin gene-related peptide. *Nature*, *308*(5961), 746–8.

Muirden, K. D., & Peace, G. (1969). Light and electron microscope studies in carragheenin, adjuvant, and tuberculin-induced arthris. *Ann. Rheum. Dis.*, *28*(4), 392–401.

Munro, S., Thomas, K. L., & Abu-Shaar, M. (1993). Molecular characterization of a peripheral receptor for cannabinoids. *Nature*, *365*(6441), 61–5.

Nalubamba, K. S., Gossner, A. G., Dalziel, R. G., & Hopkins, J. (2007). Differential expression of pattern recognition receptors in sheep tissues and leukocyte subsets. *Vet. Immunol. Immunopathol.*, *118*(3-4), 252–62.

Neugebauer, V., Han, J. S., Adwanikar, H., Fu, Y., & Ji, G. (2007). Techniques for assessing knee joint pain in arthritis. *Mol. Pain*, *3*(1), 8.

Neugebauer, V., & Schaible, H. G. (1990). Evidence for a central component in the sensitization of spinal neurons with joint input during development of acute arthritis in cat's knee. *J. Neurophysiol.*, *64*(1), 299–311.

Neugebauer, V., & Schaible, H.-G. (1988). Peripheral and spinal components of the sensitization of spinal neurons during an acute experimental arthritis. *Agents Actions*, *25*(3-4), 234–236.

Ni, X., Geller, E. B., Eppihimer, M. J., Eisenstein, T. K., Adler, M. W., & Tuma, R. F. (2004). Win 55212-2, a cannabinoid receptor agonist, attenuates leukocyte/endothelial interactions in an experimental autoimmune encephalomyelitis model. *Mult. Scler.*, *10*(2), 158–64.

Noguchi, K., Senba, E., Morita, Y., Sato, M., & Tohyama, M. (1990). Co-expression of alpha-CGRP and beta-CGRP mRNAs in the rat dorsal root ganglion cells. *Neurosci. Lett.*, *108*(1-2), 1–5.

Nong, Y. H., Titus, R. G., Ribeiro, J. M., & Remold, H. G. (1989). Peptides encoded by the calcitonin gene inhibit macrophage function. *J. Immunol.*, *143*(1), 45–9.

Norman, M. U., James, W. G., & Hickey, M. J. (2008). Differential roles of ICAM-1 and VCAM-1 in leukocyte-endothelial cell interactions in skin and brain of MRL/faslpr mice. *J. Leukoc. Biol.*, *84*(1), 68–76.

Okine, B. N., Norris, L. M., Woodhams, S., Burston, J., Patel, A., Alexander, S. P. H., Barrett, D. A., Kendall, D. A., Bennett, A. J., & Chapman, V. (2012). Lack of effect of chronic pre-treatment with the FAAH inhibitor URB597 on inflammatory pain behaviour: evidence for plastic changes in the endocannabinoid system. *Br. J. Pharmacol.*, *167*(3), 627–40.

Onaivi, E. S., Ishiguro, H., Gong, J.-P., Patel, S., Perchuk, A., Meozzi, P. A., Myers, L., Mora, Z., Tagliaferro, P., Gardner, E., Brusco, A., Akinshola, B. E., Liu, Q.-R., Hope, B., Iwasaki, S., Arinami, T., Teasenfitz, L., & Uhl, G. R. (2006). Discovery of the presence and functional expression of cannabinoid CB2 receptors in brain. *Ann. N. Y. Acad. Sci.*, *1074*, 514–36.

Orita, S., Ishikawa, T., Miyagi, M., Ochiai, N., Inoue, G., Eguchi, Y., Kamoda, H., Arai, G., Toyone, T., Aoki, Y., Kubo, T., Takahashi, K., & Ohtori, S. (2011). Pain-related sensory innervation in monoiodoacetate-induced osteoarthritis in rat knees that gradually develops neuronal injury in addition to inflammatory pain. *BMC Musculoskelet. Disord.*, *12*, 134.

Otrubova, K., Ezzili, C., & Boger, D. L. (2011). The discovery and development of inhibitors of fatty acid amide hydrolase (FAAH). *Bioorg. Med. Chem. Lett.*, *21*(16), 4674–85.

Petersen, W., & Tillmann, B. (1999). [Structure and vascularization of the knee joint menisci]. *Z. Orthop. Ihre Grenzgeb.*, *137*(1), 31–7.

Piomelli, D., Tarzia, G., Duranti, A., Tontini, A., Mor, M., Compton, T. R., Dasse, O., Monaghan, E. P., Parrott, J. A., & Putman, D. (2006). Pharmacological profile of the selective FAAH inhibitor KDS-4103 (URB597). *CNS Drug Rev.*, *12*(1), 21–38.

Pulichino, A.-M., Rowland, S., Wu, T., Clark, P., Xu, D., Mathieu, M.-C., Riendeau, D., & Audoly, L. P. (2006). Prostacyclin antagonism reduces pain and inflammation in rodent models of hyperalgesia and chronic arthritis. *J. Pharmacol. Exp. Ther.*, *319*(3), 1043–50.

Qi, J., Buzas, K., Fan, H., Cohen, J. I., Wang, K., Mont, E., Klinman, D., Oppenheim, J. J., & Howard, O. M. Z. (2011). Painful pathways induced by TLR stimulation of dorsal root ganglion neurons. *J. Immunol.*, *186*(11), 6417–26.

Rasool, C. G., Schwartz, A. L., Bollinger, J. A., Reichlin, S., & Bradley, W. G. (1981). Immunoreactive somatostatin distribution and axoplasmic transport in rat peripheral nerve. *Endocrinology*, *108*(3), 996–1001.

Raud, J., Lundeberg, T., Brodda-Jansen, G., Theodorsson, E., & Hedqvist, P. (1991). Potent anti-inflammatory action of calcitonin gene-related peptide. *Biochem. Biophys. Res. Commun.*, *180*(3), 1429–35.

Rhee, S. H., & Hwang, D. (2000). Murine TOLL-like receptor 4 confers lipopolysaccharide responsiveness as determined by activation of NF kappa B and expression of the inducible cyclooxygenase. *J. Biol. Chem.*, *275*(44), 34035–40.

Richardson, D., Pearson, R. G., Kurian, N., Latif, M. L., Garle, M. J., Barrett, D. A., Kendall, D. A., Scammell, B. E., Reeve, A. J., & Chapman, V. (2008). Characterisation of the cannabinoid receptor system in synovial tissue and fluid in patients with osteoarthritis and rheumatoid arthritis. *Arthritis Res. Ther.*, *10*(2), R43.

Richardson, J. D., Kilo, S., & Hargreaves, K. M. (1998). Cannabinoids reduce hyperalgesia and inflammation via interaction with peripheral CB1 receptors. *Pain*, *75*(1), 111–9.

Ropes, M. W., Rossmeisl, E. C., & Bauer, W. (1940). The origin and nature of normal human synovial fluid. *J. Clin. Invest.*, *19*(6), 795–9.

Ross, R. A. (2003). Anandamide and vanilloid TRPV1 receptors. *Br. J. Pharmacol.*, *140*(5), 790–801.

Ross, R. A., Gibson, T. M., Brockie, H. C., Leslie, M., Pashmi, G., Craib, S. J., Di Marzo, V., & Pertwee, R. G. (2001). Structure-activity relationship for the endogenous cannabinoid, anandamide, and certain of its analogues at vanilloid receptors in transfected cells and vas deferens. *Br. J. Pharmacol.*, *132*(3), 631–40.

Russell, F. A., Schuelert, N., Veldhoen, V. E., Hollenberg, M. D., & McDougall, J. J. (2012). Activation of PAR(2) receptors sensitizes primary afferents and causes leukocyte rolling and adherence in the rat knee joint. *Br. J. Pharmacol.*, *167*(8), 1665–78.

Saito, T. (2003). Neurogenic inflammation in osteoarthritis of the knee. *Mod. Rheumatol.*, *13*(4), 301–4.

Saito, T., & Koshino, T. (2000). Distribution of neuropeptides in synovium of the knee with osteoarthritis. *Clin. Orthop. Relat. Res.*, (376), 172–82.

Sándor, K., Bölcskei, K., McDougall, J. J., Schuelert, N., Reglodi, D., Elekes, K., Petho, G., Pintér, E., Szolcsányi, J., & Helyes, Z. (2009). Divergent peripheral effects of pituitary adenylate cyclase-activating polypeptide-38 on nociception in rats and mice. *Pain*, *141*(1-2), 143–50.

Sans, M., Panés, J., Ardite, E., Elizalde, J. I., Arce, Y., Elena, M., Palacín, A., Fernández-Checa, J. C., Anderson, D. C., Lobb, R., & Piqué, J. M. (1999). VCAM-1 and ICAM-1 mediate leukocyte-endothelial cell adhesion in rat experimental colitis. *Gastroenterology*, *116*(4), 874–83.

Savill, J., & Fadok, V. (2000). Corpse clearance defines the meaning of cell death. *Nature*, *407*(6805), 784–8.

Scanzello, C. R., & Goldring, S. R. (2012). The role of synovitis in osteoarthritis pathogenesis. *Bone*, *51*(2), 249–57.

Schaible, H.-G., von Banchet, G. S., Boettger, M. K., Bräuer, R., Gajda, M., Richter, F., Hensellek, S., Brenn, D., & Natura, G. (2010). The role of proinflammatory cytokines in the generation and maintenance of joint pain. *Ann. N. Y. Acad. Sci.*, *1193*, 60–9.

Schuelert, N., Johnson, M. P., Oskins, J. L., Jassal, K., Chambers, M. G., & McDougall, J. J. (2011). Local application of the endocannabinoid hydrolysis inhibitor URB597 reduces nociception in spontaneous and chemically induced models of osteoarthritis. *Pain*, *152*(5), 975–81.

Schuelert, N., & McDougall, J. J. (2006). Electrophysiological evidence that the vasoactive intestinal peptide receptor antagonist VIP6-28 reduces nociception in an animal model of osteoarthritis. *Osteoarthritis Cartilage*, *14*(11), 1155–62.

Schuelert, N., & McDougall, J. J. (2008). Cannabinoid-mediated antinociception is enhanced in rat osteoarthritic knees. *Arthritis Rheum.*, *58*(1), 145–53.

Schuelert, N., & McDougall, J. J. (2011). The abnormal cannabidiol analogue O-1602 reduces nociception in a rat model of acute arthritis via the putative cannabinoid receptor GPR55. *Neurosci. Lett.*, *500*(1), 72–6.

Seely, K. A., Brents, L. K., Franks, L. N., Rajasekaran, M., Zimmerman, S. M., Fantegrossi, W. E., & Prather, P. L. (2012). AM-251 and rimonabant act as direct antagonists at mu-opioid receptors: implications for opioid/cannabinoid interaction studies. *Neuropharmacology*, *63*(5), 905–15.

Segond von Banchet, G., Boettger, M. K., König, C., Iwakura, Y., Bräuer, R., & Schaible, H.-G. (2013). Neuronal IL-17 receptor upregulates TRPV4 but not TRPV1 receptors in DRG neurons and mediates mechanical but not thermal hyperalgesia. *Mol. Cell. Neurosci.*, *52*, 152–60.

Shore, D. M., & Reggio, P. H. (2015). The therapeutic potential of orphan GPCRs, GPR35 and GPR55. *Front. Pharmacol.*, *6*, 69.

Showalter, V., Compton, D., Martin, B., & Abood, M. (1996). Evaluation of binding in a transfected cell line expressing a peripheral cannabinoid receptor (CB2): identification of cannabinoid receptor subtype selective ligands. *J. Pharmacol. Exp. Ther.*, *278*(3), 989–999.

Sluka, K. A., & Westlund, K. N. (1993). Behavioral and immunohistochemical changes in an experimental arthritis model in rats. *Pain*, *55*(3), 367–77.

Sluka, K. A., Willis, W. D., & Westlund, K. N. (1995). The role of dorsal root reflexes in neurogenic inflammation. *Pain Forum*, *4*(3), 141–149.

Smart, D., Gunthorpe, M. J., Jerman, J. C., Nasir, S., Gray, J., Muir, A. I., Chambers, J. K., Randall, A. D., & Davis, J. B. (2000). The endogenous lipid anandamide is a full agonist at the human vanilloid receptor (hVR1). *Br. J. Pharmacol.*, *129*(2), 227–30.

Smith, M. D. (2011). The normal synovium. *Open Rheumatol. J.*, *5*, 100–6.

Smith, M. D., Triantafillou, S., Parker, A., Youssef, P. P., & Coleman, M. (1997). Synovial membrane inflammation and cytokine production in patients with early osteoarthritis. *J. Rheumatol.*, *24*(2), 365–71.

Sofia, R. D., Nalepa, S. D., Harakal, J. J., & Vassar, H. B. (1973). Anti-edema and analgesic properties of delta9-tetrahydrocannabinol (THC). *J. Pharmacol. Exp. Ther.*, *186*(3), 646–655.

Sokolove, J., & Lepus, C. M. (2013). Role of inflammation in the pathogenesis of osteoarthritis: latest findings and interpretations. *Ther. Adv. Musculoskelet. Dis.*, *5*(2), 77–94.

Staton, P. C., Hatcher, J. P., Walker, D. J., Morrison, A. D., Shapland, E. M., Hughes, J. P., Chong, E., Mander, P. K., Green, P. J., Billinton, A., Fulleylove, M., Lancaster, H. C., Smith, J. C., Bailey, L. T., Wise, A., Brown, A. J., Richardson, J. C., & Chessell, I. P. (2008). The putative cannabinoid receptor GPR55 plays a role in mechanical hyperalgesia associated with inflammatory and neuropathic pain. *Pain*, *139*(1), 225–36.

Staud, R., Craggs, J. G., Robinson, M. E., Perlstein, W. M., & Price, D. D. (2007). Brain activity related to temporal summation of C-fiber evoked pain. *Pain*, *129*(1-2), 130–42.

Steinhoff, M., Vergnolle, N., Young, S. H., Tognetto, M., Amadesi, S., Ennes, H. S., Trevisani, M., Hollenberg, M. D., Wallace, J. L., Caughey, G. H., Mitchell, S. E., Williams, L. M., Geppetti, P., Mayer, E. A., & Bunnett, N. W. (2000). Agonists of proteinase-activated receptor 2 induce inflammation by a neurogenic mechanism. *Nat. Med.*, *6*(2), 151–8.

Szekanecz, Z., Halloran, M. M., Volin, M. V, Woods, J. M., Strieter, R. M., Kenneth Haines, G., Kunkel, S. L., Burdick, M. D., & Koch, A. E. (2000). Temporal expression of inflammatory cytokines and chemokines in rat adjuvant-induced arthritis. *Arthritis Rheum.*, *43*(6), 1266–77.

Talme, T., Ivanoff, J., & Sundqvist, K. G. (2004). Somatostatin is a specific inhibitor of SDF-1alpha-induced T cell infiltration. *Clin. Exp. Immunol.*, *135*(3), 434–9.

Tétreault, P., Dansereau, M.-A., Doré-Savard, L., Beaudet, N., & Sarret, P. (2011). Weight bearing evaluation in inflammatory, neuropathic and cancer chronic pain in freely moving rats. *Physiol. Behav.*, *104*(3), 495–502.

Thomas, E. A., Cravatt, B. F., Danielson, P. E., Gilula, N. B., & Sutcliffe, J. G. (1997). Fatty acid amide hydrolase, the degradative enzyme for anandamide and oleamide, has selective distribution in neurons within the rat central nervous system. *J. Neurosci. Res.*, *50*(6), 1047–52.

Toguri, J. T., Lehmann, C., Laprairie, R. B., Szczesniak, A. M., Zhou, J., Denovan-Wright, E. M., & Kelly, M. E. M. (2014). Anti-inflammatory effects of cannabinoid CB2 receptor activation in endotoxin-induced uveitis. *Br. J. Pharmacol.*, *171*(6), 1448–61.

Tolone, G., Bonasera, L., & Tolone, C. (1978). Biosynthesis and release of prostaglandins by mast cells. *Br. J. Exp. Pathol.*, *59*(1), 105–9.

Tonussi, C. R., & Ferreira, S. H. (1999). Tumour necrosis factor-alpha mediates carrageenin-induced knee-joint incapacitation and also triggers overt nociception in previously inflamed rat knee-joints. *Pain*, *82*(1), 81–7.

Turkiewicz, A., Petersson, I. F., Björk, J., Hawker, G., Dahlberg, L. E., Lohmander, L. S., & Englund, M. (2014). Current and future impact of osteoarthritis on health care: a population-based study with projections to year 2032. *Osteoarthritis Cartilage*, *22*(11), 1826–32.

Urban, M. O., Jiang, M. C., & Gebhart, G. F. (1996). Participation of central descending nociceptive facilitatory systems in secondary hyperalgesia produced by mustard oil. *Brain Res.*, *737*(1-2), 83–91.

V Euler, U. S., & Gaddum, J. H. (1931). An unidentified depressor substance in certain tissue extracts. *J. Physiol.*, *72*(1), 74–87.

Vaccarino, A. L., & Chorney, D. A. (1994). Descending modulation of central neural plasticity in the formalin pain test. *Brain Res.*, *666*(1), 104–8.

Van Boxel, J. A., & Paget, S. A. (1975). Predominantly T-cell infiltrate in rheumatoid synovial membranes. *N. Engl. J. Med.*, *293*(11), 517–20.

Van der Kooij, S. M., de Vries-Bouwstra, J. K., Goekoop-Ruiterman, Y. P. M., van Zeben, D., Kerstens, P. J. S. M., Gerards, A. H., van Groenendael, J. H. L. M., Hazes, J. M. W., Breedveld, F. C., Allaart, C. F., & Dijkmans, B. A. C. (2007). Limited efficacy of conventional DMARDs after initial methotrexate failure in patients with recent onset rheumatoid arthritis treated according to the disease activity score. *Ann. Rheum. Dis.*, *66*(10), 1356–62.

Van Lent, P. L. E. M., Blom, A. B., Schelbergen, R. F. P., Slöetjes, A., Lafeber, F. P. J. G., Lems, W. F., Cats, H., Vogl, T., Roth, J., & van den Berg, W. B. (2012). Active involvement of alarmins S100A8 and S100A9 in the regulation of synovial activation and joint destruction during mouse and human osteoarthritis. *Arthritis Rheum.*, *64*(5), 1466–76.

Vedder, N. B., Winn, R. K., Rice, C. L., Chi, E. Y., Arfors, K. E., & Harlan, J. M. (1990). Inhibition of leukocyte adherence by anti-CD18 monoclonal antibody attenuates reperfusion injury in the rabbit ear. *Proc. Natl. Acad. Sci.*, *87*(7), 2643–2646.

Vergnolle, N., Bunnett, N. W., Sharkey, K. A., Brussee, V., Compton, S. J., Grady, E. F., Cirino, G., Gerard, N., Basbaum, A. I., Andrade-Gordon, P., Hollenberg, M. D., & Wallace, J. L. (2001). Proteinase-activated receptor-2 and hyperalgesia: A novel pain pathway. *Nat. Med.*, *7*(7), 821–6.

Vishwanath, R., & Mukherjee, R. (1996). Substance P promotes lymphocyte-endothelial cell adhesion preferentially via LFA-1/ICAM-1 interactions. *J. Neuroimmunol.*, *71*(1-2), 163–171.

Von Andrian, U. H., Chambers, J. D., Berg, E. L., Michie, S. A., Brown, D. A., Karolak, D., Ramezani, L., Berger, E. M., Arfors, K. E., & Butcher, E. C. (1993). L-selectin mediates neutrophil rolling in inflamed venules through sialyl LewisX-dependent and -independent recognition pathways. *Blood*, *82*(1), 182–91.

Wang, Q., Rozelle, A. L., Lepus, C. M., Scanzello, C. R., Song, J. J., Larsen, D. M., Crish, J. F., Bebek, G., Ritter, S. Y., Lindstrom, T. M., Hwang, I., Wong, H. H., Punzi, L., Encarnacion, A., Shamloo, M., Goodman, S. B., Wyss-Coray, T., Goldring, S. R., Banda, N. K., Thurman, J. M., Gobezie, R., Crow, M. K., Holers, V. M., Lee, D. M., & Robinson, W. H. (2011). Identification of a central role for complement in osteoarthritis. *Nat. Med.*, *17*(12), 1674–9.

Ward, A. E., & Rosenthal, B. M. (2014). Evolutionary responses of innate immunity to adaptive immunity. *Infect. Genet. Evol.*, *21*, 492–6.

Ware, M. A., Adams, H., & Guy, G. W. (2005). The medicinal use of cannabis in the UK: results of a nationwide survey. *Int. J. Clin. Pract.*, *59*(3), 291–5.

Wei, B. Q., Mikkelsen, T. S., McKinney, M. K., Lander, E. S., & Cravatt, B. F. (2006). A second fatty acid amide hydrolase with variable distribution among placental mammals. *J. Biol. Chem.*, *281*(48), 36569–78.

Wenzel, S. E., Fowler, A. A., & Schwartz, L. B. (1988). Activation of pulmonary mast cells by bronchoalveolar allergen challenge. In vivo release of histamine and tryptase in atopic subjects with and without asthma. *Am. Rev. Respir. Dis.*, *137*(5), 1002–8.

Wodnar-Filipowicz, A., Heusser, C. H., & Moroni, C. (1989). Production of the haemopoietic growth factors GM-CSF and interleukin-3 by mast cells in response to IgE receptor-mediated activation. *Nature*, *339*(6220), 150–2.

Woodward, D. F., Liang, Y., & Krauss, A. H.-P. (2008). Prostamides (prostaglandin-ethanolamides) and their pharmacology. *Br. J. Pharmacol.*, *153*(3), 410–9.

Woodward, D. F., Wang, J. W., & Poloso, N. J. (2013). Recent progress in prostaglandin F2α ethanolamide (prostamide F2α) research and therapeutics. *Pharmacol. Rev.*, *65*(4), 1135–47.

Yamaki, K., Thorlacius, H., Xie, X., Lindbom, L., Hedqvist, P., & Raud, J. (1998). Characteristics of histamine-induced leukocyte rolling in the undisturbed microcirculation of the rat mesentery. *Br. J. Pharmacol.*, *123*(3), 390–9.

Yu, M., Ives, D., & Ramesha, C. S. (1997). Synthesis of prostaglandin E2 ethanolamide from anandamide by cyclooxygenase-2. *J. Biol. Chem.*, *272*(34), 21181–6.

Yusof, M., Kamada, K., Gaskin, F. S., & Korthuis, R. J. (2007). Angiotensin II mediates postischemic leukocyte-endothelial interactions: role of calcitonin gene-related peptide. *Am. J. Physiol. Heart Circ. Physiol.*, *292*(6), H3032–7.

Zehentbauer, F. M., Moretto, C., Stephen, R., Thevar, T., Gilchrist, J. R., Pokrajac, D., Richard, K. L., & Kiefer, J. (2014). Fluorescence spectroscopy of Rhodamine 6G: concentration and solvent effects. *Spectrochim. Acta. A. Mol. Biomol. Spectrosc.*, *121*, 147–51.

Zeller, J., Poulsen, K. T., Sutton, J. E., Abdiche, Y. N., Collier, S., Chopra, R., Garcia, C. A., Pons, J., Rosenthal, A., & Shelton, D. L. (2008). CGRP function-blocking antibodies inhibit neurogenic vasodilatation without affecting heart rate or arterial blood pressure in the rat. *Br. J. Pharmacol.*, *155*(7), 1093–103.

Zhang, M., Martin, B. R., Adler, M. W., Razdan, R. K., Jallo, J. I., & Tuma, R. F. (2007). Cannabinoid CB(2) receptor activation decreases cerebral infarction in a mouse focal ischemia/reperfusion model. *J. Cereb. Blood Flow Metab.*, *27*(7), 1387–96.

Zhang, R.-X., Ren, K., & Dubner, R. (2013). Osteoarthritis pain mechanisms: basic studies in animal models. *Osteoarthritis Cartilage*, *21*(9), 1308–15.

Zhuo, M. (2007). A synaptic model for pain: long-term potentiation in the anterior cingulate cortex. *Mol. Cells*, *23*(3), 259–71.

Zias, J., Stark, H., Sellgman, J., Levy, R., Werker, E., Breuer, A., & Mechoulam, R. (1993). Early medical use of cannabis. *Nature*, *363*(6426), 215.

Zimmerman, B. J., Anderson, D. C., & Granger, D. N. (1992). Neuropeptides promote neutrophil adherence to endothelial cell monolayers. *Am. J. Physiol.*, *263*(5 Pt 1), G678–82.

Zygmunt, P. M., Petersson, J., Andersson, D. A., Chuang, H., Sørgård, M., Di Marzo, V., Julius, D., & Högestätt, E. D. (1999). Vanilloid receptors on sensory nerves mediate the vasodilator action of anandamide. *Nature*, *400*(6743), 452–7.

Appendix

01_02

Springer

PERMISSION LETTER

July 22, 2015

Springer reference

Current Osteoporosis Reports
August 2015, Volume 13, Issue 4, pp 216-224
Date: 30 May 2015
Mechanisms and Mediators That Drive Arthritis Pain
Eugene Krustev, Danielle Rioux, Jason J. McDougall

DOI: 10.1007/s11914-015-0275-y
Print ISSN: 1544-1873
Online ISSN: 1544-2241

Materials to be reused: Table 1

Your project

Requestor: Eugene Krustev
MSc Candidate
Department of Pharmacology
Dalhousie University
Halifax, NS
Canada
E-mail: eugene.krustev@dal.ca
University: Dalhousie University
libraries.dal.ca
Purpose: Dissertation/Thesis

With reference to your request to reuse material in which **Springer Science+Business Media** controls the copyright, our permission is granted free of charge under the following conditions:

Springer material

- represents original material which does not carry references to other sources (if material in question refers with a credit to another source, authorization from that source is required as well);
- requires full credit (Springer and the original publisher, book/journal title, chapter/article title, volume, year of publication, page, name(s) of author(s), original copyright notice) to the publication in which the material was originally published by adding: "With permission of Springer Science+Business Media";
- figures, illustrations, and tables may be altered minimally to serve your work. Any other abbreviations, additions, deletions and/or any other alterations shall be made only with prior written authorization of the author and/or Springer Science+Business Media;
- Springer does not supply original artwork or content.

This permission

- is non-exclusive;
- is valid for one-time use only for the purpose of defending your thesis limited to university-use only and with a maximum of 100 extra copies in paper. If the thesis is going to be published, permission needs to be reobtained.
- includes use in an electronic form, provided it is an author-created version of the thesis on his/her own website and his/her university's repository, including UMI (according to the definition on the Sherpa website: http://www.sherpa.ac.uk/romeo/);
- is subject to courtesy information to the author (address is given in the publication);

Springer

PERMISSION LETTER

- is personal to you and may not be sublicensed, assigned, or transferred by you to any other person without Springer's written permission;
- is only valid if no personal rights, trademarks, or competitive products are infringed.

This license is valid only when the conditions noted above are met.

Permission free of charge does not prejudice any rights we might have to charge for reproduction of our copyrighted material in the future.

Rights and Permissions
Springer Science+Business Media
Tiergartenstr. 17
69121 Heidelberg
Germany